MUC1 interacts with Wnt-effector β-catenin in human oesophageal squamous cell carcinoma cell lines

Ciara Metcalfe

A dissertation submitted to the Faculty of Science, University of the Witwatersrand, Johannesburg, in fulfilment of the requirements for the degree of Master of Science.

Johannesburg, 2006

DECLARATION

I declare that this dissertation is my own, unaided, work. It is being submitted for the Degree of Master of Science in the University of the Witwatersrand, Johannesburg. It has not been submitted before for any other degree or examination in any other University.

_____

Ciara Metcalfe

_____ day of_____ 20____

ABSTRACT

MUC1, a mucin-like transmembrane glycoprotein, is highly overexpressed and aberrantly localized in several invasive carcinomas. MUC1 is proposed to play numerous roles in the transformed behaviour of cells in which it is expressed. A number of these roles are facilitated by the interaction of MUC1 with β-catenin, a protein that is central to both cellular adhesion as well as Wnt-responsive gene transcription. The aim of this study was to investigate MUC1 expression, localization, and interaction with β-catenin, as a means of providing insight into the behaviour of human oesophageal squamous cell carcinoma. This cancer-type is exceptionally aggressive and is a major cause of cancer-related morbidity and mortality in South Africa. MUC1 is expressed and aberrantly localized in oesophageal squamous cell carcinoma cell lines, as demonstrated by RT-PCR, western blotting and indirect immunofluorescence. Moreover, evidence from co-immunoprecipitation assays shows that the MUC1 cytoplasmic tail and β-catenin form a complex both at the cell membrane and importantly, within the nucleus of these cell lines. This is the first demonstration of such a complex in the nucleus of a carcinoma derived from stratified, as opposed to simple, epithelia. Data presented here further indicates that activation of the epidermal growth factor receptor results in modulation of the association between MUC1 and β-catenin at the cell membrane. MUC1 membrane-localization, and interaction with β-catenin, may modulate cellular adhesion through steric interference of cell surface adhesion molecules as well as through sequestration of β-catenin away from adherens junctions. On the other hand, MUC1 association with β-catenin may enhance β-catenin signalling either through the stabilization of β-catenin, or as an essential functional component of the β-catenin/LEF/TCF transcription factor complex.

Furthermore, results presented in this study identify oesophageal squamous cell carcinoma as a prime candidate for MUC1-specific immunotherapy. This finding is of substantial importance considering the ineffectual nature of existing therapies used in the treatment of oesophageal carcinoma.

LIST OF ASSOCIATED PUBLICATIONS AND PRESENTATIONS

Metcalfe C and Veale RB: **The MUC1 cytoplasmic tail, and its interaction with beta-catenin, in human oesophageal squamous cell carcinoma cell lines.** *BMC Cancer* Corrections submitted.

Metcalfe C and Veale RB: **MUC1, a mucin-like oncoprotein, interacts with the Wnt effector, beta-catenin, in human oesophageal squamous cell carcinoma cell lines.** *SASBMB XXth Conference,* Pietermaritzburg. 3-5 July 2006

Dahan Y, Metcalfe C, Veale RB: **Urokinase receptor and matrix metalloprotease-7 expression in human oesophageal squamous carcinoma cells- the role of nuclear beta-catenin?** *SASBMB XXth Conference,* Pietermaritzburg. 3-5 July 2006

Metcalfe C and Veale RB: **Expression of the multi-faceted protein, MUC1, in human oesophageal carcinoma cell lines.** *SASBMB XIXth Conference,* Stellenbosch. 16-20 January 2005

Things should be made as simple as possible, but not any simpler.

Albert Einstein

ACKNOWLEDGEMENTS

According to the renowned geneticist, Professor Bryan Sykes, "Like any walk of life, science has its ups and downs, its heroes and its villains". It is because of the following people that there were more ups than downs and more heroes (and heroines) than villains. Heartfelt thanks to:

My supervisor, Professor Rob Veale, for his wisdom, for his patience, for believing in me; without him this work would not have been possible.
Elsabé Scott, for teaching me the finer art of tissue culture, for providing cells, and for always knowing where to find things.
The members of the Cell Biology lab, Belinda Bezuidenhout, Bronwyn Thomson, Catherine Worsley, Glenn Driver, Lindsay McCutcheon, Mark Killick, Nicolene Shaw and Yael Dahan, for all the helpful advice, especially in the drafting of this dissertation, and for making me laugh when things weren't going according to plan. Special thanks go to Yael for bravely taking on the task of proof reading this dissertation.
Caroline Lalkhan, for her assistance with the confocal microscope.

Personal thanks go to my parents, Bernadette and Sean Metcalfe, for all their love, support, guidance, and encouragement, and also to Helen and Bill Langridge for being there when I needed them.

Many thanks also go to the National Research Foundation, the Deutscher Akademischer Austausch Dienst, and the University of the Witwatersrand, for funding.

CONTENTS

LIST OF FIGURES

LIST OF TABLES

LIST OF ABBREVIATIONS AND SYMBOLS

α	alpha
APC	adenomatous polyposis coli
APS	ammonium persulphate
β	beta
Bis	*N′,N′*,-methylenebis-acrylamide
bp	base pair
BSA	bovine serum albumin
β-TrCP	beta-transductin-repeat-containing protein
°C	degrees Celsius
C-terminal	carboxy-terminal
CBP	CREB binding protein
CDK	cyclin dependant kinase
cDNA	complementary deoxyribonucleic acid
CHO	Chinese hamster ovary
cm	centimetre(s)
CT	cytoplasmic tail
CTL	cytotoxic T-lymphocyte
dH_2O	distilled water
DMEM	Dulbecco's modified eagles medium
DNA	deoxyribonucleic acid
dNTP	deoxynucleotide triphosphate
Dsh	dishevelled
DTT	dithiothreitol
E-cadherin	epithelial-cadherin
ECM	extracellular matrix
EDTA	ethylenediaminetetra-acetic acid
EGF	epidermal growth factor
EGFR	epidermal growth factor receptor
EMT	epithelial-mesenchymal transition

ERK	extracellular signal regulated kinase
EtBr	ethidium bromide
FAK	focal adhesion kinase
FCS	foetal calf serum
FITC	fluorescein isothiocyanate
γ	gamma
x g	gravitational units
g	gram(s)
Grb2	growth factor receptor binding protein 2
GSK3β	glycogen synthase kinase 3β
HEK	human embryonic kidney
HOSCC	human oesophageal squamous cell carcinoma
HRP	horseradish peroxidase
Ig	immunoglobulin
IL-2	interleukin-2
ILK	integrin-linked kinase
IP	immunoprecipitation
JNK	c-Jun NH_2 terminal kinase
Kb	kilobase
kDa	kilodalton
LEF	lymphoid enhancer factor
µ	micro
µg	microgram(s)
µl	microlitre(s)
M	molar
mA	milliampere(s)
MAPK	mitogen-activated protein kinase
min	minute(s)
ml	millilitre(s)
mM	millimolar
MMLV-RT	Moloney murine leukemia virus reverse transcriptase

MMP7	matrix metalloproteinase 7
mRNA	messenger ribonucleic acid
nm	nanometre(s)
PAGE	polyacrylamide gel electrophoresis
PBS	phosphate buffered saline
PCR	polymerase chain reaction
PI3K	phosphoinositide 3-kinase
PKC	protein kinase C
PMSF	phenyl-methyl-sulphonyl fluoride
Rb	retinoblastoma
RNA	ribonucleic acid
RT	reverse transcriptase
SAPK	stress-activated protein kinase
SDS	sodium dodecyl sulphate
SH	src homology domain
SOS	son of sevenless
STAT	signal transducer and activator of transcription
TAE	tris acetic acid EDTA
TCA	tri-chloroacetic acid
TCF	T-cell factor
TEMED	*N′,N′,N′,N′*-tetramethylene-diamine
TGFα	transforming growth factor alpha
Tris	tris(hydroxymethyl)aminomethane
UV	ultraviolet
V	volts
WHCO	Wits human carcinoma of the oesophagus

CHAPTER 1: GENERAL INTRODUCTION AND LITERATURE SURVEY

1.1 Cancer is the product of multiple genetic defects

Mammalian cells have multiple safeguards to protect them against the potentially lethal effects of cancer gene mutations. No single genetic defect causes cancer, and only when several genes are defective does an invasive cancer develop (for reviews see Knudson, 2002, Mareel and Leroy, 2002, Vogelstein and Kinzler, 2004). Alterations in three types of genes are responsible for tumorigenesis: stability genes, oncogenes and tumour-suppressor genes.

Stability genes include mismatch repair, nucleotide-excision repair and base-excision repair genes that are responsible for repairing subtle mistakes made during normal DNA replication or induced by exposure to mutagens (Hanahan and Weinberg, 2000). Stability genes also include those that control processes involving large portions of chromosomes such as chromosomal segregation (for review see Friedberg, 2003). Stability genes are considered the "caretakers" that keep genetic alterations to a minimum. Mutations in stability genes have the effect of increasing the rate at which mutations may occur in other genes, such as in oncogenes and tumour-suppressor genes (Vogelstein and Kinzler, 2004).

Oncogenes are mutated in ways that render the gene constitutively active, or active under conditions in which the wild-type gene is not. These mutations are often referred to as gain-of-function mutations (Hanahan and Weinberg, 2000). An activating mutation in one allele of an oncogene is generally sufficient to confer a selective growth advantage to the cell. An example of an oncogene is BRAF, a tyrosine kinase which when mutated from a valine to a glutamate (located within the activation loop of the kinase domain) becomes constitutively active. Activated BRAF then phosphorylates downstream targets such as extracellular signal regulated kinase (ERK), leading to aberrant growth (Davies, 2002). Another common example of an oncogene is cyclin D1 which promotes

progression of the cell through the cell cycle and therefore has a direct impact on proliferation when mutated (Baldin *et al*., 1993).

Tumour-suppressor genes, on the other hand, are targeted by what are known as loss-of-function mutations, whereby the mutations reduce the activity of the gene product (Hanahan and Weinberg, 2000). These inactivations may arise from missense mutations at residues that are essential for activity, from mutations that result in a truncated protein, from insertions and/or deletions, or from epigenetic signalling (Vogelstein and Kinzler, 2004). Epigenetic signalling refers to such events that are not directly controlled by gene sequence. For example, an epigenetic change may refer to a covalent modification of DNA or chromatin (perhaps methylation) that results in up- or down-regulation of a specific gene product. In contrast to an oncogene, mutation of both alleles of a tumour-suppressor gene is usually required in order for the effect to be expressed physiologically. There are two tumour-suppressor gene pathways that are thought to be crucial to the initiation and/or progression of almost all (if not all) carcinomas, that is, cancers of epithelial origin. These are the pRb pathway and the p53 pathway. pRb refers to the retinoblastoma gene product that was originally discovered in a hereditary tumour of the eye (for review see Classon, 2002). It controls the transition of a cell from a resting stage in the cell cycle (G0 or G1) to a replicating phase (S) of the cell cycle. The p53 protein is a transcription factor that normally inhibits cell growth and stimulates cell death when induced by cellular stress. p53 may be mutated "genetically" through a point mutation that inactivates its capacity to bind to its recognition sequence, or epigenetically, through the amplification of the mouse double minute 2 (MDM2) gene which functionally inactivates p53 by binding to it (for review see Mayo, 2002). Another common tumour-suppressor gene that is of interest in this study is the adenomatous polyposis coli (APC) gene. Although first discovered in the colon, APC mutations are now thought to occur in numerous cancer-types (Polakis, 2000).

Oncogenes and tumour-suppressor genes drive the neoplastic process by increasing tumour cell number through the stimulation of cell division, the inhibition of cell death, or cell cycle arrest (Hanahan and Weinberg, 2000). Mutations in the three classes of

cancer genes (i.e. stability genes, oncogenes and tumour-suppressor genes) may occur either in the germline or in single somatic cells. Mutations in the germline are usually subtle point mutations or small deletions or insertions, and result in hereditary predisposition to cancer (Vogelstein and Kinzler, 2004). Predisposition to cancer is due to the fact that each somatic cell of that individual (derived from the mutated germline) already contains a mutation, or mutations, that may contribute to neoplasia.

Mutations occurring in somatic cells can be either small subtle changes such as in germline cells or may be gross changes such as chromosomal rearrangement. The first somatic mutation in an oncogene or tumour-suppressor gene that causes a clonal expansion initiates the neoplastic process (Nowell, 2002). Subsequent mutations may occur over time and result in additional rounds of clonal expansion and thus in tumour progression. It is these subsequent mutations that often confer "malignant" traits to the neoplastic cells. Malignancy is the ability of neoplastic cells to migrate to distant sites and establish secondary metastases (Knudson, 2002). Whereas primary and benign (solid) tumours can generally be removed through surgery, widely metastatic tumours are difficult to excise and are exceptionally difficult to treat (Mareel and Leroy, 2002). Thus, it is malignancy, rather than tumorigenicity, that is ultimately responsible for the great majority of neoplastic deaths (Vernon and LaBonne, 2004).

1.2 Metastasis is a complex multi-step process

The processes of invasion and metastasis are extremely complex and cells must accumulate several mutations, each rate-limiting, in numerous behaviour-related genes in order to achieve malignant status (Bussemakers and Schalken, 1996, Mareel and Leroy, 2002). Neoplastic cells must acquire a motile phenotype, escape from the primary tumour, degrade the extracellular matrix, migrate to distant sites, arrest in the capillaries, and migrate through the basement membrane and underlying tissue to the metastatic site (Bussemakers and Schalken, 1996). Thus it is evident that in order to successfully metastasize tumour cells must exhibit considerable flexibility in numerous characteristics. This flexibility is reflected in a complex and dynamic expression pattern of cell adhesion

molecules, proteases, protease inhibitors, motility factors and growth factors (Pignatelli and Vessey, 1994, Bussemakers and Schalken, 1996). Of particular interest in this study is the impact of the changing dynamics of cell adhesion during metastasis.

1.3 Cell adhesion is central to both embryonic development as well as malignant transformation

Multicellular organisms require mechanisms for intercellular cohesion and communication (Hynes and Zhou, 2000). These requirements are largely met by the ability of cells to adhere to one another as well as to components of the extracellular matrix (ECM). Cell adhesion is vital in controlling and mediating development; it is an absolute requirement for the generation of coherent sheets or tubes of epithelial cells with distinct apical-basal polarity, which in turn is a requisite for the appropriate formation of an organism (Carthew, 2005). A system of dynamic cell adhesion resulting in cell motility is also required for a functional immune system (see CD44, immunoglobulins and selectins below).

In general, adhesion molecules are intimately involved in the control of processes such as morphological differentiation, cellular proliferation, motility, as well as malignancy (Harington and Syrigos, 2000). The particular adhesive characteristics of a cell are determined by the combined expression of individual proteins characterized as cell adhesion molecules. There are at least 5 families of cell adhesion molecules, including: integrins, cadherins, immunoglobulins, CD44 and selectins.

CD44 transmembrane glycoproteins bind to components of the ECM, including hyaluronic acid, osteopontin, collagen and laminin and therefore mediate cell-ECM adhesion. These proteins allow for the attachment of circulating lymphocytes to vascular endothelium and are predominantly involved in lymphocyte homing and T-cell activation (Goodison *et al*., 1999). Immunoglobulins are a large group of cell surface glycoproteins that share an immunoglobulin (Ig)-like extracellular domain and are also important in the immune response of T-cells (Springer, 1990). Selectins, on the other hand, are a group of

cell surface lectins that mediate the adhesion between leukocytes, platelets and endothelial cells (Carlos and Harlan, 1994). Selectins mediate leukocyte rolling which is important for the recruitment of leukocytes to areas of injury and inflammation (Carlos and Harlan, 1994). Although modulation of expression of CD44 proteins, immunoglobulins and selectins has been associated with the ability of cells to metastasize, we will focus more on integrin and cadherin expression and function, since they are central to epithelial attachment.

1.4 Integrins mediate interactions between the cell and components of the acellular environment

Adhesion of cells to the ECM is crucial for control of cell behaviour. It connects the ECM to the intracellular cytoskeleton and transduces bidirectional signals between the extracellular environment and the intracellular compartment (Sepulveda *et al.,* 2005). Reduced cell-ECM adhesion allows cells to circumvent the control induced by the extracellular environment. Importantly, a dynamic formation and dissolution of cell-ECM contacts is needed for cancer cell migration and subsequent arrest at the secondary site (Mareel and Leroy, 2002).

Integrins are a family of ubiquitously expressed integral transmembrane glycoproteins that exist as α/β heterodimers at cell adhesion sites known as focal adhesions (Hynes, 2002). The human genome is thought to encode as many as 18 α and 8 β subunits, from which 24 different functional integrins are formed (Danen, 2005). The extracellular domains of integrins function as cell surface receptors for components of the ECM, including laminin, collagen and fibronectin. Their affinity for a particular component of the ECM depends on the combination of α and β subunits from which that integrin is formed (Van der Flier and Sonnenberg, 2001, Hynes, 2002). For example, α6β4 integrins bind to laminin, while α2β1 integrins bind to collagen. More than one integrin combination is able to bind to a particular ECM component (Hynes, 2002). The integrin intracellular domain interacts directly or indirectly, via linker proteins, to the actin cytoskeleton (Nair *et al*., 2005). Integrin-mediated adhesion is a regulated process,

whereby integrins must be stimulated by soluble mediators such as chemokines and growth factors or insoluble components such as the ECM, in order to adhere. Interestingly, integrins have been reported to function in signalling by "inside out" signalling, where a cell alters the adhesive state of its integrin receptors, as well as "outside in", which refers to the transmission of a signal from the ECM into the cell which may result in modulation of gene expression (Danen, 2005). Integrin signalling involves a number of important down-stream non-receptor kinases. Examples of these are focal adhesion kinase (FAK) which is activated in response to integrin clustering, as well as integrin-linked kinase (ILK) which is a unique intracellular adaptor that links integrins and growth factors to the actin cytoskeleton and a range of other signalling pathways (Giancotti and Rouslatti, 1999). Integrin binding and functionality is pivotal in controlling cell attachment, cell migration, cell cycle progression and apoptosis.

The relationship between integrin expression and cancer is complex. Up- or down-regulation of integrin expression may contribute to oncogenic transformation, primary tumour growth and invasion, depending on the specific integrin, the cell type and on the oncogenic mutations involved. For example, forced expression of α5β1 in transformed Chinese hamster ovary cells restored fibronectin matrix assembly and suppressed growth in soft agar and tumour formation in immunodeficient mice (Giancotti and Rouslatti, 1990). Growth in soft agar indicates the ability of cells to proliferate by an anchorage-independent mechanism, which is a hallmark of cancer. Normal cells exhibit anchorage-dependence, whereby cells that are not attached to a substrate experience growth arrest and apoptosis. Therefore forced expression of α5β1 appeared to induce a degree of anchorage-dependence to the transformed cells, indicating that reduced expression of this integrin mediates a shift to anchorage-independence. On the other hand, increased expression of αv integrins contributes to primary tumour growth in human melanoma (Felding-Habermann *et al*., 1992). Moreover, changes in expression from one integrin type to another may aid in cell migration (Danen, 2005). In some carcinomas, tumour cell detachment from laminin in the basement membrane and subsequent attachment to fibronectin in the stroma is mediated by the down-regulation of laminin-binding α4β6 integrins and up-regulation of fibronectin-binding α5β1 integrins (Danen, 2005). Tumour

cells thus gain and lose expression of specific integrins during the course of tumour progression in accordance with the different environmental constraints they may encounter.

1.5 Cadherins mediate interactions between neighbouring cells

Cell-cell adhesion is responsible for determining and maintaining tissue integrity and regulates major cellular processes including motility, growth, differentiation and survival. The adhesion of cells to their neighbours also counteracts the escape of cells into neighbouring tissues (Conacci-Sorrell *et al*., 2002, Mareel and Leroy, 2002). Reduced cell-cell adhesion may therefore allow the cells to escape from their site of origin and may significantly enhance the proliferative and migratory potential of the cells (Harington and Syrigos, 2000, Conacci-Sorrell *et al*., 2002).

Cadherins are a family of calcium dependant integral membrane proteins that function in homotypic cell-cell adhesion (Harington and Syrigos, 2000, Hirohashi and Kanai, 2003). The cadherin family is divided into three subfamilies: classic cadherins, which are components of the adherens junctions, and desmocollins and desmogleins, which are both components of desmosomes (Nair *et al*., 2005). Adherens junctions are responsible for mediating cell-cell adhesion via the actin microfilaments of neighbouring cells. Desmosomes, rather than binding actin microfilaments, bind intermediate filaments. Of particular interest to this study is the classic cadherin, E (epithelial)-cadherin. E-cadherin plays an important role in tissue formation and maintenance during embryonic development, and in the induction and maintenance of normal architecture and function in adult tissues (Takechi, 1988). The critical importance of E-cadherin to normal development and tissue function is demonstrated both by the very early expression of E-cadherin, at the two cell stage, as well as by the lethality of E-cadherin gene knockouts in mice, also at a very early stage during embryogenesis (Larue *et al*., 1994). Reduced E-cadherin expression has been shown to promote epithelial cell invasiveness, dedifferentiation and metastasis in various carcinomas, supporting a role for this protein as an “invasion suppressor molecule” (Pecina-Slaus, 2003, Vogelstein and Kinzler,

2004). Importantly, hereditary predisposition to gastric cancer results from germline mutations in the CDH1 gene that encodes E-cadherin (Conacci-Sorrell *et al*., 2002). Providing further support for the notion of E-cadherin as an invasion suppressor gene is the apparent relationship between down-regulation of the E-cadherin molecule and epithelial-mesenchymal transition (EMT) (Cano *et al*., 2000, Conacci-Sorrell *et al*., 2002, Pecina-Slaus, 2003, Vernon and LaBonne, 2004). EMT is essential for normal embryonic development and refers to the process whereby epithelial cells acquire mesenchymal fibroblast-like properties and show reduced cell-cell adhesion, a loss of polarity and increased motility (Vernon and LaBonne, 2004, Larue and Bellacosa, 2005). In normal development EMT is vital to the gastrulation movements that reorganize embryonic germ layers, as well as to the development of other migratory cell types such as the neural crest (Shook and Keller, 2003). Neural crest cells in particular must undergo EMT in order to migrate extensively prior to giving rise to the diverse array of tissue-types characteristic of vertebrates (Locascio and Nieto, 2001). Interestingly, tumour progression and malignant transformation appear to be associated with EMT-like events. Indeed it has been suggested that EMT is essential for the progression of non-invasive tumour cells into malignant carcinomas (Vernon and LaBonne, 2004, Larue and Bellacosa, 2005). Several oncogenic pathways, including growth factor, integrin and Wnt/β-catenin pathways, have been implicated in the induction of EMT (Larue and Bellacosa, 2005). However, it appears that the critical molecular event in EMT is the down-regulation of E-cadherin.

E-cadherin function is mediated by its linkage to the actin cytoskeleton via cytoplasmic proteins known as catenins (Harington and Syrigos, 2000, Conacci-Sorell, 2002, Hirohashi and Kanai, 2003). The intracellular domain of E-cadherin binds to β-catenin (or less often to γ-catenin) which then binds to α-catenin which is in turn bound to the actin cytoskeleton (see Figure 1.1). α-catenin thus plays an important role in linking E-cadherin, which itself interacts homotypically with E-cadherin molecules of adjacent cells, to the actin cytoskeleton, but does not bind directly to E-cadherin. β-catenin provides the structural link between E-cadherin and α-catenin (Harington and Syrigos,

2000). The cadherin-catenin system thereby effectively forms an intercellular bridge linking the actin cytoskeleton of one cell to the actin cytoskeleton of an adjacent cell.

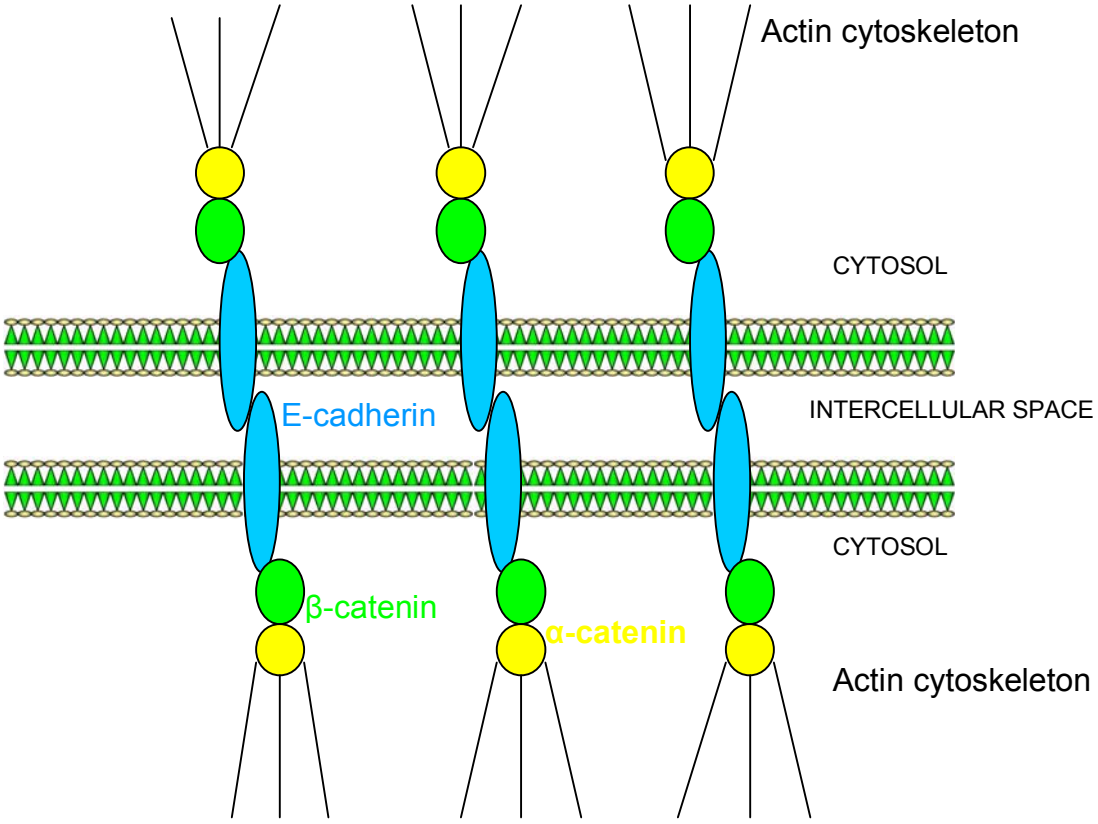

Figure 1.1: The adherens junction. The adherens junction forms an intercellular bridge linking the actin cytoskeleton of one cell to the actin cytoskeleton of an adjacent cell. Extracellular domains of E-cadherin molecules form homodimers. Intracellularly, E-cadherin is linked to the cytoskeleton via β-catenin and α-catenin.

β-catenin was first described in mammals as a member of the adherens junction, as detailed above (Ozawa *et al*., 1989a). Further study, however, indicated that β-catenin is an orthologue of the *Drosophila* protein, Armadillo, a segment polarity gene that controls patterning and organogenesis in the embryo. Just as Armadillo functions downstream of the Wingless protein, β-catenin functions downstream of Wnt (the orthologue of *Drosophila* Wingless) (Kikuchi, 2000, Logan and Nusse, 2004). Wnt proteins are a family of highly conserved secreted signalling molecules that regulate cell-cell interactions during embryogenesis (Cadigan and Liu, 2006). Wnt signalling induces nuclear translocation of β-catenin which alters gene transcription and has the downstream effect of modulating aspects of cell behaviour and morphology. These changes may include reduced cell polarity and an increase in cell migration (Logan and Nusse, 2004, Cadigan and Liu, 2006). The importance of β-catenin in embryonic development is clearly demonstrated by the early in utero death of β-catenin gene knockout mice (Haegel *et al*., 1995). β-catenin therefore has a dual role; on one hand it is an essential functional component of the adherens junction and on the other hand it is a crucial effector of Wnt signalling. Tumour genetics has revealed that mutations in members of the Wnt-β-catenin pathway result in the up-regulation of genes, such as c-myc, cyclin D1 and matrix metalloproteinase 7 (MMP7), which may enhance tumorigenic and/or metastatic potential (Novak and Dedhar, 1999, Wong and Pignatelli, 2002). These mutations occur in approximately 90% of colorectal carcinomas as well as in other cancer types such as hepatocellular carcinomas and gastric cancers (Bienz and Clevers, 2000, Polakis, 2000, Brembeck *et al*., 2006). Members of the Wnt-β-catenin signalling pathway thus appear to be important contributors to tumorigenesis and tumour progression. There are several other membrane-associated proteins for which cancer-related signalling roles have been identified; an important one being MUC1.

1.6 MUC1, a transmembrane mucin, is overexpressed by numerous carcinomas

MUC1 was first identified in human milk, where it is shed from the milk secreting epithelial cells, as a high molecular weight glycoprotein rich in serines, threonines and prolines (Gendler *et al*., 1990, Patton *et al*., 1995, Taylor-Papadimitriou *et al*., 1999). It

has since been confirmed as a type-I transmembrane mucin that is expressed on the apical surface of most simple epithelia, including mammary gland, female reproductive tract, lung, kidney, stomach, gall bladder and pancreas (Brayman *et al*., 2004).

The apical surface of simple epithelia is often exposed to a relatively harsh environment. Mucins have a protective role and function to maintain cellular integrity, provide lubrication, prevent dehydration and offer protection against proteolysis. Mucins protect against microbial attack by sterically inhibiting access to the cell surface (Van Klinken *et al*., 1995, Hollingsworth and Swanson, 2004). They are a large family of glycoproteins that are encoded by a total of 21 *MUC* genes: MUC1, MUC2, MUC3A, MUC3B, MUC4, MUC5AC, MUC5B, MUC6-13 and MUC15-20 (Moniaux *et al*., 2001). Mucins are classified as either membrane-bound, which include MUC1, MUC3B and MUC4, or secreted, which include MUC2, MUC5AC, MUC5B and MUC6 (Moniaux *et al*., 2001). The secreted, or gel-forming, mucins are expressed exclusively by specialized epithelial cells and form complex arrays of intermolecular disulphide-linked mucin multimers, i.e. mucus. Membrane-bound mucins are implanted at the apical surface of simple epithelia (Moniaux *et al*., 2001). Although characterized as membrane-bound these mucins also contribute to mucus formation by shedding their extracellular domain, which is mediated by a cleavage event (Gendler and Spicer, 1995). Alternatively spliced isoforms of membrane-bond mucins may also be secreted into the mucus (Moniaux *et al*., 2004).

Mucins (both secreted and membrane-bound) are typically very large molecules with extended structures due to the abundance of proline residues and a high degree of glycosylation (Hollingsworth and Swanson, 2004). MUC1 is no exception. The human MUC1 gene spans 4 to 7 kb (depending on the allele) and is comprised of 7 exons that can be alternatively spliced to form transcripts from 3.7 to 6.4 kb in length. The full length protein consists of a short cytoplasmic domain and a transmembrane domain, both of which are highly conserved among species, and a large extracellular domain containing a variable number of tandem repeats (Gendler and Spicer, 1995, Lagow *et al*., 1999). The conserved cytoplasmic domain is thought to have signalling capabilities, which will be discussed in greater detail in the following chapters.

MUC1 is synthesized as one large precursor, containing only N-linked glycans, which is immediately proteolytically cleaved while still in the endoplasmic reticulum. Cleavage occurs between the mucin-like extracellular domain and the remainder of the molecule, including the transmembrane and cytoplasmic domains (Hilkens *et al.,* 1992, Taylor-Papadimitriou *et al.,* 1999). The two components remain tightly associated as a heterodimer in a stable, non-covalent, but SDS-sensitive manner (see Figure 1.2). The core protein has an estimated weight of 120 to 225 kDa, and the mature glycosylated form ranges from 250 to 500 kDa (the size varies according to the number of tandem repeats in the ectodomain). Importantly, the extended extracellular domain of MUC1 is thought to modulate cell-cell and cell-ECM interactions by steric hindrance of cadherin and integrin molecules, however this is only the case when apical restriction is lost, an event common in cancer cells (Hilkens *et al*., 1992, Wesseling *et al*., 1995, Wesseling *et al*., 1996).

MUC1 is expressed ubiquitously on the ducts and glands of simple epithelial tissues. A number of studies indicate that MUC1 is overexpressed, aberrantly localized and aberrantly glycosylated in various carcinomas, including those of the breast, pancreas and colon (for review see Gendler, 2001). Importantly, MUC1 is thought to be overexpressed and aberrantly localized by approximately 90% of breast carcinomas. Moreover, MUC1 overexpression is associated with metastasis and poor clinical outcome in a variety of tumours (Satoh *et al*., 2000). To illustrate, MUC1 is highly expressed in invasive ductal carcinomas of the pancreas and invasive cholangiocarcinomas of the liver, which both show invasive growth and a poor prognosis. However, it is rarely expressed in intraductal papillary mucinous tumours of the pancreas and bile duct carcinomas of the liver, which show a favourable prognosis (Yonezawa and Sato, 1997). Similarly, it was shown that high levels of expression of MUC1 in renal cell carcinoma correlates with the aggressiveness of the disease and the tendency to form metastases (Fujita *et al*., 1999).

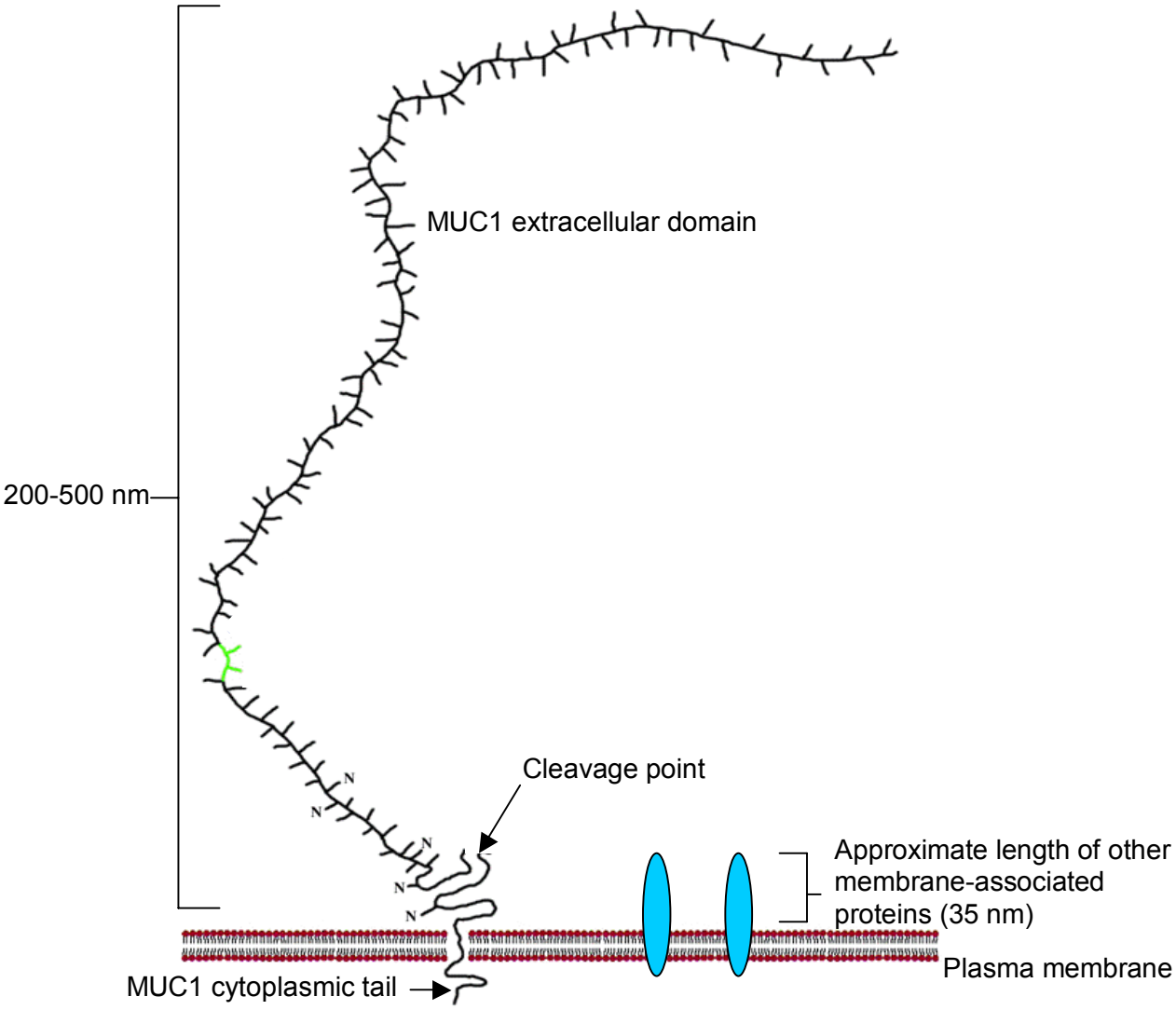

Figure 1.2: MUC1 exists at the cell surface as a heterodimer. One component of the dimer consists of the extracellular domain containing a variable number of tandem repeats, and the other component consists of a short extracelluar fragment, the transmembrane domain and the cytoplasmic tail (Hilkens *et al.,* 1992).

1.7 MUC1 contributes to multiple aspects of cell behaviour

As previously discussed, tumorigenesis and particularly metastasis are extremely complex events. Mutations in oncogenes and tumour-suppressor genes are required to generate a sub-population of cells that have a growth advantage (Vogelstein and Kinzler, 2004). Further mutations and epigenetic modifications are then required to create a population of cells that have metastatic capabilities (Bussemakers and Schalken, 1996, Vogelstein and Kinzler, 2004). Those cells must exhibit a number of specialized characteristics to allow them to detach from the primary tumour, invade the local stroma, enter either the lymphatic or blood circulatory systems, evade the immune system, arrest at the secondary site and establish a tumour (Bussemakers and Schalken, 1996). MUC1 expression is proposed to contribute to the transformed behaviour of invasive cancer cells through a variety of different mechanisms. These mechanisms are mediated predominantly by its aberrant localization over the entire cell surface, its exceptionally large extracellular domain and its aberrant glycosylation (Gendler, 2001). Together these factors contribute to anti-adhesion, cell proliferation, survival, cell migration and the modulation of immune system functioning.

One of the major focuses of scientists investigating MUC1 biology has been the impact of MUC1 expression on cell adhesion. The large extracellular domain of MUC1 extends well beyond the extracellular domains of most other membrane-associated proteins, including the cell adhesion molecules (Hilkens *et al*., 1992, Wesseling *et al*., 1996). This has the effect of shielding adhesion molecules from their ligands. On the other hand, aberrant glycosylation of MUC1 may generate novel epitopes that act as ligands for adhesion molecules present on, for example, endothelial cells (Hilkens *et al*., 1992). In Chapters 2 and 3 we explore, in greater detail, the implications of MUC1 expression on cell adhesion.

Up-regulation of MUC1 expression may contribute to the regulation of differentiation and proliferation of tumour cells. Various studies have implicated MUC1 in pathways-such as the mitogen-activated protein kinase (MAPK) pathway and the Wnt-β-catenin

pathway- that result in the up-regulation of genes that promote progression through the cell cycle (detailed below). Briefly, MUC1 is thought to potentiate epidermal growth factor signalling through recruitment of intracellular members of the signalling pathway to the epidermal growth factor receptor (EGFR), where they are activated (Panday *et al*., 1995, Schroeder *et al*., 2001). With regards to the Wnt-β-catenin pathway, MUC1 has been implicated in the nuclear translocation of β-catenin, potentially mimicking an active Wnt pathway (Wen *et al.,* 2003). These concepts will be addressed more fully in Chapter 4, as well as in the final discussion.

In addition to enhancing proliferation through the up-regulation of growth promoting genes, MUC1 may also actively inhibit apoptosis and enhance survival, in particular in response to genotoxic agents. In short, MUC1 has been shown to activate the anti-apoptotic phosphoinositide 3-kinase (PI3K) pathway, and has also been shown to suppress the pro-apoptotic p53 response (Raina *et al*., 2004, Ren *et al*., 2004). These concepts will also be addressed more fully at a later stage. What is important to note here however, is that MUC1 is exceptionally dynamic and modulates cell behaviour through a variety of mechanisms.

1.8 MUC1 may contribute to the survival of metastatic cells in circulation by assisting in evasion of the immune system

Not all tumour cells in a primary lesion are able to metastasize to distant organs. Tumour cells with a high metastatic potential arise within primary tumours at an early stage and become predominant during the progression of the disease to an advanced stage (Nicolson, 1982). Moreover, the glycoproteins expressed on the tumour cells of a metastatic phenotype are qualitatively and quantitatively different from those of the non-metastatic phenotype (Nicolson, 1982).

Mucin function is intimately connected with their pattern of glycosylation. Oligosaccharides on proteins have a multifunctional role in the folding, stability and targeting of glycoproteins. N-linked glycans (of which there are 5 potential binding sites

on MUC1) are added in the endoplasmic reticulum, during translocation of proteins, and are used by the chaperones calnexin and calreticulin, to retain proteins within this compartment until they are properly folded (Trowbridge and Helenius, 1998). Both O- and N-linked glycans provide protection from degradation, while clusters of O-linked glycans can act as an apical targeting signal (Trowbridge and Helenius, 1998). Each MUC1 tandem repeat contains 5 potential sites for O-glycosylation. The addition of N-acetyl galactosamine to serine or threonine initiates O-glycosylation in mammalian cells. This reaction is catalysed by a family of N-acetylgalactosaminyltransferases (Taylor-Papadimitriou *et al*., 1999). O-glycans are then synthesized by the addition of sugars individually and sequentially as the mucin passes through the Golgi. Since the concentrations of glycosyltransferases as well as their cofactors and substrates vary from tissue to tissue the degree of MUC1 glycosylation also varies from tissue to tissue. For example, MUC1 of the pancreas is more heavily glycosylated (80%), than that of the mammary gland (50%) (Taylor-Papadimitriou *et al*., 1999). Oncogenic transformation is often accompanied by a change in the profile of expression of glycosyltransferases which results in the modification of glycosylation patterns of MUC1 in cancer cells (Taylor-Padaimitriou *et al*., 1999).

The long and complexly branched carbohydrates on MUC1 expressed by normal epithelial cells ordinarily mask MUC1 core proteins at the cell surface, however, MUC1 in cancer cells has a reduced number of sites that are glycosylated and tend to express much shorter carbohydrates (Von Mensdorff-Pouilly *et al*., 2000, Kontani *et al.*, 2001). This results in the exposure of numerous repetitive cryptic epitopes (due to the tandem repeats) on the core protein of the molecule. In cancer patients, this altered molecule is shed into the circulation, where it comes into contact with the immune system, which may now recognize it as “foreign” (Taylor-Papadimitriou and Finn, 1997, Von Mensdorff-Pouilly *et al*., 2000). The aberrant glycosylation of MUC1 was thus proposed to be important in inducing significant cytotoxic T-lymphocyte (CTL) response in patients with cancer (Kontani *et al.,* 2001).

There are conflicting reports on the susceptibility of MUC1 expressing cells to CTLs. Van de Wiel-Van Kemenade *et al.* (1993) reported that melanoma cells transfected with the MUC1 gene are resistant to killing by cytotoxic T-cells. In agreement, Fujita *et al.* (1999) state that even though MUC1-specific CTLs can be generated, the sialylated MUC1 mucin inhibits cytotoxic lymphocyte-target cell interactions, and even induces apoptosis of lymphocytes. They propose that a greater concentration of MUC1 on renal carcinoma cells may conceal putative recognition sites for these killer lymphocytes, which would increase the chance of survival and colonization of MUC1-expressing cells by allowing them to evade immune surveillance. In contrast, von Mensdorff-Pouilly *et al*. (2000) found that the natural humoral immune response against aberrantly glycosylated MUC1 positively influenced survival of breast cancer patients. On one hand, alterations in MUC1 glycosylation alerts the immune system and induces the production of MUC1-specific CTLs, but on the other hand (and not as clearly defined) MUC1 expression may aid in the escape of cells from the immune system.

In addition to impacting upon its interactions with the immune system, changes in MUC1 glycosylation have been reported to generate sialyl Lewis^{x} and sialyl Lewis^{a} epitopes which are not present in normal cells (Taylor-Papadimitriou and Finn, 1997). These epitopes may act as ligands for selectins found on endothelial cells (which line lymph and blood vessels) and may therefore aid in the movement and migration of transformed cells.

1.9 Intracellular MUC1 is associated with a poor prognosis

MUC1 expression in tumours from breast, lung, kidney and thyroid correlates with an aggressive tumour and increased metastasis. However, a recent immunohistological study conducted on breast carcinomas indicates that it is likely to be the aberrant intracellular localization of MUC1 (rather than simply expression) which is associated with a poor prognosis for the patient (Rahn *et al*., 2001). MUC1 staining, when restricted to the apical region was associated with a better prognosis than when MUC1 was found over the entire cell membrane and within the cytoplasm. Interestingly, it was found that delivery of MUC1 to the cell surface in Chinese hamster ovary (CHO) cells is absolutely dependent

on the addition of O-linked glycans to the core protein (Altschuler *et al*., 2000). In glycosylation-defective CHO cells, only half as much MUC1 was delivered to the cell surface when it was synthesized with shorter glycans as compared with MUC1 with normal glycans (Altschuler *et al*., 2000). MUC1 with shorter glycans was also internalized by clathrin-mediated endocytosis at twice the rate of MUC1 with normal glycans. This is not surprising considering that a fully glycosylated isoform can extend up to 500 nm above the cell surface, inhibiting packaging into clathrin-coated vesicles, which may be only 150 nm in diameter. MUC1 that was not transported to, and maintained at, the cell membrane accumulated within the cytoplasm (Altschuler *et al*., 2000). Thus aberrant glycosylation resulting in increased intracellular MUC1 may be important for the role of MUC1 as a contributor to malignant cell behaviour.

Although the MUC1 ectodomain, and in particular its glycosylation, is important in determining clathrin-mediated endocytosis, it appears that the MUC1 cytoplasmic tail also plays a role in modulating endocytosis. Kinlough *et al*. (2004) prepared a MUC1 chimera, where the ectodomain was replaced by the ectodomain of Tac, a cell surface glycoprotein that had been used previously in chimeric constructs to analyze C-terminal cytoplasmic targeting signals. Replacement of the MUC1 mucin-like ectodomain of 810 amino acids with the Tac ectodomain of 239 amino acids drastically altered the level of endocytosis (a 2.7 fold increase), as predicted. Four cytoplasmic tail tyrosine residues of the Tac-MUC1 chimera (Y8, Y20, Y46 and Y60) were selected to be individually mutated by virtue of the sequences surrounding them. The Y20 mutation reduced Tac-MUC1 endocytosis by 30% while the Y60 mutation reduced Tac-MUC1 endocytosis by 50%. The Y20 site (YHPM) represents, and was confirmed as a binding site for AP-2, which is known to link its associated proteins to clathrin. The Y60 site (YTNP) was confirmed as a binding site for growth factor receptor binding protein 2 (Grb2). The role of Grb2 in clathrin-mediated endocytosis has been characterized for the internalization and degradation of EGFR. Briefly, Grb2 is recruited to a src homology domain (SH) 2 on activated EGFR and thereby links the ubiquitin ligase Cbl to the receptor through interaction with its SH3 binding site. Grb2-Cbl complex binding to stimulated EGFR causes recruitment of the receptor to the edge of clathrin-coated pits (Stang *et al*., 2004).

It is thus hypothesized that a similar mechanism exists with respect to Grb2-mediated recruitment of MUC1 to clathrin-coated pits (Kinlough *et al*., 2004). It would therefore appear that MUC1 internalization is regulated by the glycosylation of the extracellular domain as well as by the interaction of the cytoplasmic tail with AP-2 and Grb2.

1.10 Human oesophageal squamous cell carcinoma (HOSCC) displays an exceptionally aggressive phenotype

Oesophageal squamous cell carcinoma is a common malignancy that exhibits an extremely poor prognosis (Nair *et al*., 2005). The 5-year survival rate of patients diagnosed with HOSCC is less that 10% (McCabe and Dlamini, 2005). This poor outlook is determined largely by the fact that patients present late, by which time the primary tumour has metastasized. HOSCC ranks as the ninth most common malignancy worldwide with the incidence varying dramatically among different regions (McCabe and Dlamini, 2005). High-risk areas include south-eastern Africa (primarily the area previously known as the Transkei), the "Asian oesophageal cancer belt" from eastern Turkey, through the southern former Soviet Union (Kazakhstan, Turkmenistan, Uzbekistan, Tajikistan), Iraq, Iran, into western and northern China, Hong Kong, Japan, as well as France, and parts of South America (for reviews see Lam, 2000, Kuwano *et al*., 2005). HOSCC in South Africa is the second most common cancer among all South African men combined, and the most common cancer in black males. In 2004, the incidence at Baragwanath hospital in Johannesburg, was reported to be one case per day (Isaacson, 2005).The Eastern Cape has recorded a rise in incidence of oesophageal cancer from 16 per 100 000 before 1970 to over 40 per 100 000 thereafter (Von Zeyneck, 1973, McCabe and Dlamini, 2005).

The striking variation in geographical distribution is thought to be a reflection of exposure to specific environmental factors (Kuwano *et al*., 2005). These factors are however, poorly defined. Two major risk factors are tobacco smoking and alcohol consumption. Other factors that may contribute to the pathogenesis of HOSCC are diets deficient in vitamins and protective antioxidants (lack of green leafy vegetables, citrus

fruit, micronutrients, zinc, riboflavin, vitamin A), intake of carcinogens and thermal injuries (acquired as a result of preference for hot drinks and soups) (Lam, 2000). Mycotoxins, nitrosyl compounds (contained in smoked foods) and possibly infection with human papilloma virus are also thought to be important in HOSCC pathogenesis (Lam, 2000, Kuwano *et al*., 2005).

1.11 A range of genes have been implicated in HOSCC pathology

Like other gastrointestinal carcinomas, HOSCC evolves through a series of well defined histological steps, culminating in metastatic disease (Stemmermann *et al*., 1994). The principal precursor lesion of HOSCC is epithelial dysplasia. Microscopically, this lesion represents an accumulation of atypical cells with nuclear hyperchromasia, abnormally clumped chromatin, and loss of polarity. HOSCC is then thought to develop through a progressive sequence from mild to severe dysplasia, to carcinoma *in situ*, and finally to invasive carcinoma. These tumours frequently present as fungating, ulcerating, or infiltrating lesions in the oesophageal epithelium (Stemmermann *et al*., 1994). Clearly, these changes are a phenotypic demonstration of the genetic and epigenetic events driving the progression towards an invasive HOSCC.

A number of genes have been implicated in the pathogenesis of HOSCC (for reviews see Lam, 2000, Lehrbach *et al*., 2003, Kuwano *et al*., 2005). These include (but are not limited to) genes already briefly mentioned, such as p53, pRb, cyclin D1, E-cadherin and EGFR. p53 and pRb are the 2 major pathways that control cell cycling. The p53 tumour-suppressor gene regulates cell cycle arrest, DNA repair and apoptosis and as such is considered the “guardian of the genome”. It is the most frequently mutated gene in all human malignancies (Hollstein *et al*., 1991). The incidence of p53 mutation in HOSCC is approximately 50%, and most of these mutations are point mutations. Overexpression of MDM2 (which inhibits p53 functioning), or inactivation of p14ARF (which suppresses MDM2 activity) also result in deactivation of the p53 pathway and are associated with carcinogenesis (Parenti *et al*., 1995, Kuwano *et al*., 2005).

The retinoblastoma gene product (pRb) negatively regulates transcription by forming a complex with the E2F transcription factor. When pRb is phosphorylated by the cyclin/cyclin dependent kinase (CDK) complex E2Fs are released, activating transcription and cell division. Deletions or mutations of pRb are common features of many tumours; however, the role of pRb in HOSCC is controversial with mutations being found in 0% to 100% of HOSCC patients, depending on the study (Lam, 2000). Cyclin D1 binds to and activates CDK4 or CDK6. The cyclin D1-CDK4/CDK6 complex phosphorylates pRb, freeing E2F and allowing progression of the cell through the cell cycle (Baldin *et al*., 1993). Overexpression of cyclin D1 is generally associated with amplification of the cyclin D1 gene. In HOSCC, amplification of cyclin D1 has been reported for between 23% and 65% of patients (Lam, 2000). In addition, there is some evidence to suggest that cyclin D1 gene amplification is predictive of a poor prognosis in human HOSCC (Nakagawa *et al*., 1995, Shamma *et al*., 1998).

The invasion suppressor gene, E-cadherin is down-regulated in numerous carcinomas including HOSCC (Pecina-Slaus, 2003). Importantly, reduction in the expression of E-cadherin in patients with HOSCC was shown to be strongly associated with post-operative blood borne recurrence, resulting in a poorer prognosis than those patients showing normal expression before surgery (Tamura *et al*., 1996). A more recent study, evaluating the relationship between E-cadherin expression and clinicopathological features in HOSCC, obtained similar results. Takeno *et al*. (2004) showed that patients with reduced E-cadherin expression correlated with tumour invasion. Moreover, they showed that examination of reduced E-cadherin expression is important in assessing biologic behaviour, including clinical outcome, in HOSCC.

1.12 Overexpression of the epidermal growth factor receptor is a common characteristic of HOSCC

Overexpression of the epidermal growth factor receptor in HOSCC is of particular interest considering that it has been implicated in MUC1 signalling (Schroeder *et al*., 2001). The EGFR is a transmembrane receptor tyrosine kinase that when activated by the

appropriate ligand, such as the epidermal growth factor (EGF) or transforming growth factor α (TGFα), triggers numerous growth-related (i.e. mitogenic) signalling pathways (for review see Normanno *et al*., 2006). The EGF ligand/receptor system is involved in early embryonic development and in the renewal of stem cells in normal tissues such as the skin, liver and colon (Salomon *et al*., 1990, Normanno *et al*., 2006). Deregulation of this system, often by overexpression of the receptor or mutation of the receptor to a constitutively active isoform, is associated with the pathogenesis of human cancer. Processes that are regulated by EGFR signalling and are important for tumour development include growth, differentiation, metastatic spread, survival and apoptosis (Yarden and Sliwkowski, 2001).

EGFR is overexpressed in numerous malignancies and particularly in HOSCC. In fact, HOSCC is considered a prototypic system for demonstrating amplification and overexpression of the EGFR gene (Stemmermann *et al*., 1994). EGFR is overexpressed in 29% to 92% of HOSCC tumour samples and cell lines, depending on the study (Ozawa *et al*., 1989b, Kuwano *et al*., 2005). Moreover, binding assays demonstrate that HOSCCs exhibit 10 times more EGFR than gastric cancer cells (Yano *et al*., 1991). EGFR overexpression in HOSCC correlates with the degree of dysplasia, the frequency of lymph node metastasis and in general with a poor prognosis (Yano *et al*., 1991, Kuwano *et al*., 2005). Hirai *et al*. (1998) noted that the 5-year survival rate of Japanese patients with HOSCC was much lower with a high expression of EGFR. Furthermore, a study of 14 HOSCC patients showed that EGFR overexpression was associated with a minimal response to chemoradiotherapy (Kuwano *et al*., 2005).

1.13 The mechanisms resulting in the aggressive HOSCC phenotype are not clearly defined

Oesophageal squamous cell carcinoma remains as one of the most difficult neoplasms to treat effectively, largely due to either local tumour invasion of surrounding tissue or to metastasis. Although a number of genes associated with HOSCC tumorigenesis have been identified (as discussed above), the actual molecular mechanisms governing the

aggressive behaviour characteristic of HOSCC remain undefined (Nair *et al*., 2005). In order to develop effective treatment and diagnostic strategies for HOSCC it will be essential to gain an understanding of the processes underlying HOSCC malignancy.

MUC1 is considerably dynamic and multi-faceted and has been associated with aggressive behaviour in numerous cancer types (Hattrup and Gendler, 2006). However, studies defining the expression and the potential roles of MUC1 in HOSCC are limited. One study has shown that normal squamous cell epithelium of the oesophagus expresses low levels of MUC1 at the apical membrane (Sagara *et al*., 1999). In HOSCC however, MUC1-specific immunohistochemistry indicated the presence of MUC1 within the cytoplasm as well as at the membrane (Sagara *et al*., 1999). Importantly, this study also indicated that MUC1 in HOSCC exhibited a different glycosylation pattern to that of MUC1 in normal oesophageal epithelium. This was demonstrated by the different affinities of 2 antibodies (assumed to be glycosylation dependent) for the MUC1 expressed in either the normal or HOSCC samples (Sagara *et al*., 1999). A second immunohistochemistry-based study demonstrated MUC1 expression in 32% of HOSCC samples (Kijima *et al*., 2001). A third study was conducted in China to determine the relationship between MUC1 expression in HOSCC and disease prognosis (Song *et al.,* 2003). In this case, 78.9% of specimens were positive for MUC1 immunostaining. Moreover, they came to the conclusion that the expression of MUC1 correlated negatively with patient survival, and proposed that MUC1 expression may play an important role in the invasion and metastasis of HOSCC.

It is proposed therefore to investigate the expression and potential roles of MUC1 in HOSCC, not simply because this knowledge is thus far severely limited, but because we hope it will give insight into a potentially important molecular mechanism contributing to the aggressive, malignant phenotype that is characteristic of HOSCC.

1.14 Specific aims and objectives

The specific aims and objectives of this study are detailed below and each aim refers to 5 HOSCC cell lines. The aims were to:

1) determine if the MUC1 gene is expressed.
2) determine if the MUC1 protein is present.
3) determine the distribution pattern of the MUC1 protein.
4) determine if the MUC1 cytoplasmic tail and β-catenin physically interact at the cell membrane.
5) investigate whether the association of MUC1 and β-catenin at the cell membrane is modulated by EGFR activation.
6) determine if β-catenin concentration at the cell membrane is modulated by EGFR activation.
7) determine if the MUC1 cytoplasmic tail is located in the nucleus.
8) determine if β-catenin is located in the nucleus.
9) investigate the possibility of a nuclear MUC1 cytoplasmic tail/β-catenin complex.
10) determine if nuclear β-catenin concentration is modulated by EGFR activation.
11) assess the gene expression of matrix metalloproteinase 7.
12) determine if the matrix metalloproteinase 7 protein is present.
13) establish if the matrix metalloproteinase 7 produced is active.

CHAPTER 2: THE POTENTIAL IMPLICATIONS OF MUC1 EXPRESSION IN HOSCC.

2.1 Introduction

MUC1 is a sialylated transmembrane glycoprotein with a large mucin-like domain consisting of 20-amino acid repeats rich in serines, threonines and prolines (Wesseling *et al*., 1996, for review see Gendler, 2001). The number of repeats varies from 30 to 90 as a result of genetic polymorphism, causing a variation in the length of the extracellular domain of 1000 to 2200 amino acids (Gendler *et al*., 1987). The large number of proline residues is thought to give the extracellular domain an extended structure, which becomes rigid as a result of the addition of O-linked carbohydrate side chains to the serines and threonines (Hilkens *et al*., 1992). Analysis by electron microscopy has shown that MUC1 protrudes 200-500 nm beyond the plasma membrane (Wesseling *et al*., 1995). In contrast, the extracellular domains of most other membrane molecules do not extend more than 35 nm above the plasma membrane (Wesseling *et al*., 1995). It has thus been proposed that MUC1 shields numerous proteins, and in particular cell adhesion molecules, from their ligands, thereby inhibiting their functioning.

Cell adhesion to the extracellular matrix is mediated largely by the integrin family of adhesion proteins (Danen, 2005). The inhibitory effects of MUC1 expression on integrin-mediated cell attachment were clearly demonstrated in a study conducted by Wesseling *et al*. (1995). They assessed melanoma cells that had been transfected with full length MUC1 cDNA and determined that a large proportion of the transfected cells no longer attached to the culture dish but grew in suspension. In addition, they showed that adhesion of the transfected cells to laminin, fibronectin, collagen type I and type II as well as to Matrigel was substantially reduced. Importantly, it was shown that involvement of the cytoplasmic tail in integrin-mediated cell adhesion was unlikely, as transfectants expressing a MUC1 construct with no cytoplasmic tail showed comparable inhibition of adhesion to integrin ligands. Wesseling *et al*. (1995) therefore suggest that the large

extended extracellular domain of MUC1 reduces the number of possible integrin-ligand encounters which, in turn, renders adhesion of the cell to ECM components difficult. A subsequent study provided an alternative mechanism for MUC1 inhibition of cellular adhesion, in this case, of E-cadherin mediated cell-cell adhesion. E-cadherin functions via homotypic interaction whereby an E-cadherin molecule on one cell binds to an E-cadherin molecule on an adjacent cell to form a homodimer. Wesseling *et al*. (1996) investigated the role of the MUC1 extracellular domain on the inhibition of E-cadherin-mediated cell-cell adhesion. They transfected a murine fibroblast cell line (L929), reliant on E-cadherin for cell-cell adhesion, with both full length and shortened MUC1 cDNA constructs. Results obtained in cell-cell aggregation assays indicated that MUC1 expression can override E-cadherin mediated cell-cell adhesion by a mechanism that is largely dependant on the length of the MUC1 backbone. Their data provide support for the theory that the extended extracellular domain of MUC1 inhibits cellular adhesion via steric interference of smaller adhesion molecules.

In contrast to MUC1 inhibition of integrin functioning, where only the extracellular domain of MUC1 plays a role, MUC1 inhibition of E-cadherin adhesion involves the cytoplasmic tail as well as the extracellular domain. The contribution of the MUC1 cytoplasmic tail to the disruption of E-cadherin mediated adhesion will be dealt with in detail in Chapter 3.

As well as possessing anti-adhesive effects, MUC1 can promote cell adhesion in some cases. Extravasation and vascular migration of malignant cells involves the interaction of selectins, cell adhesion molecules at the surface of endothelial cells lining the blood vessels, with corresponding carbohydrate ligands on the surface of malignant cells (Kannagi, 2004). Importantly, malignant transformation and overexpression of MUC1 is usually associated with abnormal glycosylation of MUC1, which results in the synthesis and expression of altered carbohydrate determinants, such as sialyl Lewis^{x} and sialyl Lewis^{a}. These sialyl Lewis epitopes are selectin ligands and are thus thought to be associated with the haematogenous metastasis of cancer (Hanski *et al*., 1993, Zhang *et al*., 1996). MUC1 also acts as a ligand for ICAM-1, a cell adhesion molecule expressed

by activated endothelial cells (Regimbald *et al*., 1996). MUC1 can therefore promote heterotypic cell-cell adhesion (to ICAM-1 positive endothelial cells) and may facilitate metastasis by taking advantage of ICAM-1-mediated migratory pathways which are intended for transendothelial and stromal leukocyte movement (Rahn *et al*., 2001). Moreover, a more recent study demonstrated that the MUC1/ICAM-1 interaction triggers an intracellular oscillatory calcium-based signal in MUC1-expressing epithelial cells (Rahn *et al*., 2004). The oscillatory response is strongly suggestive of a definite signal as the frequency and amplitude of calcium oscillations generated during the experiment are thought to encode instructions to activate specific proteins. Possible downstream calcium-sensitive targets of this signal include gelsolin, calpain and calmodulin, which are involved in cytoskeletal restructuring, focal adhesion disassembly, and cell contraction (Rahn *et al*., 2004). Thus, the MUC1/ICAM-1 interaction results in a calcium-based pro-migratory signal that may enhance the metastatic potential of MUC1-expressing epithelial cells.

The modulation of cellular adhesive characteristics by MUC1 is clearly an important aspect to consider when looking at the potential roles of MUC1 in the context of cancer. However, it is by no means the only contribution of MUC1 to the transformed behaviour of tumorigenic/metastatic cells. Mucins, including MUC1, are intimately involved in cell protection; normally expressed by simple epithelia lining ducts, they protect cells from proteolytic degradation and constitute a barrier against infection (Hollingsworth and Swanson, 2004). It has thus been suggested that cancer cells may use mucins, and in particular MUC1, in much the same way as normal epithelia, to protect from adverse growth conditions and to control the local microenvironment during invasion and metastasis (Patel *et al*., 2005). This concept, of MUC1-mediated cellular protection, is reinforced by the observation that apical restriction is lost in cancer cells and MUC1 is located over the entire cell surface, further enhancing its protective role.

MUC1 is thus a dynamic protein, as depending on context it may confer either anti-adhesive or adhesive properties to cells in which it is overexpressed. The implications of this dynamic approach to cellular adhesion are substantial, considering that the adhesion

properties of neoplastic cells play a pivotal role in the development and progression of the malignant phenotype. Reduced cell-ECM adhesion allows neoplastic cells to circumvent the control of differentiation induced by the normal extracellular environment, while reduced intercellular adhesion allows malignant cells to escape from their site of origin and acquire a more motile and therefore invasive phenotype (Harington and Syrigos, 2000). On the other hand, MUC1-mediated increased adhesion to vessel walls allows neoplastic cells to make use of the lymphatic and vascular systems to migrate to distant sites (Zhang *et al.,* 1996). The contribution of MUC1 to cell survival, in terms of its integral protective function and its anti-apoptotic role, is also important in conferring a possible "metastatic advantage".

Investigations into MUC1 expression have thus far primarily been limited to those on cancers derived from simple epithelia, as opposed to stratified epithelia. This study examines the expression and cellular localization of MUC1 in 5 cell lines derived from moderately differentiated human oesophageal squamous cell carcinomas.

2.2 Methods & Materials

2.2.1 Cell lines

Five South African moderately differentiated human oesophageal squamous cell carcinoma cell lines, each with metastatic capabilities, were obtained from the Cell Biology Laboratory, School of Molecular and Cell Biology, University of the Witwatersrand. The cell lines are designated WHCO1, WHCO3, WHCO5, WHCO6 (Veale and Thornley, 1989) and SNO (Bey *et al*., 1976). Human embryonic kidney cell line, HEK293 (Graham *et al*., 1977), was kindly donated by Dr Clem Penny, Medical School, University of the Witwatersrand. The cells were maintained in Dulbecco's Modified Eagles Medium (DMEM)/Hams F12 (3:1) supplemented with 10% Foetal Calf Serum (FCS) in an atmosphere of 5% carbon dioxide (CO_2) at 37°C. Cells were harvested using trypsin/ethylenediaminetetra-acetic acid (EDTA) (see Appendix 7.1).

2.2.2 Antibodies

Monoclonal mouse anti-MUC1 (VU-4-H5) antibody (Zymed®) was used for the indirect immunofluorescence procedure as well as for the western blotting. Goat fluorescine isothiocyanate (FITC)-conjugated anti-mouse IgG (Serotech) antibody was used as the secondary antibody for the indirect immunofluorescence procedure, while horseradish peroxidase (HRP)-conjugated rabbit anti-mouse IgG was used as the secondary antibody for the western blotting. The anti-MUC1 antibody is directed against a non-glycosylated 60-mer triple tandem repeat on the MUC1 polypeptide core.

2.2.3 RNA extraction

Total RNA was extracted from all cell lines using Trizol® Reagent (Life Technologies, GibcoBRL). Trizol is a monophasic solution of phenol and guanidine isothiocyanate that maintains the integrity of RNA while disrupting cells and dissolving cell components. Cells at 80% confluency in 10 cm Nunc™ dishes (1 dish per cell line) were washed 3

times in phosphate buffered saline (PBS) pH 7.6 (see Appendix 7.2), scraped, and transferred to a sterile eppendorf tube. Cells were lysed by the application of 1 ml Trizol followed by a brief vortex. 200 µl chloroform was added to the lysate, which was then hand-shaken briefly before being centrifuged at 12 000 x g and 4°C for 15 minutes (min). The upper aqueous phase was transferred to a sterile tube, and the RNA was precipitated with the addition of 500 µl of isopropanol. The sample was centrifuged at 12 000 x g and 4°C for 10 min, and then washed with 75% ethanol, air-dried and resuspended in 50 µl nuclease free distilled water (dH_2O) (Sigma). Samples were stored at -70°C.

2.2.4 Agarose gel electrophoresis

A 1% agarose gel was prepared by the addition of 0.3 g agarose to 30 ml TAE (see Appendix 7.3). The mixture was heated in the microwave to dissolve the agarose. 1.5 µl of ethidium bromide (EtBr) (see Appendix 7.3) was added once the mixture had begun to cool. The gel mixture was then poured into a Sigma-Aldrich MiniZ33 Horizontal Gel Caster, a 10-well comb was slotted into the gel which was then left to set at room temperature for 45 min. The comb was pulled out and the gel was placed in the Sigma-Aldrich Electrophoresis Unit, making sure the gel was fully submerged in TAE. All samples were prepared as a 1:1 ratio of RNA:loading buffer (see Appendix 7.3), or in the case of the 1Kb plus DNA ladder™ (GibbcoBRL), 1 kb ladder:loading buffer (also 1:1). After loading the samples into the wells, the gel was electrophoresed at 72 V for 1 hour. The gel was viewed on an ultraviolet (UV) transilluminator.

2.2.5 cDNA synthesis

RNA was reverse transcribed into cDNA using Moloney Murine Leukemia Virus Reverse Transcriptase (MMLV-RT). 1 µl of RNA from each cell line, each in a separate eppendorf tube, was mixed with 2 µl random primers (Roche) and incubated at 70°C for 5 min. 5 µl buffer (5X), 0.6 µl RNAsin, 2 µl dNTP mix, 1 µl MMLV-RT and 12.4 µl dH_2O (Sigma) (see Appendix 7.4) were added to each tube. The reaction mixture was then incubated for a period of 1 hour at 37°C. The reaction was stopped by heating the

mixture to 90°C for 5 min. Tubes were placed immediately on ice. 25 µl of phenol:chloroform (25:24) was added to each tube before vortexing for 10 seconds and then centrifuging at 12 000 x g for 5 min at room temperature. The aqueous phase was removed and placed in a sterile eppendorf tube. An equal volume of chloroform was added to each tube before vortexing for 10 seconds and then centrifuging at 12 000 x g for 5 min at room temperature. The aqueous phase was removed and transferred to a sterile eppendorf to which an equal volume of chloroform was added. The samples were vortexed and centrifuged as above and the aqueous phase again transferred to a sterile tube. Three times the volume of 100% ethanol and one tenth the volume of 3 M sodium acetate pH 5.2 were added (giving a final concentration of 25% ethanol and 0.3 M sodium acetate). The cDNA was precipitated overnight at -20°C. Precipitated cDNA was centrifuged at 12 000 x g and 4°C for 20 min, the supernatant was removed and the pellet air-dried before being resuspended in 10 µl nuclease free dH_2O (Sigma). 2 µl of cDNA was run on a 1% agarose gel (as above) to ensure RNA had been successfully reverse transcribed.

2.2.6 Reverse transcriptase-polymerase chain reaction (RT-PCR)

It is important to note that RT-PCR was conducted as a 2-step system whereby the reverse transcription had already been carried out (see cDNA synthesis above). The following primers, generated against the cytoplasmic tail of MUC1 using the interactive primer design program, GeneFisher (http://bibiserv.techfak.uni-bielefeld.de/genefisher), were used for PCR analysis (see Appendix 7.5 for sequence input and parameters):

Forward 5′ ACGGAAGCAGCCTCTCGA 3′ (MUC1-F)
Reverse 5′ GCCCCTACAAGTTGGCAGA 3′ (MUC1-R)

The reaction mixtures were prepared on ice under sterile conditions. Each PCR tube was set up to contain: 5 µl PCR buffer (10X) (Roche) (see Appendix 7.6), 1 µl dNTP mix, 1 µl MUC1-F, 1 µl MUC1-R, 5 µl Taq polymerase (Roche), 1 µl template (1µl cDNA, representative of each cell line) and 36 µl dH_2O (final volume 50 µl). Samples were

amplified for 30 cycles under the following conditions: 1 min at 95°C (denaturing), 1 min at 55°C (primer annealing) and 1 min 30 seconds at 72°C (primer extension). Cell line HEK293 is known not to express MUC1 and was thus included in this experiment to serve as a negative control, to confirm the specificity of the reaction (Wang *et al.,* 2004). A water control, containing no template cDNA, was used as an additional negative control. PCR products were electrophoresed on a 1% agarose gel as above.

2.2.7 Preparation of whole-cell lysates

HOSCC cells at 80% confluency (1 dish per cell line) were washed 3 times in PBS, before being scraped and transferred to a sterile eppendorf tube. 200 µl of Laemmli lysis buffer (Laemmli, 1970) pH 6.8 (see Appendix 7.7) was added to the cells before briefly vortexing and boiling for 5 min. Samples were centrifuged at 12 000 x g for 5 min at 4°C before being stored at -20°C.

2.2.8 Protein estimation

Estimation of protein concentration was carried out according to Bramhall *et al.* (1969). Whatman filter paper was cut to fit into a glass dish. The filter paper was washed in distilled water for 30 min and dehydrated by rinsing in 95% ethanol (5 min) followed by 99.99% ethanol (5 min) and then acetone (5 min). The filter paper was air-dried in a fume hood. Cell lysates (3 µg) (prepared above), as well as bovine serum albumin (BSA) samples of known concentration (2 µg/µl BSA in lysis buffer) equal to 1 µg, 3 µg, 6 µg, 12 µg, 16 µg and 20 µg, were spotted onto the filter paper. Spots were air-dried and placed in tri-chloroacetic acid (TCA) (see Appendix 7.8) for 40 min, in order to precipitate the protein onto the filter paper. The filter paper was then placed in Coomassie Blue (see Appendix 7.8) for 1 hour, before being destained (see Appendix) for 2 hours. The filter paper was air-dried and protein spots cut out, each was placed in 5 ml elution solution (see Appendix 7.8) to remove the protein stain from the filter paper. The absorbance of each solution was determined using a Beckman DU-64 spectrophotometer at a wavelength of 596 nm. A standard curve of absorbance versus protein concentration

was constructed using readings from the samples of known concentration. Protein concentrations of the unknown samples were then determined using the standard curve.

2.2.9 Polypeptide resolution by sodium dodecyl sulphate polyacrylamide gel electrophoresis (SDS-PAGE)

Each protein sample (10 µg) was resolved using the Laemmli (1970) discontinuous buffer system on a 10% sodium dodecyl sulphate (SDS) polyacrylamide gel. The Mighty Small™ SE245 Dual Gel Caster (Hoefer Scientific) was used to construct the gel. The 10% separating gel was prepared by adding together: 1 g acrylamide, 2.5 ml separating buffer, 400 µl SDS solution, 400 µl *N′,N′*,-methylenebis-acrylamide (bis) and dH_2O to make the volume up to 10 ml (see Appendix 7.9 for all solutions used for SDS-PAGE). The gel solution was mixed and immediately prior to pouring, 180 µl ammonium persulphate (APS) and 25 µl of *N′,N′,N′,N′*-tetramethylene-diamine (TEMED) was added. A thin layer of 0.2% SDS in dH_2O was poured on top of the gel to exclude air and thereby enhance polymerization. The separating gel was allowed to polymerize at room temperature (approximately 20 min). Unpolymerized gel and SDS was removed before adding the stacking gel. The 5% stacking gel was prepared by adding together: 0.5 g acrylamide, 2.5 ml stacking buffer, 400 µl SDS solution, 400 µl bis and dH_2O to make the volume up to 10 ml. 180 µl APS and 25 µl TEMED were added immediately prior to pouring. A 10-well comb was placed between the gel plates and the gel allowed to polymerize (approximately 20 min). Once polymerized, the gel was placed in the Mighty Small™ Electrophoresis Unit which contained reservoir buffer pH 8.3. The comb was removed and the wells filled with reservoir buffer. PageRuler™ Prestained Protein Ladder (Fermentas) (3 µl) was loaded into the first lane as the molecular weight marker. Whole-cell lysates (10 µg) representative of each cell line were loaded in adjacent wells. The gel was electrophoresed at a constant current (25 mA) for 1 hour. Resolved protein was visualized by staining the gel with Coomassie Blue for 1 hour and then destaining in methanol/acetic acid (see Appendix 7.9) for 1 hour. The gel was scanned using a Hewlett Packard ScanJet 5200c.

2.2.10 Western Blot Analysis

Each protein sample (10 μg) was separated on a 10% SDS-PAGE gel, as above. Resolved protein was transferred to Nitroband nitrocellulose membrane (MSI) using a Bio-Rad Criterion™ Blotter (Bio-Rad) containing western blot transfer buffer pH 8.3 (4°C) (see Appendix 7.10 for all western blot solutions) for 2 hours. The membrane was then washed three 3 in PBS and kept in PBS overnight at 4°C. The following day, the membrane was blocked in a casein-based blocking buffer (Blotto) for 1 hour at room temperature. Thereafter, the membrane was incubated in mouse anti-MUC1 (1:1000) for 1 hour at room temperature, washed 6 times for 5 min each in PBS, before being incubated in secondary antibody, horseradish-peroxidase (HRP)-conjugated anti-mouse IgG (1:5000), for 1 hour at room temperature in the dark. Unbound secondary antibody was removed by washing in PBS (6 times for 5 min each). The secondary antibody was detected by placing the membrane in a solution of peroxide:luminol (1:1) from the Supersignal® West Pico Chemiluminescent Kit (Pierce), for 5 min in the dark, and then exposing it to Hyperfilm™ MP autoradiography film (Amersham) for 2 min. (Note: All antibodies were diluted in PBS.)

2.2.11 Indirect Immunofluorescence

Cells from exponentially growing cultures were seeded onto sterile glass cover-slips. Cells were allowed to settle and adhere to the cover-slip for at least 16 hours. The following day, tissue culture media was aspirated and cells were rinsed 3 times in PBS prior to being fixed in 4% paraformaldehyde (see Appendix 7.11) for 30 min at room temperature. Cells were rinsed 5 times in PBS and were then permeabilized in 0.25% Triton X-100. The cells were rinsed twice in PBS and then the cover-slips were dipped into dH_2O. The cover-slips were air-dried briefly and then areas of cells were delineated using a DAKO pen. Cells were rehydrated with PBS for 30 min before incubation in anti-MUC1 antibody (20 μl of 1:500 per well) for 1 hour at room temperature. Samples were rinsed 6 times (1 min for each wash) in PBS. 20 μl FITC-conjugated anti-mouse antibody (1:500) was applied to each well, also for 1 hour at room temperature. The negative

control was treated as above; however, no primary antibody was applied to the cells. After removing unbound secondary antibody (6 one min PBS washes) 10 µl elvanol (see Appendix 7.11), containing anti-bleach (P-phenylenediamine), was added to each well. Glass slides were placed on top of each cover-slip. Cells were viewed immediately under a Zeiss LSM 410 confocal microscope (FITC excitation wavelength 490 nm, emission wavelength 525 nm).

2.3 Results

2.3.1 MUC1 expression in 5 moderately differentiated HOSCC cell lines

RNA extraction was assessed on a 1% agarose gel prior to cDNA synthesis. Bands at 650 bp and 1500 bp (Figure 2.1) represent the 18s and 28s ribosomal RNA subunits respectively, and indicate that the extraction was successful (see Appendix 7.12 for standard curve). cDNA was subsequently assessed on an agarose gel, and produced a smear, due to the presence of a multitude of transcripts of different lengths, that is characteristic of successful reverse transcription of RNA into cDNA (Figure 2.2). The presence of a 400 bp fragment (see Appendix 7.12 for standard curve) in lanes corresponding to the HOSCC cell lines is evidence that each of those 5 HOSCC cell lines positively express MUC1 (Figure 2.3). The lack of non-target fragments and smears is a good indication that the reaction was highly specific and well optimized. Lanes representing HEK293 and water-control reactions did not contain a 400 bp fragment, or any other fragment, further confirming the specificity of the reaction.

2.3.2 MUC1 protein isoforms in HOSCC cell lines

The presence of the MUC1 protein in 5 HOSCC cell lines was determined by western blotting. Resolution of whole-cell lysates, prior to western blot analysis, indicated that the extraction and the protein estimation procedures were successful. Each lane of the SDS-PAGE gel (Figure 2.4) appeared to have a similar distinct banding pattern (rather than a smear) as well as similar concentrations of protein, as demonstrated by the same degree of Coomassie Blue staining in each lane. (See Appendix 7.13 for standard curve generated during protein estimation). Western blotting generated multiple bands in all lanes, representative of different MUC1 isoforms, or variants, in each cell line (Figure 2.5). The MUC1 isoforms ranged considerably in terms of their molecular weight. However, the 4 most distinct isoforms (indicated using blue arrows) are all greater than 70 kDa, with 2 of those isoforms being greater in size than the largest molecular weight marker of 170 kDa. (See Appendix 7.14 for standard curve of relative molecular weight

versus distance migrated). All cell lines exhibit the same isoforms. Visual assessment indicates that WHCO5 exhibits a marginally darker banding pattern, potentially indicating a slightly higher MUC1 concentration, when compared to the other cell lines.

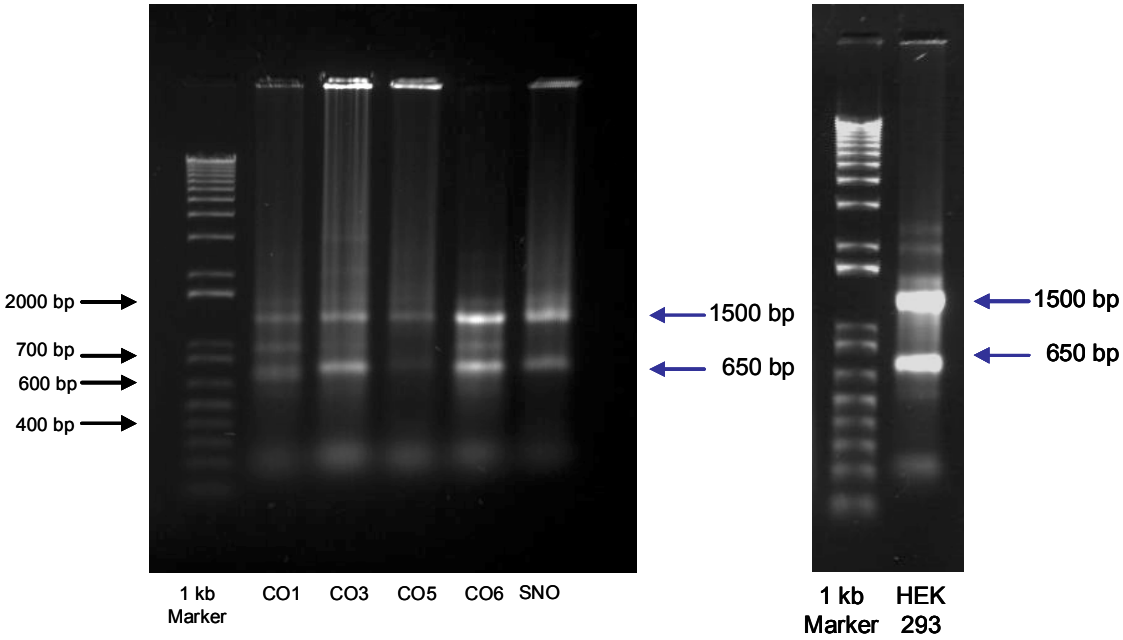

Figure 2.1: RNA extracts from 5 HOSCC cell lines and a human embryonic kidney (HEK) cell lines. RNA samples were electrophoresed on a 1% agarose gel. Bright bands at 1500 bp and 650 bp indicate that the RNA extraction was successful. CO1=WHCO1, CO3=WHCO3, CO5=WHCO5, CO6=WHCO6

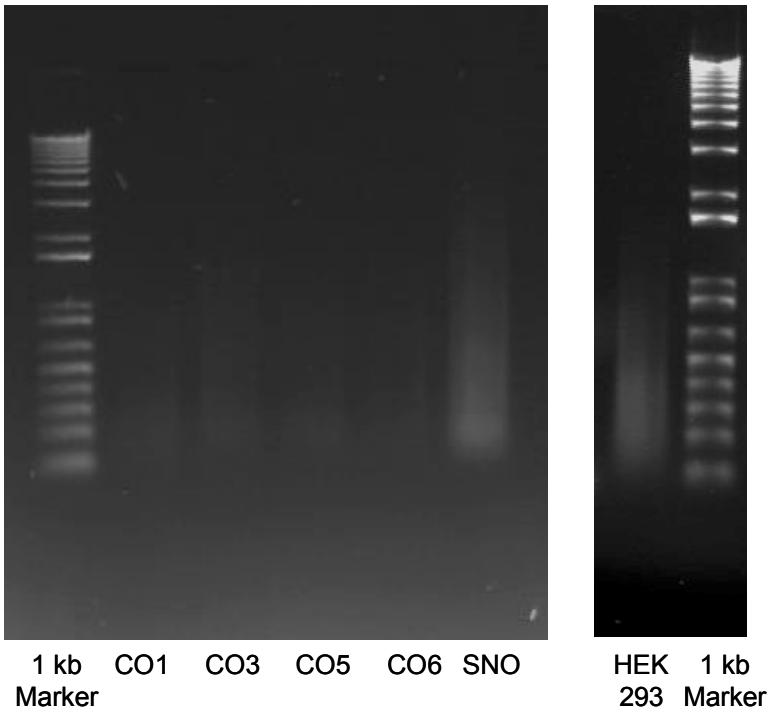

Figure 2.2: cDNA was synthesized by reverse transcription of mRNA. Numerous cDNA transcripts of varying lengths result in a characteristic smear when electrophoresed on a 1% agarose gel. CO1=WHCO1, CO3=WHCO3 etc.

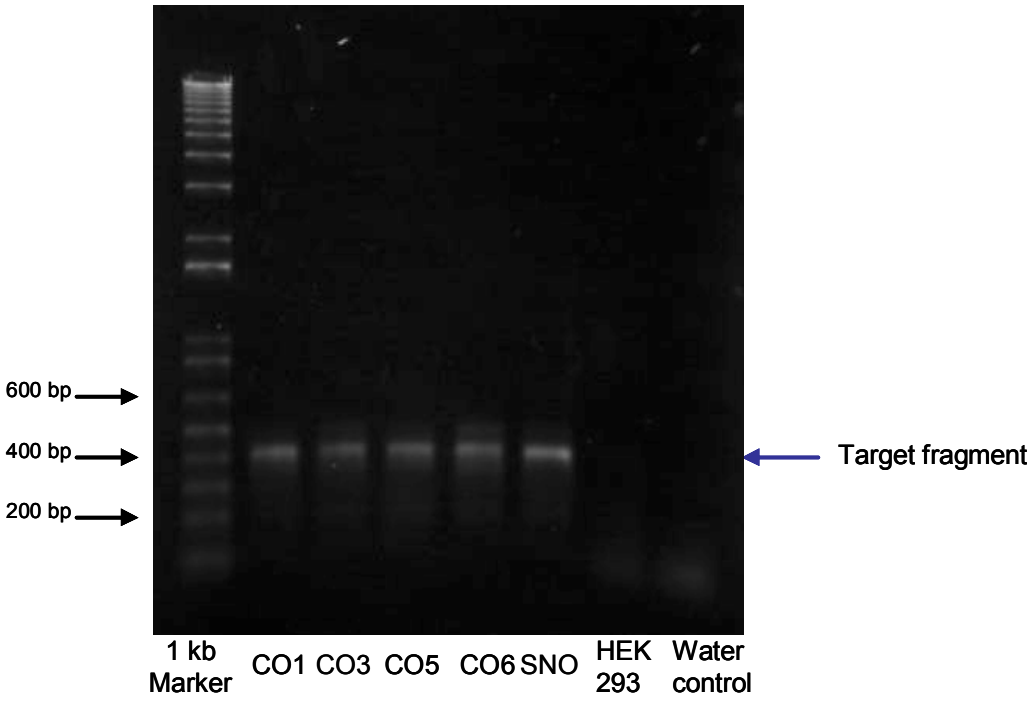

Figure 2.3: MUC1-specific RT-PCR was conducted using cDNA template from 5 HOSCC cell lines. The presence of a 400 bp target fragment in lanes representative of each of those HOSCC lines is indicative of positive MUC1 expression. The absence of a band in lanes representative of HEK293 cells and the (template-free) water-control confirms the specificity of the reaction. CO1=WHCO1, CO3=WHCO3 etc.

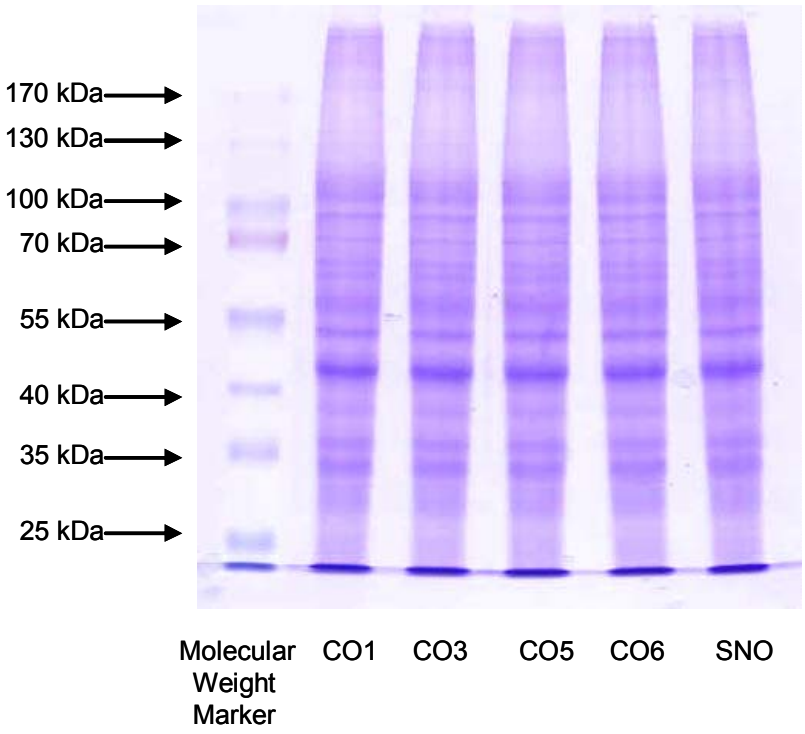

Figure 2.4: Whole-cell lysates from HOSCC cell lines were analyzed by 10% SDS-PAGE. The presence of multiple bands of equal intensity across lanes representative of each cell line indicates that the extraction procedure was successful and that the protein estimation was accurate. CO1=WHCO1, CO3=WHCO3 etc.

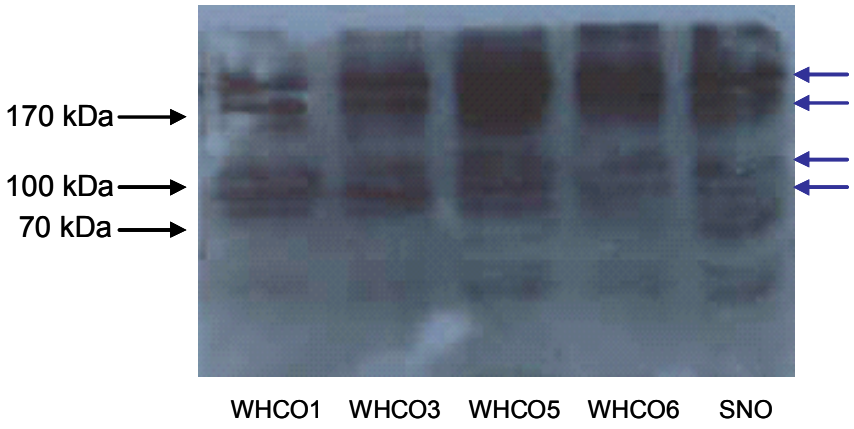

Figure 2.5: MUC1-specific western blot. Whole-cell lysate (15µg) was resolved using 10% SDS-PAGE, and then transferred to nitrocellulose membrane. The membrane was then immunoblotted using an antibody generated against the tandem repeat region of the MUC1 extracellular domain (mouse VU-4-H5). The secondary antibody was goat HRP-conjugated anti-mouse IgG. Multiple bands indicate the presence of a number of MUC1 protein isoforms in whole-cell extracts representative of all 5 HOSCC cell lines investigated. Blue arrows indicate the 4 major MUC1 isoforms.

2.3.3 Cellular distribution of MUC1 in HOSCC cell lines.

In healthy epithelia, MUC1 expression is limited to the apical borders of cells lining the lumen, in these HOSCC cell lines however, apical restriction is lost, and MUC1 is present over the entire cell surface as well as in the cytoplasm (Figures 2.6 and 2.7). In order to clarify the use of terminology, it must be stated that while the reactions producing the immunofluorescence images are not "staining" in the histological sense, they are commonly, and here, referred to as "staining".

Figure 2.6a (WHCO1) provides a clear illustration of loss of polarization. MUC1 specific immunofluorescent staining is bright around the entire cell membrane, and in addition, there is a substantial amount of staining within the cytoplasm. There are small, but highly distinct clear patches apparent in the cells (see Figure 2.6b for a higher magnification). These small clear patches are considerably smaller than the nucleus and are likely to be as a result of stringent exclusion of the extracellular domain of MUC1 (against which the antibody is directed), from the nucleoli (see red arrow).

WHCO3 (Figure 2.7, see arrow) shows a pattern of MUC1 expression similar to that of WHCO1, with MUC1 being expressed around the entire cell membrane in conjunction with visible staining in the cytoplasm. WHCO6 (Figure 2.7), like WHCO1 and WHCO3, demonstrates MUC1-specific staining over the cell membrane. What is not apparent in these images however, is the distribution of MUC1 within a colony of cells. The large colony of WHCO5 cells exhibits staining predominantly around the outside of the colony. There does however appear to be some staining around the membrane of cells within the colony (see WHCO5 red arrow), although it is not distinct. Some cells in the colony exhibit small clear patches (see WHCO5 yellow arrow), similar to those seen in Figure 2.6b, perhaps also indicating exclusion of the MUC1 extracellular domain from the nucleoli in this cell line.

SNO (Figure 2.7) exhibits strong circumferential staining of all cells within the colony. Strong staining is seen both at cell-cell junctions (see SNO red arrow) as well as in the

absence of cell-cell junctions (i.e. around the outside of the colony) (see SNO yellow arrow). Here, as in Figure 2.6a, a clear demonstration of loss of polarization is observed, with MUC1 being expressed over the entire cell surface.

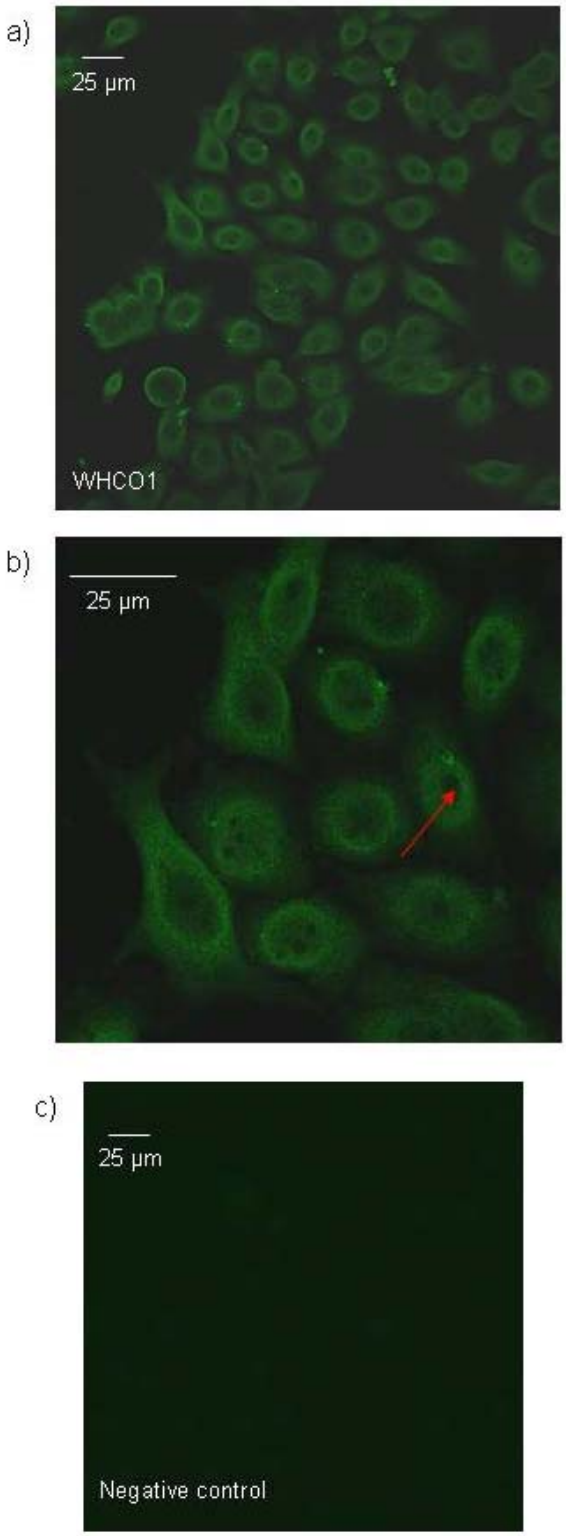

Figure 2.6: MUC1 cellular distribution was investigated by indirect immunofluorescence using an antibody directed against the tandem repeat region of the MUC1 extracellular domain. a) Bright staining around the entire cell membrane of WHCO1 cells shows that polarization has been lost in these cells. Interestingly, MUC1 also appears to be localized (to a lesser degree) to the cytoplasm. However, there appears to be strict exclusion of the MUC1 extracellular domain from the nucleoli (red arrow). b) Magnification of (a). c) Negative control.

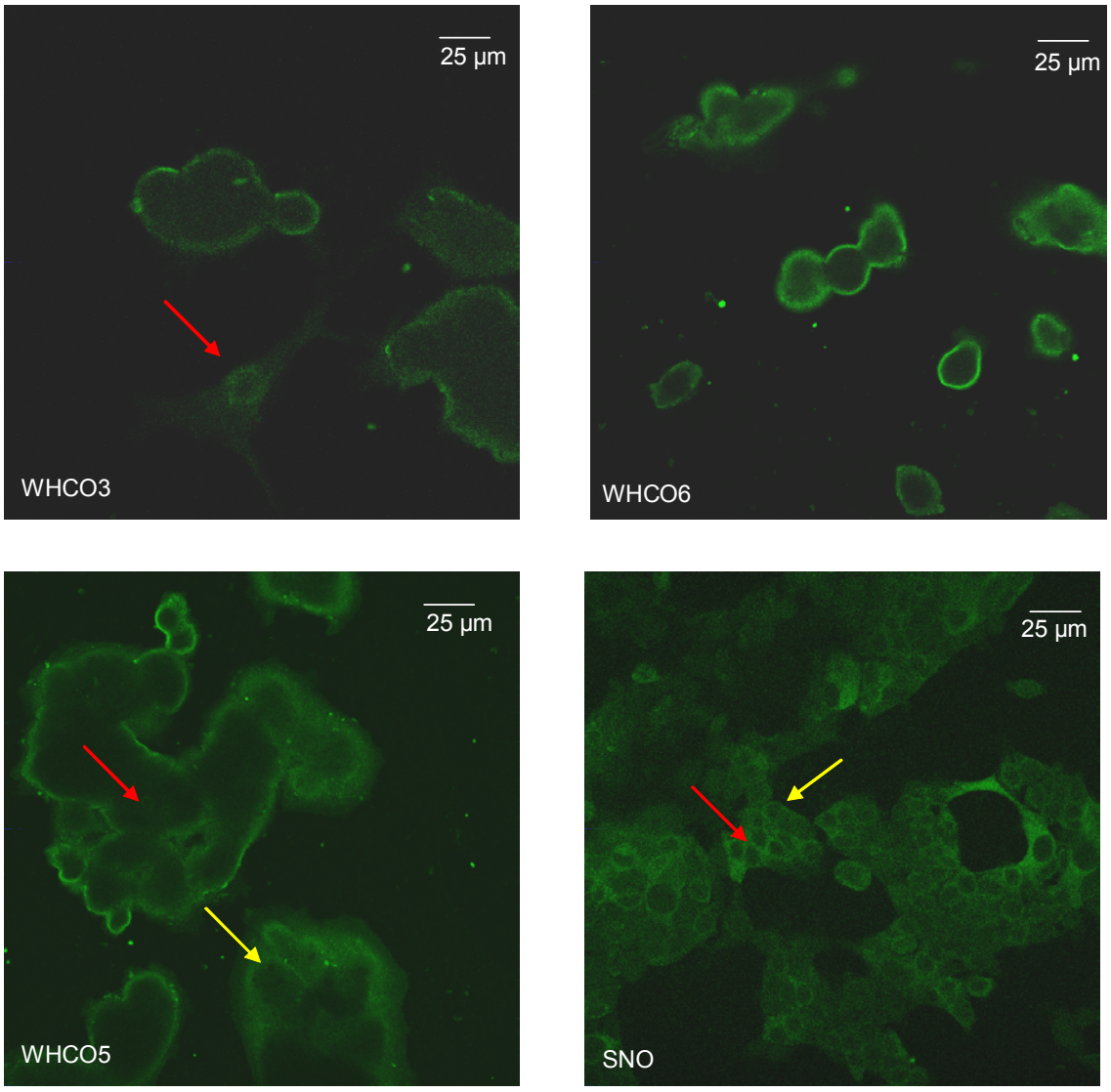

Figure 2.7: MUC1-specific indirect immunofluorescence was conducted on HOSCC cell lines. Arrows indicate regions or cells of interest. WHCO3 and WHCO6 generated a similar pattern of binding as was seen for WHCO1. MUC1 is located around the entire cell membrane and to a lesser degree within the cytoplasm. The large colonies of cells representing WHCO5 show MUC1-specific staining primarily around the outside of the colony. SNO cells exhibit staining over their entire cell membrane, including at cell-cell junctions.

2.4 Discussion

MUC1 expression has a distinct clinicopathological association with metastasis and poor clinical outcome in a variety of tumours (Taylor-Papadimitriou *et al*., 1999, Satoh *et al*., 2000). Here, we demonstrate that MUC1 is expressed, and that the MUC1 protein is present, in 5 moderately differentiated human oesophageal squamous cell carcinoma cell lines.

The data presented indicate that the MUC1 gene is expressed in all of the 5 HOSCC cell lines investigated. The question thus becomes: what is controlling the expression of MUC1 in these HOSCC cells? Although positive MUC1 expression has been established in a number of carcinomas and haematoligic malignancies, the mechanism by which MUC1 expression is controlled is not clearly understood. In some B-cell lymphomas MUC1 overexpression is activated by a specific chromosomal translocation, whereby the MUC1 gene is brought into the vicinity of the Ig heavy chain enhancer (Gendler, 2001). This event seems restricted to B-cell lymphomas and has not been noted in any other cancers. Considering that this mechanism has been limited to B-cell lymphomas it is not likely to play a role in MUC1 expression in these HOSCC cells.

Activation by signal transducers and activators of transcription (STATs) may present a more likely mechanism for MUC1 expression in HOSCC. STAT1 and STAT3 in particular, have been noted to bind to a STAT-binding site in the MUC1 promoter in breast carcinomas (Gaemers *et al*., 2001). Constitutive activation of STATs is a phenomenon common in breast carcinomas which is a cancer-type where MUC1 is overexpressed in over 90% of cases. It is therefore possible that increased STAT activity contributes to the overexpression of MUC1 in breast carcinomas. Interestingly, activation of EGFR, which is known to be highly overexpressed in these particular HOSCC cell lines, as well as in HOSCC in general, has been shown to induce STAT1 and STAT3 activation in oesophageal keratinocytes (Andl *et al*., 2003). It is therefore possible that in these cell lines EGFR stimulation triggers MUC1 expression via STAT activation.

In addition to containing a STAT-binding site, the MUC1 promoter contains potential binding sites for a number of other transcriptional regulators, among them Sp-1, AP1-4, Nuclear Factor-1, Nuclear Factor-κB, an E-box, GC-boxes, as well as oestrogen and progesterone receptor sites (Gendler, 2001). It is thus possible that increased activity of any of these transcriptional regulators, or a combination thereof, could contribute to MUC1 expression in these HOSCC cell lines. MUC1 gene duplication has not been reported to occur in any other cancer-types and is therefore unlikely to be the cause of MUC1 expression in these cell lines.

The presence of numerous bands in each lane of the western blot indicates that there may be a number of MUC1 variants or isoforms present in the HOSCC cells. Nine different MUC1 splice variants have previously been isolated, these are MUC1 A, B, C, D, X, Y, Z, REP and SEC (Patton *et al*., 1995, Gendler, 2001). Six of these splice variants (A, B, C, D and REP) may be contributing to the numerous bands detected in the western blot. Variants X, Y and Z, however, would not be detected as they lack the entire tandem repeat domain, which is required for binding of the particular antibody used in this study. Although MUC1 SEC lacks the transmembrane domain and is therefore secreted (hence the name SEC), some may remain intracellularly and may therefore be detected in the whole-cell lysates. In addition to splice variants, further MUC1 variants are created both through genetic polymorphisms, where a single allele determines the number of tandem repeats in the MUC1 backbone, as well as through differential glycosylation of each of those tandem repeats (Patton *et al*., 1995). Numerous MUC1 variants can therefore be produced via a combination of alternative splicing, a variable number of tandem repeats and differential/aberrant glycosylation. It is possible however, that some bands are due to non-specific binding of the antibody to other proteins, especially when considering the lower molecular weight bands, as even the smaller splice variants, when under-glycosylated, would not be expected to be under 120 kDa (Kinlough *et al*., 2004). However, binding of the same antibody in the immunocytochemistry does not appear to exhibit random binding, and staining matched previous reports, indicating that the antibody is in fact specific to MUC1.

MUC1 expression in cancer cells is most often accompanied by aberrant glycosylation and it appears that MUC1 expression in these cells is not an exception. Providing evidence for this notion is the fact that the antibody used here binds only to an under-glycosylated, and therefore aberrantly glycosylated, epitope in the tandem repeat domain. The specificity of the antibody for the under-glycosylated epitope has been clearly demonstrated by Zymed®, the manufacturer of the antibody, as well as by independent experimentation (Schol *et al*., 1998). Aberrant, and specifically under-, glycosylation, has been reported to expose sialyl Lewis^{x} and sialyl Lewis^{a} determinants, that act as ligands for selectins (Moniaux *et al*., 2004). This is significant in terms of the role selectin binding may play in enhancing the metastatic potential of the cells, as discussed earlier. Thus on one hand aberrant glycosylation may give the cells a metastatic advantage by allowing them to migrate along the endothelium of the blood vessels (Kannagi, 2004). On the other hand, however, exposure of novel epitopes may alert the immune system and cells expressing that particular epitope will be targeted for destruction, obviously inhibiting metastasis (von Mensdorff-Pouilly *et al*., 2000, Kontani *et al.,* 2001). However, as has been previously discussed, the interaction between MUC1 and the immune system is considerably more complex than the above statement would suggest. Some groups believe that MUC1, far from alerting the immune system, physically shields invading cells from immune recognition and subsequent destruction by the cellular arm of the immune system (Taylor-Papadimitriou and Burchell, 2002). Other groups suggest that MUC1 actively inhibits the functioning of the immune system (Chan *et al*., 1999, Kontani *et al*., 2001). It is evident that numerous questions remain to be answered before a consensus is reached in terms of exactly how MUC1 interacts with the immune system.

Immunofluorescence images show that polarization is lost and that MUC1 is located over the entire cell membrane as well as in the cytoplasm in the HOSCC cell lines, with the possible exception of WHCO5. In WHCO5, MUC1 is predominantly located around the edge of the colony of cells, as opposed to being located around each individual cell. This may be an indication that WHCO5 maintains some degree of polarity. In a cell culture context, the edge of a cell colony may be likened to the apical side of the cell (where MUC1 is normally expressed) in that the cell has a “free” surface that is not attached to

other cells. This provides a possible explanation for the slightly different localization pattern of MUC1 in WHCO5.

The circumferential staining of SNO in particular is interesting because the size of MUC1 (up to 500 nm) appears to be incompatible with the normal intercellular space (~30 nm). Contrary to the expectations that adjacent cells would be forced apart by steric forces, the SNO cell aggregates appear cohesive. At least 4 other studies (3 in breast and 1 in non small cell lung carcinomas) have made this same observation (Hayes *et al*.,1991, McCuckin *et al*., 1995, Guddo *et al*., 1998, Rahn *et al*., 2001). These same studies have shown that although the cells appear cohesive this pattern of staining is associated with a higher incidence of lymph node metastasis and a poor prognosis. Thus although the cells may give the impression of being cohesive it is likely that cell-cell interaction is to some degree still hindered.

Aberrant glycosylation (as indicated by antibody binding) may explain the circumferential as well as the intracellular localization of MUC1 in these cells. As mentioned earlier, O-linked glycans may be important in targeting proteins to the apical membrane. In addition, aberrant, particularly under-glycosylation may increase the rate of MUC1 internalization by clathrin-mediated endocytosis (Altschuler *et al*., 2000). Thus, the demonstrated loss of apical restriction, and intracellular accumulation of MUC1 is in keeping with the suggestion that it is aberrantly glycosylated in these HOSCC cells.

The implications of MUC1 expression over the entire cell membrane and in the cytoplasm, are substantial, particularly in terms of the adhesive characteristics of the cells. The studies conducted by Wesseling *et al*. (1995 and 1996) (detailed earlier in this chapter) clearly show that MUC1 expression inhibits both ECM and cell-cell adhesion. The studies indicate that MUC1 membrane localization therefore potentially enhances the metastatic potential of the cell by allowing cells to ignore normal controls elicited by interaction of integrins with the ECM as well as allowing them to detach from the primary tumour and invade the host stroma. A more recent immunohistochemical study conducted on colorectal adenocarcinoma has demonstrated a relationship between

circumferential and/or cytoplasmic MUC1 staining (similar to the MUC1 staining pattern generated for the HOSCC cells) and patient prognosis. Ultimately, the authors showed that patients exhibiting circumferential and/or cytoplasmic MUC1 localization were associated with a significantly lower 5 year survival rate than patients who had no MUC1 expression or only apical MUC1 staining. They also showed that subcellular staining pattern of KL-6/MUC1 may be an important indicator for unfavourable behaviours such as lymph node and liver metastasis (Guo *et al*., 2006). Thus, taking into account these new findings, together with earlier findings of Guddo *et al*. (1998) and Rahn *et al*., (2001) it must be considered that the pattern of MUC1 localization as demonstrated in these HOSCC cells may impact upon cell behaviour and potentially enhance metastatic capabilities.

The data presented here unequivocally demonstrates that MUC1 is expressed, that the protein complement is present, and that it is aberrantly located in 5 oesophageal squamous cell carcinoma cell lines. The potential implications of MUC1 expression in these lines are both substantial and diverse, considering that MUC1 is thought to contribute to multiple aspects of transformed cell behaviour. MUC1 expression potentially impacts upon cell adhesion, migration and survival. In the following chapters we shall further explore the possible roles of MUC1 in these HOSCC cell lines.

CHAPTER 3: MUC1 ASSOCIATION WITH β-CATENIN IS MODULATED BY ACTIVATION OF EGFR IN HOSCC CELL LINES

3.1 Introduction

MUC1 physically interacts with a number of important cell signalling molecules, including glycogen synthase kinase 3β (GSK3β), Grb2/son of sevenless (SOS), c-Src, β-catenin and the epidermal growth factor receptor (EGFR) (Gendler, 2001, Wang *et al.,* 2004). This chapter focuses on the interplay that exists between MUC1, β-catenin and EGFR. Although the concept of EGFR overexpression in HOSCC has previously been introduced, it is now essential to have a brief understanding of EGFR signalling.

EGFR (also known as erbB1) is a member of a family of transmembrane tyrosine receptor kinases known as erbB receptors. EGFR, as well as family members erbB2, erbB3 and erbB4, are expressed dynamically during development and are also commonly implicated in cancer initiation and progression (Normanno *et al.,* 2006). Ligand binding induces dimerization of receptors, which can be either homodimerization, or heterodimerization among members of the ErbB family. Dimerization results in activation of the intrinsic tyrosine kinase domain, leading to the recruitment and activation of a variety of effector proteins including the non-receptor kinase c-Src, phosphatidylinositol 3-kinase (PI3K), Shc, phospholipase Cγ, STAT, Grb2/SOS and others (Yarden and Sliwkowski, 2001). The activation of many of these proteins results in the downstream phosphorylation of nuclear translocating kinases, including stress-activated protein kinase (SAPK)/ c-Jun NH_2-terminal kinase (JNK) and the MAP kinases, which subsequently results in the regulation of processes that are crucial in cellular proliferation, differentiation and apoptosis (Yarden and Sliwkowski, 2001) (Figure 3.1).

As previously discussed, EGFR overexpression has frequently been observed in human tumours and in tumour cell lines, and is thought to play a critical role in cancer progression by increasing the transduction of mitogenic signals (Yarden and Sliwkowski, 2001). EGFR is often overexpressed in HOSCC and its overexpression is associated with

frequency of metastasis and a poor prognosis (Andl *et al.,* 2003, Sunpaweravong *et al.,* 2004, Gibault *et al.,* 2005). Moreover, and what has not been previously discussed, is that EGFR is proposed to be a key player in the dysfunction of cadherin-mediated cell-cell adhesion in HOSCC, resulting in an increased metastatic potential (Shiozaki *et al.,* 1995)

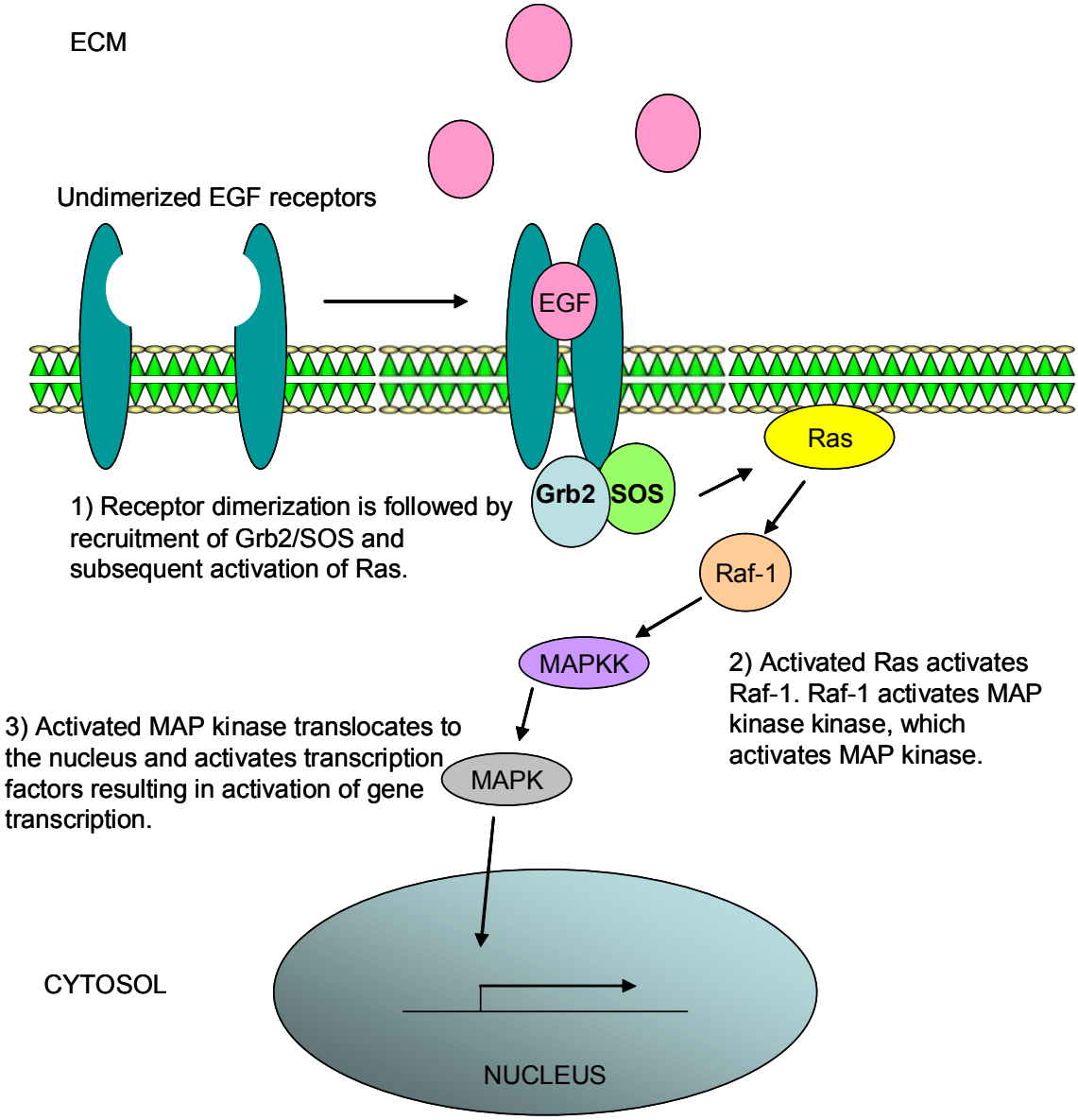

Figure 3.1: EGFR signalling. The EGFR signalling pathway activates membrane-bound Ras which results in a cascade of events leading to transcriptional activation of a number of growth promoting genes.

In a study conducted by Shiozaki *et al.* (1995), EGF treatment of the HOSCC cell line TE-2R induced a morphological shift in the cells from round to fibroblastic. As well as altering the morphology of the cells EGF treatment resulted in change of colony formation from compact to sparse, and in addition, the invasive potential of the cells increased. These cellular responses are concomitant with loss of adherens junction formation commonly associated with down-regulation of E-cadherin expression. However, further investigation indicated that these cellular responses were not accompanied by a decreased expression of E-cadherin, nor were they accompanied by reduced expression of the other adherens junction components, α-catenin or β-catenin (Shiozaki, 1995). It was determined however, that the E-cadherin molecule experienced a change in localization, from the lateral adhesion site to the whole cell surface. The results further indicated that activated EGFR counteracts E-cadherin-mediated junctional assembly through phosphorylation of β-catenin; a phosphorylation event that inhibits the functioning of the cadherin-catenin system. These results were in keeping with previous findings (Shibamoto *et al.,* 1994). Thus, rather than down-regulating the expression of any component of the adherens junction, EGF inhibits the assembly of the junction through tyrosine phosphorylation of β-catenin.

MUC1 has been implicated in the disruption of adherens junctions (Kondo *et al*., 1998). The MUC1 cytoplasmic tail (CT) interacts with β-catenin at a SAGNGGSSL motif similar to the β-catenin binding site on E-cadherin (Yamamoto *et al.,* 1997). It has been shown that MUC1 and E-cadherin compete for binding from the same pool of β-catenin (Yamamoto *et al.,* 1997, Kondo *et al*., 1998, Li *et al.,* 1998). Thus, when MUC1 is expressed, some of the available pool of β-catenin associates with MUC1 and reduces the β-catenin available for association with E-cadherin, resulting in a reduction of adherens junctions (Kondo *et al*., 1998, Schroeder *et al*., 2003). This is, however, a simplified version of events, and the interaction between MUC1 and β-catenin appears to be dynamically controlled by a number of kinases, one of which is EGFR (Li *et al.,* 1998, Li *et al.,* 2001a, Li *et al.,* 2001b, Ren *et al.,* 2002). We will look at the overall network of control of the association in order to get a clearly defined view of the role of EGFR in modulating the interaction between MUC1 and β-catenin.

The 72 amino acid MUC CT has a number of potential sites for tyrosine and serine/threonine phosphorylation, and at least 3 of these appear to be important in regulating the association between MUC1 and β-catenin (Li *et al.,* 1998, Wang *et al.,* 2003). GSK3β binds to, and phosphorylates MUC1, on serine 44 (S44) in a TDRSPYE domain adjacent to the β-catenin binding domain. This GSK3β-mediated phosphorylation event decreases the binding of MUC1 to β-catenin (Li *et al.,* 1998). In a study conducted to determine the functional significance of this relationship, MUC1 was overexpressed in MUC1-negative HEK293 cells. This resulted in a down-regulation of interaction between β-catenin and E-cadherin. Importantly however, overexpression of GSK3β (which would presumably inhibit association between MUC1 and β-catenin) along with MUC1 restored the interaction between β-catenin and E-cadherin (Li *et al.,* 1998). Thus GSK3β activity effectively abrogated MUC1-mediated sequestration of β-catenin away from E-cadherin.

In contrast to GSK3β-mediated down-regulation of MUC1/β-catenin interaction, EGFR and c-Src activation increase the association between MUC1 and β-catenin, an event which sequesters additional β-catenin away from E-cadherin and thereby further reduces cell-cell adhesion (Li *et al.,* 2001a, Li *et al.,* 2001b). EGFR physically associates with MUC1 at the cell membrane, and its activation phosphorylates MUC1 at tyrosine 46 (Y46) on the YEKV motif on the CT. Phosphorylation of this tyrosine induces the interaction of MUC1 with β-catenin and with c-Src (Li *et al.,* 2001a). Interestingly, a separate study detailed EGFR-independent c-Src phosphorylation of MUC1, also on the YEKV motif, and indicated that this event inhibited binding of GSK3β to MUC1 CT and thereby increased binding of β-catenin to MUC1 CT (Li *et al.,* 2001b). What is not clear is whether or not EGFR activation directly phosphorylates the YEKV motif or if it functions via activation of c-Src. However, the study by Li *et al*. (2001b) demonstrates that c-Src-dependant phosphorylation of the YEKV site on the MUC1 CT is necessary for the formation of MUC1 CT/β-catenin complexes. It is therefore likely that EGFR activation results in the activation of c-Src which subsequently phosphorylates MUC1, rather than EGFR directly phosphorylating MUC1 CT (see Figure 3.2). This would explain the association between MUC1 and c-Src after EGFR activation.

This chapter details the determination of whether MUC1 and β-catenin form a complex at the membrane of HOSCC cells, and investigates if this complex is modulated by the activation of EGFR by EGF.

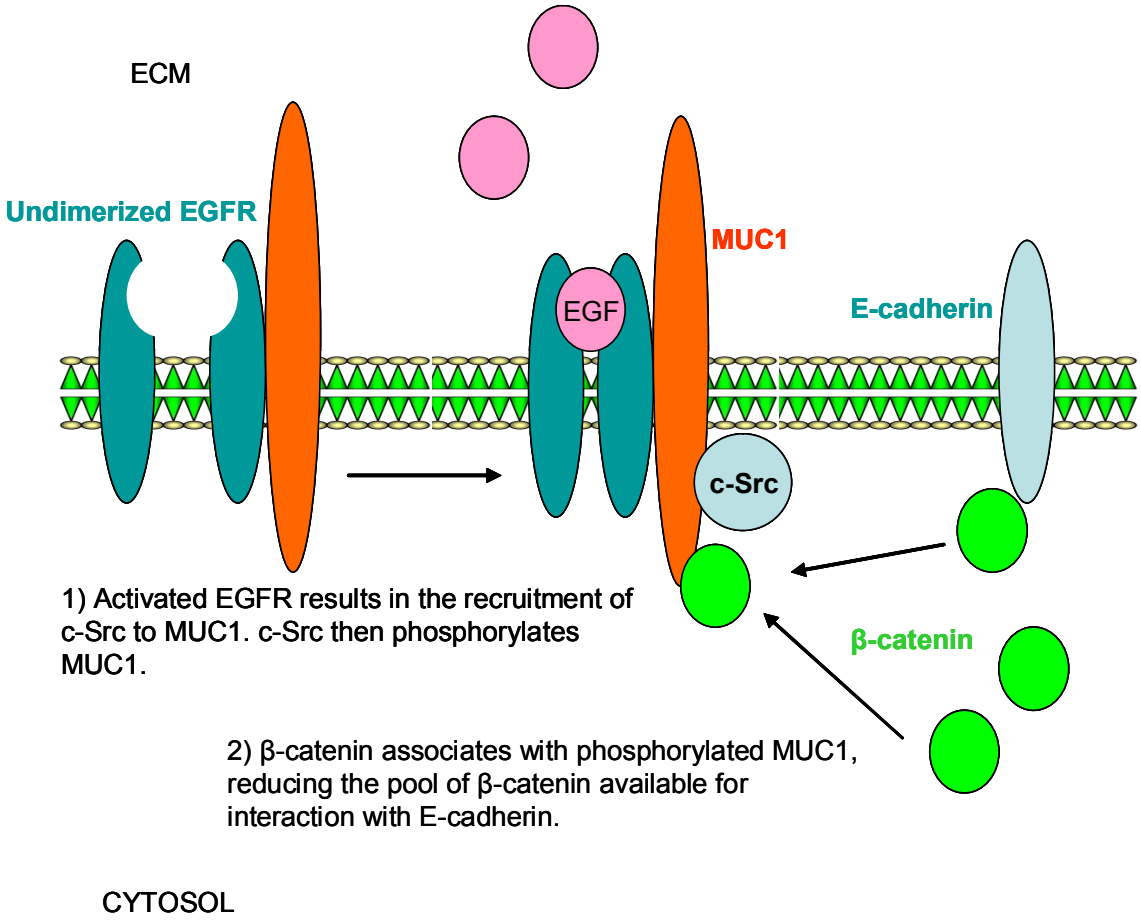

Figure 3.2: EGFR activation impacts upon cell adhesion. EGFR activation has been reported to modulate the interaction between MUC1 and β-catenin, through c-Src-mediated MUC1 phosphorylation, in breast carcinoma (Li *et al.,* 2001a).

3.2 Methods & Materials

3.2.1 Antibodies

Rabbit anti-β-catenin antibody (Sigma) was used for immunoprecipitation of membrane extracts. HRP-bound anti-rabbit IgG antibody (Sigma) was used as the secondary antibody to detect anti-β-catenin. MUC1 CT detection was conducted using Armenian hamster CT2 antibody (kindly donated by Dr Sandra Gendler, Mayo Clinic, Scottsdale, Arizona, USA). HRP-conjugated goat anti-Armenian hamster IgG antibody (Jackson Immunoresearch Laboratories) was used to detect CT2 in western blot analysis.

3.2.2 Epidermal growth factor treatment

Cells were cultured, as described in Chapter 2, in tissue culture medium containing 10 ng/ml EGF for a period of 5 min, 30 min, 1 hour or 3 hours at 37°C in a humid CO_2 incubator. EGF treatment was conducted on each cell line.

3.2.3 Membrane extraction

Membrane extractions were carried out on EGF-treated as well as untreated cells representative of each cell line (i.e. one untreated dish per cell line as well as one dish for every EGF treatment period, totalling 5 dishes per cell line). Tissue culture medium was aspirated and the cells were washed 3 times in PBS before being transferred to a sterile eppendorf tube. Cells were centrifuged in a Tomy Capsule HF-120 bench top centrifuge (1200 x g) for 5 min and the supernatant was removed and discarded. Cells were then resuspended in 200 µl of Tris-based TritonX-100 membrane extraction buffer pH 8.5 (see Appendix 7.15) for 2 hours on ice. Samples were then centrifuged at 12 000 x g and 4°C for 5 min. The supernatants were kept for further analysis and the pellets were discarded.

3.2.4 Protein estimation

Protein estimation was carried out according to the procedure detailed in Chapter 2.

3.2.5 SDS-PAGE resolution of membrane extracts

Protein (10 μg) from all membrane extracts was separated on 10% SDS-PAGE in order to ensure success of the extraction. The gel was prepared and electrophoresis was conducted according to the procedure outlined in Chapter 2.

3.2.6 β-Catenin immunoprecipitation

Immunoprecipitation (IP) is a method whereby a protein, along with proteins that are physically associated with it, can be purified from a complex mixture of proteins. The procedure makes use of an antibody directed against the protein of interest, together with a matrix that binds the antibody. Protein (150 μg) from all membrane extracts were incubated with 2 μl undiluted anti-β-catenin antibody overnight at 4°C in IP buffer pH 8.0 (see Appendix 7.16), to allow binding of the antibody to the protein. The following day 7 mg Protein G agarose beads (Sigma) were added to each sample. Protein G binds IgG at neutral to basic pH. The IP mixture was incubated at 4°C overnight, to allow the binding of the Protein G beads to the antibody/protein immune complexes. The following day samples were centrifuged at 12 000 x g and 4°C for 1 min. The supernatant was discarded and the pellet (now consisting of Protein G beads, anti-β-catenin, and β-catenin and associated proteins) was washed 3 times in IP buffer. After the final wash 40 μl of Laemmli lysis buffer (see Appendix 7.7) was added to the pellet, before incubation for 5 min at 95°C. This step releases β-catenin and its associated proteins from the agarose beads. The samples were then centrifuged for 5 min at 12 000 x g at room temperature and the supernatants, representing β-catenin immunoprecipitates, were kept for western blot analysis.

3.2.7 Western Blot Analysis

Untreated and EGF-treated protein extracts corresponding to each cell line were analysed on a separate blot (i.e. 5 blots, each representative of a single cell line, were carried out). Equal volumes of immunoprecipitates were subjected to electrophoresis on a 10% SDS-PAGE gel and transferred to nitrocellulose membrane as in Chapter 2. Nitrocellulose membranes were blocked in a casein-based blocking buffer (Blotto) for 1 hour at room temperature. Resolved protein was incubated in either CT2 antibody (1:500) for 1 hour 30 min, or anti-β-catenin (1:5000) for 1 hour, followed by 6 five min washes with PBS. Membranes were then incubated in either HRP-conjugated anti-Armenian hamster IgG antibody (1:1000) (to detect CT2 antibody) or HRP-conjugated anti-rabbit IgG (1:10 000) (to detect anti-β-catenin antibody), both for 1 hour. Detection of antibody binding was carried out with the Supersignal® West Pico Chemiluminescent Kit (Pierce) as detailed in Chapter 2.

3.2.8 Densitometry

Densitometric analysis of the western blots was conducted using LabWorks ™ Image Acquisition and Analysis Software (Version 4.5). This program has the advantage of being able to specifically select the band of interest, thereby circumventing problems associated with background and non-specific smears around bands of interest. Levels of concentration/association were represented as a percentage of the maximum concentration/association generated in these experiments, where maximum association was considered 100%. While experiments were carried out more than once, the data was not sufficient for statistical analysis.

3.3 Results

3.3.1 Membrane extracts from HOSCC cell lines constitute a wide range of polypeptides.

Prior to immunoprecipitation it was necessary to determine the protein content of the membrane extracts so that a uniform amount of protein, in this case 150 μg, was used in each immunoprecipitation experiment. It is evident from SDS-PAGE analysis that the membrane extraction procedure produced numerous polypeptides, possibly including both β-catenin and the MUC1 CT (Figure 3.3). The relative uniformity, in terms of staining in each lane, indicates that the same amount of protein has been loaded in each lane and therefore demonstrates that the protein estimation was accurate and successful.

3.3.2 MUC1 and β-catenin co-immunoprecipitate from membrane extracts.

Membrane extracts, from untreated and EGF-treated HOSCC cells, were immunoprecipitated with anti-β-catenin and then resolved using SDS-PAGE prior to western blot analysis with the CT2 antibody. Distinct 28 kDa bands in all lanes in blots depicted in Figure 3.4a indicate that MUC1 and β-catenin co-immunoprecipitate from the membrane in all cell lines both prior to EGF treatment, as well as after treatment. The CT2 (anti-MUC1 CT) antibody used in this experiment has been reported to generate a distinctive western blotting result whereby the MUC1 CT is detected in a broad band from 28 kDa to 20 kDa (Li *et al.,* 2003a and personal communication from Dr Gendler's laboratory, Mayo Clinic, Scottsdale, Arizona). Since the single 28 kDa band was noted to be different from the previously reported MUC1 CT western blotting banding-pattern, it was deemed necessary to include negative controls for this experiment. HEK293 cells known not to express MUC1 were subject to the same treatment as the HOSCC cells. As an additional negative control, WHCO6 membrane-protein was treated according to the above-outlined protocol with the exception that no anti-β-catenin antibody was added to the protein extract. As a positive control, 20 μg SNO whole-cell lysate was electrophoresed in a lane between the negative control samples and immunoprecipitated

samples (Figure 3.4b). The absence of bands in lanes representative of the negative controls confirms that the experiment is specific for the MUC1 CT/β-catenin interaction (Figure 3.4b). Moreover, the banding pattern generated by the SNO whole-cell lysate parallels what has previously been reported for specific CT2 binding, and thus provides further evidence that the immunoblotting procedure is specifically detecting MUC1 CT. This data thus provides a clear demonstration of the presence of a MUC1/β-catenin complex at the membrane of these HOSCC cell lines.

3.3.3 EGFR activation modulates the association of MUC1 and β-catenin at the membrane of HOSCC cell lines

The graph included as part of Figure 3.4 was generated using the densitometric data obtained from the western blots (see Appendix 7.17 for raw data) and depicts the changes in association between MUC1 and β-catenin that occur at the cell membrane in response to EGF treatment over time. The responses of each cell line, in terms of the modulation of MUC1/β-catenin association, were complex. There were both increases and decreases in MUC1/β-catenin association over the 3 hour period, rather than a simple increase or decrease over the assessed time interval. What is clear, however, is that cell lines WHCO3, WHCO5, WHCO6 and SNO exhibit a substantial increase in association between MUC1 and β-catenin some time within the 3 hour treatment period.

WHCO6 exhibited the greatest increase in association, escalating from only 12% of the maximum association to 100% after 3 hours of EGF treatment (see methods). Cell lines WHCO3 and SNO achieved maximum association after 1 hour, while WHCO5 increased from 62% of the maximum association in the untreated sample to 100% in only 5 min. Although WHCO3, WHCO6 and SNO took longer to achieve maximum association their respective increases were more considerable than that of WHCO5, with WHCO3 increasing from only 25% association in the untreated sample to 100% after 1 hour of treatment, and SNO exhibiting only 40% of the maximum association in the untreated sample. WHCO1, on the other hand, showed the least overall increase in association

between MUC1 and β-catenin at the cell membrane, with only a negligible increase after 30 min (Figure 3.4).

A common trend for all cell lines, except for WHCO6, is the reduction in association of MUC1 and β-catenin after 3 hours of EGF treatment. For example, WHCO1 exhibits maximum association after 30 min of treatment, this association is drastically reduced to only 3% after 3 hours of treatment. Similarly, WHCO3 is at maximum association after 1 hour of treatment, and this drops to only 22% association after 3 hours.

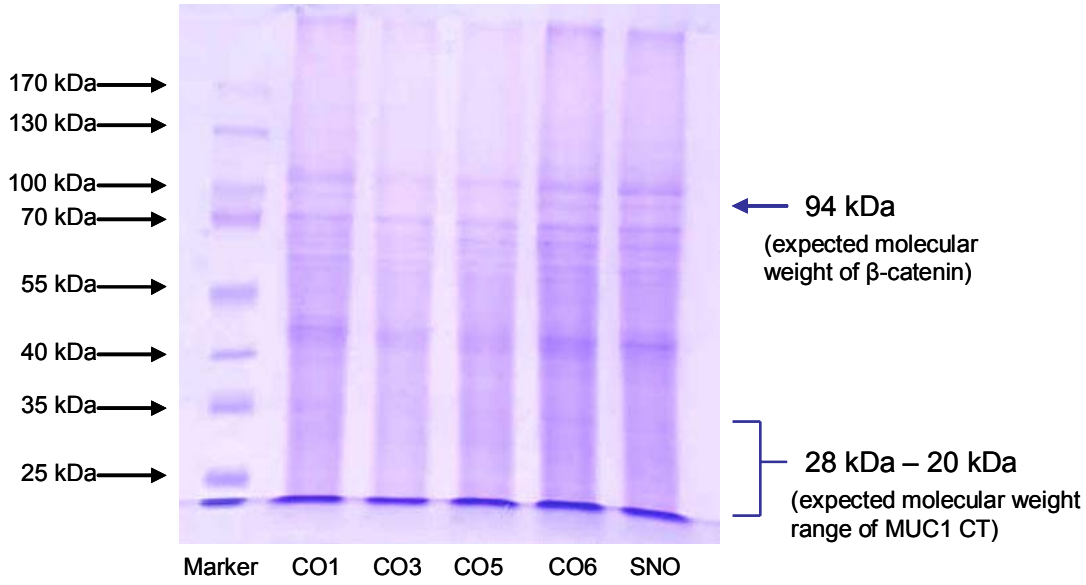

Figure 3.3: Membrane protein-extract from each of the HOSCC cell lines was resolved by SDS-PAGE (10%). The presence of distinct bands in all lanes indicates that the extraction procedure was successful.

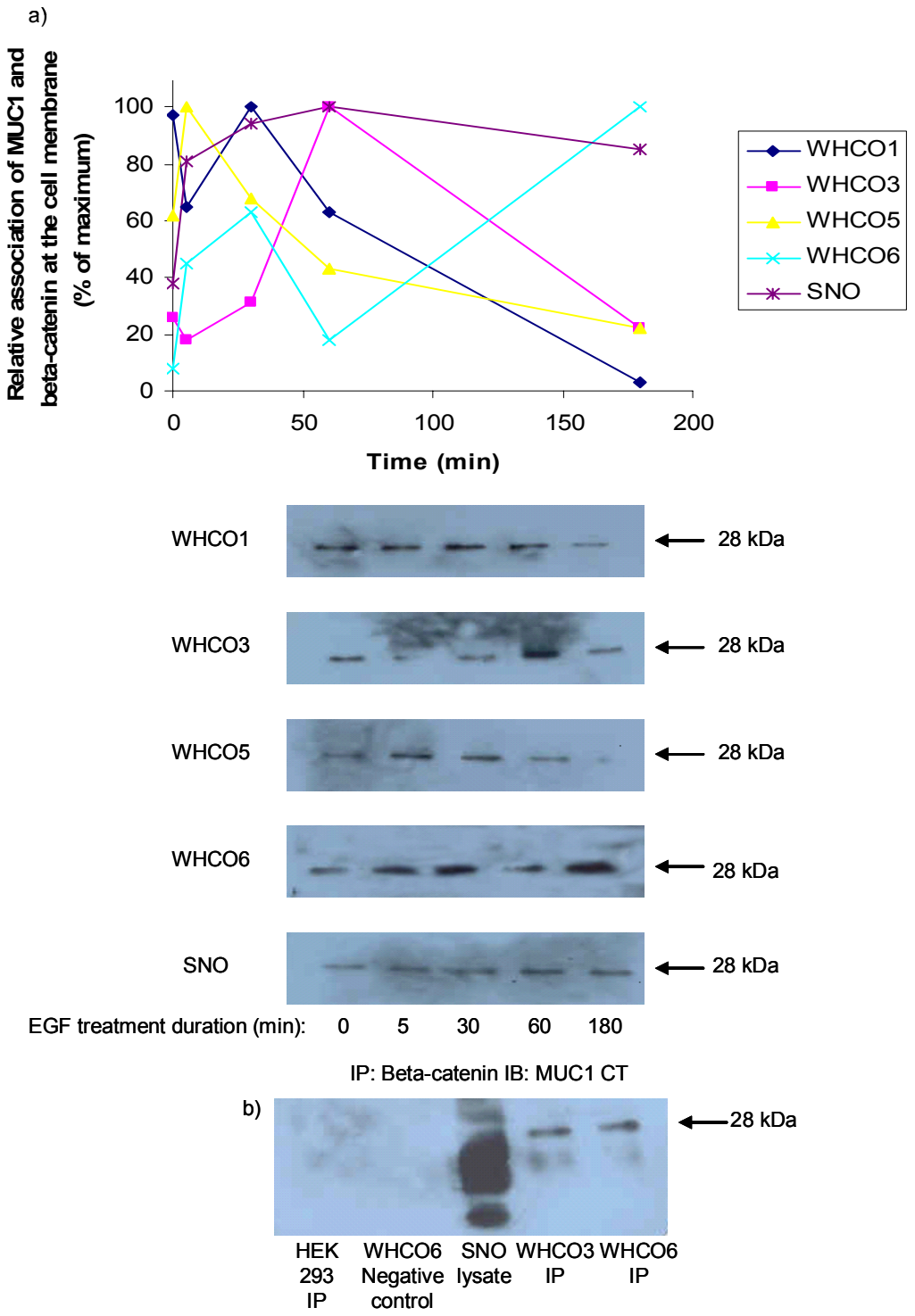

Figure 3.4: EGFR activation modulates the interaction between MUC1 CT and β-catenin. a) Graphical representation of densitometric analysis of bands created through MUC1 CT-specific immunoblotting of β-catenin immunoprecipitates. b) Membrane extracts from HEK293 and WHCO6 (subject to the same treatment as experimental samples, with the exception that no anti-β-catenin antibody was added) served as negative controls. The absence of bands in lanes representative of HEK293 and WHCO6 negative controls confirms the specificity of the experiment. IP=Immunoprecipitating antibody, IB=Immunoblotting antibody

3.3.4 EGF treatment modulates the concentration of β-catenin at the cell membrane

EGFR activation results in the phosphorylation of β-catenin, an event that inhibits binding of β-catenin to E-cadherin (discussed above). This may elicit changes in concentration of membranous β-catenin as it is possible that once freed from E-cadherin, β-catenin would translocate away from the membrane. Thus in order to add value to the results presented in Figure 3.4, and to ensure that the results were not merely a reflection of β-catenin concentration at the membrane it was important to monitor β-catenin concentration at the cell membrane. Also, should the results indicate that β-catenin moves away from the membrane after 3 hours of treatment it would provide an explanation for the apparent reduction in association of MUC1 and β-catenin at that time period.

Membrane extracts that had been immunoprecipitated with β-catenin for the pervious experiment were resolved by SDS-PAGE and probed with anti-β-catenin. The graph depicted in Figure 3.5, similar to that in Figure 3.4, was generated from densitometric data from the western blot results (see Appendix 7.18 for raw data) and depicts changes in concentration of β-catenin at the cell membrane in response to EGF treatment.

Results indicate that exposing the HOSCC cells to EGF does result in changes of β-catenin concentration at the cell membrane (Figure 3.5). This is in keeping with what has previously been reported for these cells (Jones and Veale, 2003). Again, these changes appear to be complex, with neither a steady increase nor a steady decrease occurring over the 3 hour treatment period. What is important to note, however, is that changes in concentration of β-catenin at the membrane are not as dramatic as the changes in degree of association between MUC1 and β-catenin occurring over the same time period. For example, in WHCO3 the relative concentration of β-catenin at the membrane increases from 83% of maximum to 100% over the period of an hour, whereas MUC1/β-catenin association shows a substantially more dramatic increase, from 25% to 100% in that same time. Similarly, Figure 3.4 demonstrates that in WHCO5, the MUC1/β-catenin association increases from 62% of the maximum to 100% in 5 min, whereas Figure 3.5

demonstrates that the concentration of β-catenin at the membrane increases from 55% of the maximum to only 59% in the same period. It is also important to note that in the WHCO6 and SNO cell lines, the concentration of the MUC1/β-catenin complex increases, even while the concentration of membrane β-catenin decreases (Figures 3.4 and 3.5). These data suggest that the demonstrated increases in association between MUC1 and β-catenin are not merely as a result of increased β-catenin concentration at the membrane.

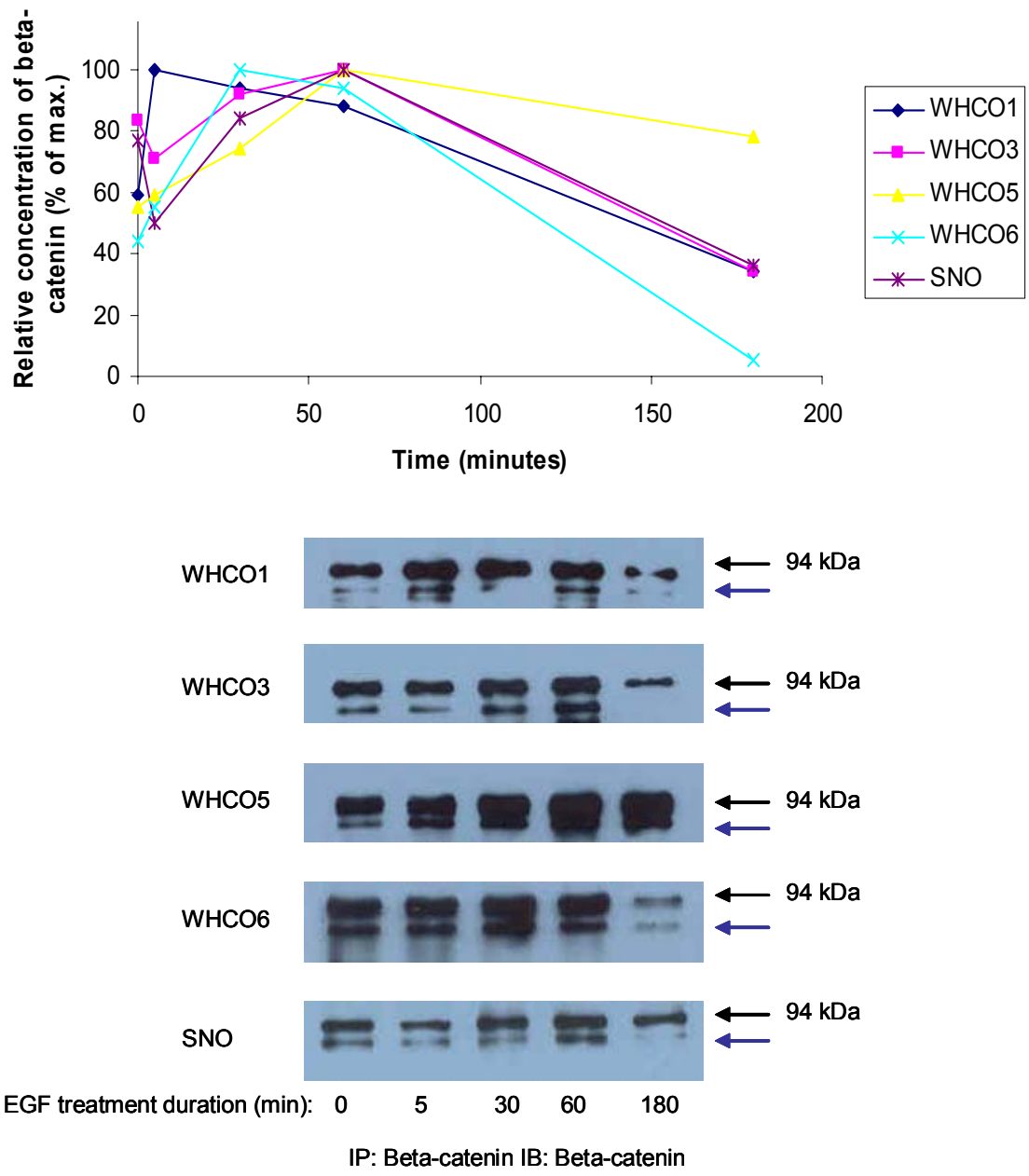

Figure 3.5: EGF modulation of the concentration of β-catenin at the cell membrane of 5 HOSCC cell lines. Representation of densitiometric analysis of western blots designed to investigate the modulation of membranous β-catenin concentration in response to EGFR activation. IP=Immunoprecipitating antibody IB=Immunoblotting antibody. Blue arrow indicates β-catenin degradation product (Jones and Veale, 2003).

3.4 Discussion

In this chapter, evidence is provided showing that the MUC1 CT associates with β-catenin at the cell membrane of all 5 HOSCC cell lines investigated. MUC1 expression, and association with β-catenin, has been shown to inhibit adherens junction formation by sequestering β-catenin away from E-cadherin and the adherens junctions (Li *et al.,* 1998). Thus, the demonstrated association between MUC1 and β-catenin at the cell membrane of these cell lines is likely to have similar implications for cellular adhesion.

Importantly, the results further indicate that EGFR activation modulates the association between MUC1 and β-catenin at the cell membrane of these cell lines. There are both increases and decreases in the association of these proteins with EGF treatment over time. The increases in association between MUC1 and β-catenin will be discussed before going on to discuss the decreases in association.

Although the downstream effects of EGFR activation were discussed earlier, it will be summarized here to aid in the interpretation of the results. Following EGF binding, inactive monomeric EGFR undergoes homodimerization or heterodimerization with other members of the ErbB family. Activation of EGFR is associated with phosphorylation of specific tyrosine residues in its cytoplasmic tail and thereby the recruitment of effector proteins that contain SH2 domains (Normanno *et al.,* 2006). Of importance here is that EGFR activation is associated with the formation of a complex containing c-Src. c-Src interaction with EGFR thus brings c-Src into proximity with MUC1, which is itself constitutively associated with EGFR (Li *et al.,* 2001a). c-Src then interacts with a YEKV motif on the MUC1 CT and phosphorylates the tyrosine. This phosphorylation event inhibits the association of GSK3β with MUC1 and thus induces binding of β-catenin. This signalling cascade is likely to result in the substantial increases in association between MUC1 and β-catenin that are seen in WHCO5 after 5 min of EGF treatment, in WHCO1 after 30 min of treatment, in WHCO3 and SNO after 1 hour of treatment and in WHCO6 after 3 hours of treatment.

Regardless of the time it takes to reach maximum association, these increases are significant in terms of the effects that increases in MUC1 and β-catenin association are thought to have on cell adhesion (Taylor-Papadimitriou *et al*., 1999). As previously discussed, MUC1 expression, and subsequent association with β-catenin at the cell membrane, reduces the β-catenin available for interaction with E-cadherin and the adherens junctions. Here we have shown that not only does MUC1 associate with β-catenin at the cell membrane, but that this association can be greatly increased by activation of EGFR, a receptor that is known to be highly overexpressed in HOSCC, and in these cell lines in particular (Veale and Thronley, 1989). The demonstrated increases in association between MUC1 and β-catenin would sequester additional β-catenin away from the adherens junctions thereby further inhibiting cell adhesion and potentially enhancing the invasive potential of these cells.

There is a substantial reduction in association between MUC1 and β-catenin after 3 hours of treatment in all cell lines (except for WHCO6). In order to determine if this was due to translocation of β-catenin away from the membrane we monitored the concentration of β-catenin by probing the immunoprecipitates with anti-β-catenin. The results indicated that β-catenin concentration at the membrane is reduced in all cases after 3 hours of treatment with EGF. It is therefore possible that the reduction in association is a reflection of a reduction of membrane-associated β-catenin; however there is an alternative explanation. A recent study has shown that when MUC1 is overexpressed it associates with β-catenin, and that this complex translocates to the nucleus during disruption of cadherin-mediated cell-cell adhesion (Wen *et al.,* 2003). This nuclear aspect of MUC1/β-catenin signalling will be dealt with in greater detail in the following chapters. However, this concept may be important here as the "3 hour result" may not necessarily depict a reduction in association between MUC1 and β-catenin at the membrane, but rather indicates movement of the entire complex away from the membrane. Put simply, the hypothesis is that after reaching maximum association the MUC1/β-catenin complex translocates away from the membrane into the cytoplasm and potentially into the nucleus. This hypothesis is supported in part by the data presented here as well as by the demonstration by Wen *et al.* (2003) that the MUC1/β-catenin complex translocates to the nucleus. The presence of

a MUC1/β-catenin nuclear complex in these cell lines, and the implications of such a complex will be investigated in later chapters.

WHCO6, unlike the other cell lines, exhibits maximum association between MUC1 and β-catenin after 3 hours of EGF treatment. It is likely however, that if an additional time point, for example 4 hours, was included WHCO6 would follow the trend of the other cell lines and would exhibit a reduction in concentration of the complex. This is supported by the observation that at 3 hours after EGF treatment WHCO6 already exhibits a substantial reduction in membrane-associated β-catenin.

The hypothesis that after reaching maximum association MUC1 and β-catenin translocate away from the membrane explains the reduction in the complex after maximum association has been reached. However, that theory does not explain the reduction in association exhibited by WHCO1 and WHCO3 prior to maximum association. In WHCO3 the reduction in association between MUC1 and β-catenin, from 26% of the maximum to 18% after 5 min of treatment, is accompanied by a reduction in membranous β-catenin, from 83% of the maximum to 71% over the same time period. It is therefore possible that, as suggested earlier, EGFR-mediated phosphorylation of β-catenin has allowed movement of β-catenin away from the membrane. This means that the apparent reduction in association is likely to be a reflection of less β-catenin in the immunoprecipitated sample. The same cannot be said for WHCO1 however, as the reduction in association from 97% to 65% of the maximum is accompanied by an increase in membranous β-catenin from 59% to 100% association. Thus in this case the reduction in association between MUC1 and β-catenin cannot be attributed to a decreased concentration of β-catenin at the cell membrane as β-catenin concentration has in fact increased. There must therefore be an alternative explanation for the reduction in association between MUC1 and β-catenin. Reduced interaction may involve changes in expression of other proteins involved in regulating the MUC1/β-catenin interaction (such as GSK3β or c-Src), however, further analysis would have to be conducted in order to determine the validity of this statement.

In addressing the observation that there are both increases and decreases in MUC1/β-catenin association in response to EGFR activation, it is also important to consider that the EGF treatments were conducted on intact cells rather than extracted and isolated proteins. The results of the experiment therefore reflect events occurring in a complex system. There are a host of interacting factors contributing to the modulation of association of MUC1 and β-catenin. These factors may include concentration of β-catenin and MUC1 as separate entities at the cell membrane, and the activity of c-Src and GSK3β, as well as protein kinase C δ (PKCδ) which has also been shown to influence β-catenin binding to MUC1 (Gendler, 2001). In addition, the intracellular recycling of EGFR, which serves to regulate the rate of EGFR degradation and signalling, may also impact upon the cellular response to exposure to EGF (Ceresa, 2006). With this in mind, it is not surprising that there were both increases and decreases in association between MUC1 and β-catenin, as well as differences across the cell lines within the 3 hour treatment period.

EGFR is highly overexpressed in numerous carcinomas including carcinomas of the oesophagus (Kuwano *et al.,* 2005). In these carcinomas, EGFR activation is associated with changes in cellular morphology, modulation of adhesive characteristics and an increase in invasive capabilities; properties that are linked to EGFR-mediated disruption of adherens junctions. The predominant cause for EGFR-mediated disruption of adherens junctions was thought to occur through a phosphorylation event that inhibited binding of β-catenin to E-cadherin (Shibamoto *et al.,* 1994, Hazan and Norton, 1998). Here, we suggest, and provide evidence for, an alternative mechanism for EGFR-mediated disruption of adherens junctions in HOSCC. MUC1 and β-catenin associate at the cell membrane and this association can be substantially increased by EGFR activation. This event is likely to sequester β-catenin away from E-cadherin thereby inhibiting the functioning of adherens junctions and resulting in reduced cell-cell adhesion. Moreover, this alternative mechanism for EGFR-mediated disruption of adherens junctions is in keeping with the evidence that indicates EGFR activation results in the dysfunction of the junction, rather that down-regulation of any of its components.

Importantly, the disruption of adherens junctions has consequences that impact upon more than cell adhesion, and may have implications relating to processes as diverse as signal transduction, cell growth, differentiation, site-specific gene expression, morphogenesis, immunologic function as well as inflammation (Harington and Syrigos, 2000). Thus, the potential reduction in adherens junction formation conferred by MUC1 expression, in combination with EGFR activation, may have a vast array of implications for the tumorigenic and metastatic behaviour of these cells.

CHAPTER 4: MUC1 IS IMPLICATED IN β-CATENIN SIGNALLING

4.1 Introduction

In the previous chapters is has been demonstrated that MUC1 localizes to the cell membrane and interacts with the adherens junction component, β-catenin, in 5 moderately differentiated HOSCC cell lines. Here, the possibility is investigated that, similar to recent findings in cancers of the pancreas and colon, the MUC1 cytoplasmic tail (CT) localizes to the nucleus and forms a nuclear complex with β-catenin in these cell lines. In order to fully appreciate the potential impacts and functional significance of MUC1 nuclear association with β-catenin it is first important to have an understanding of β-catenin signalling.

β-catenin participates in E-cadherin mediated cell-cell adhesion and as such is considered a structural protein (Ozawa *et al*., 1989a, Ben-Ze'ev and Geiger, 1998). However, there is an additional aspect to β-catenin's role in the cell, where it functions in the nucleus as a co-activator of gene transcription (Nelson and Nusse, 2004, Harris and Peifer, 2005). This transcriptional role of β-catenin is constitutively suppressed by the ubiquitin-proteosome-dependent degradation of "free" or non-junctional β-catenin (Salomon *et al*., 1997, Bienz, 2004, Harris and Peifer, 2005). β-catenin is targeted to the proteosome through its phosphorylation by a multiprotein complex consisting of GSK3β, and the scaffolding proteins adenomatous polyposis coli (APC) and axin. After serine phosphorylation (by GSK3β) β-catenin (the N-terminus in particular) is recognized by the ubiquitin ligase, β-transductin-repeat-containing protein (β-TrCP), which catalyses the attachment of ubiquitin peptides, and subsequently results in the degradation of β-catenin (for review see Kikuchi, 2000).

Wnt, a homeobox gene introduced earlier, regulates the ability of this multiprotein complex to trigger β-catenin degradation (Bienz and Clevers, 2000, Bienz, 2004). The binding of Wnt to its receptor, frizzled, activates dishevelled which then interacts with axin. Dishevelled (Dsh) recruits several other proteins, such as GSK-binding protein and

phosphatase 2C resulting in the disassembly of the multiprotein complex and the accumulation of β-catenin within the cytoplasm and nucleus (Nelson and Nusse, 2004) (see Figure 4.1). In the nucleus, β-catenin interacts with lymphoid enhancer factor (LEF)/ T-cell factor (TCF) transcription factors, displacing co-repressors Groucho and CREB binding protein (CBP), allowing transcription of specific target genes such as cyclin D1, c-myc and MMP7 (Roose and Clevers, 1999, Bienz, 2004). Importantly, the accumulation of nuclear β-catenin is associated with various cancers, including colorectal carcinomas as well as squamous cell carcinomas of the oesophagus (Morin, 1999, De Castro *et al*., 2000, Ninomiya *et al*., 2000). Induction of genes such as cyclin D1 and c-myc are thought to provide the molecular basis for growth regulation by β-catenin, whereas the induction of MMP-7 expression is thought to promote cell invasion.

Accumulation of nuclear β-catenin in cancers is not however, necessarily due to constitutive activation of the Wnt pathway. Often, mutations in key components of the degradation machinery, such as APC and axin are responsible for the deregulation of β-catenin turnover (Bienz and Clevers, 2000, Park *et al*., 2005). Similarly, mutations in β-catenin itself occasionally result in the inability of the multiprotein complex to phosphorylate it, resulting in stabilization and accumulation of β-catenin (Park *et al*., 2005). However, although nuclear accumulation of β-catenin has been reported in HOSCC, the associated mutations have not (Powell *et al*., 1994, Ninomiya *et al*., 2000). Therefore, another mechanism for cytoplasmic and nuclear accumulation of β-catenin in HOSCC must exist.

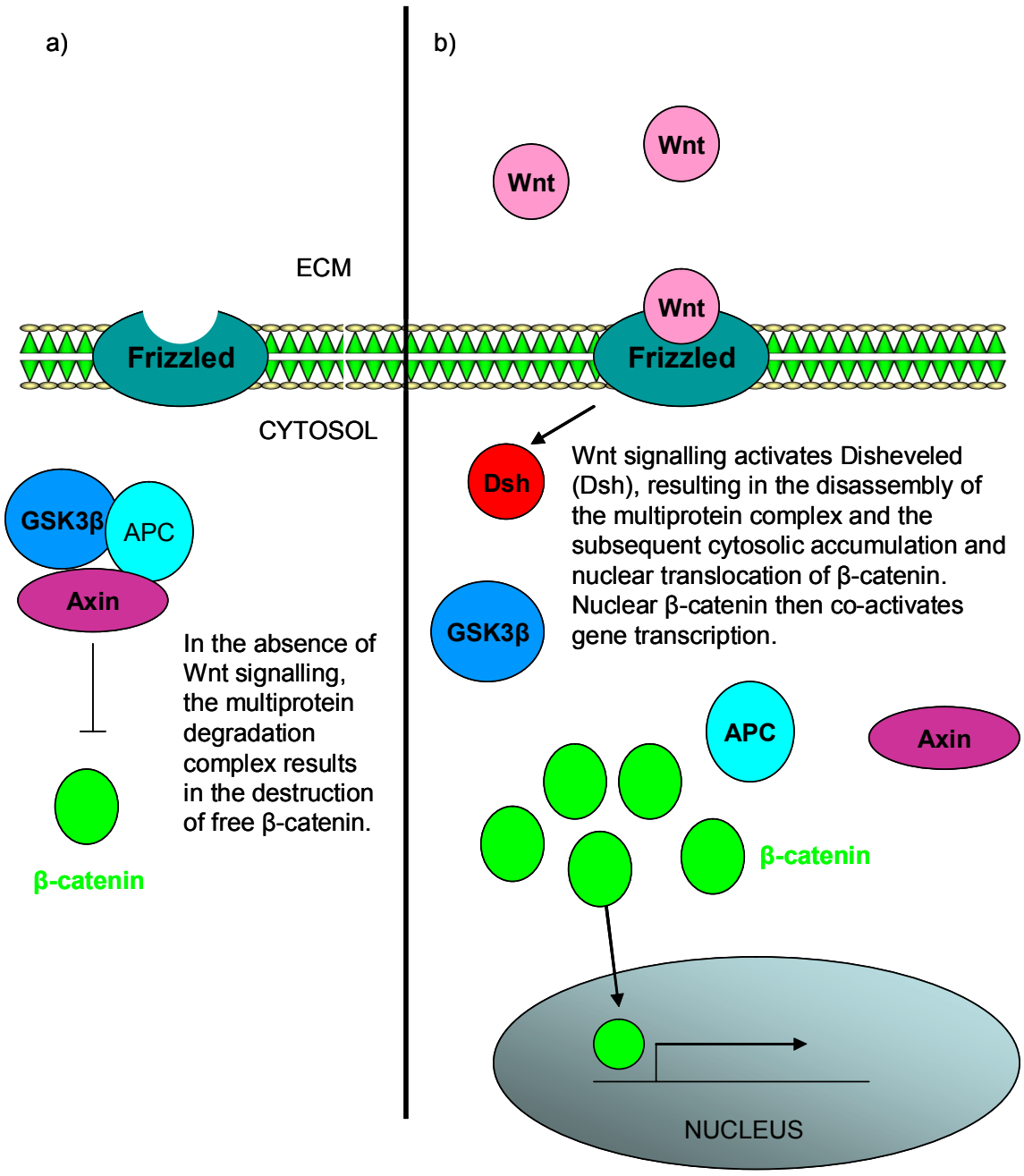

Figure 4.1: Wnt signalling controls β-catenin-mediated gene expression.

a) In the absence of Wnt signalling free β-catenin is highly unstable and is rapidly degraded by the multiprotein complex. b) Wnt signalling results in the stabilization of β-catenin and its subsequent translocation to the nucleus where it acts as a transcriptional co-activator.

A recent study has documented the increase of steady state levels of nuclear β-catenin in response to MUC1 overexpression in pancreatic cancer cell lines (Wen *et al*., 2003). In addition, their results show that a fragment of the MUC1 CT undergoes cytosol-to-nucleus trafficking in association with β-catenin. They suggest that the MUC1 CT stabilizes β-catenin and thereby influences its activity as a transcriptional co-activator. In a subsequent study, a different group of researchers demonstrated that MUC1, not only simply associates with β-catenin in the nucleus, but coactivates β-catenin mediated transcription (Huang *et al*., 2003). They clearly show that MUC1 contributes to transcription of the β-catenin/TCF/LEF responsive gene, cyclin D1, and that this transcription is abrogated by a mutation that inhibits MUC1 binding to β-catenin. Thus, while Wen *et al.* (2003) suggest that MUC1 may be important in stabilizing β-catenin and aiding in its accumulation and subsequent translocation to the nucleus, Huang *et al.* (2003) suggest that MUC1 is an essential component of the β-catenin/TCF/LEF transcription factor complex. These findings, as well as the reports that the MUC1/β-catenin complex is found in the nucleus of multiple myeloma cells as well as in rat fibroblasts, support a role for MUC1 in β-catenin mediated signalling (Li *et al*., 2003b, Li *et al*., 2003c).

This chapter details the investigation of nuclear localization of the MUC1 CT and β-catenin, and examines the possibility of a MUC1/β-catenin complex in the nucleus of HOSCC cell lines. Also investigated is the potential modulation of nuclear concentration of β-catenin in HOSCC cells in response to EGFR activation.

4.2 Methods & Materials

4.2.1 Antibodies

The Armenian hamster CT2 antibody and FITC-conjugated anti-Armenian hamster IgG antibody (Jackson Immunoresearch Laboratories,) were used for indirect immunofluorescence. Other antibodies used in this chapter have been previously described.

4.2.2 Nuclear extractions

Nuclear extractions were carried out using Sigma CelLytic™ NuClear™ Extraction Kit (Sigma) according to the manufacturer's instructions. Cells (2 x 10 cm Nunc™ dishes to give a packed cell volume of 100 µl) were rinsed 3 times in PBS before being transferred to a sterile eppendorf tube. The tubes were centrifuged in a Tomy Capsule HF-120 bench top centrifuge (1200 x g) for 5 min, and the supernatant was removed and discarded, leaving the pellet of rinsed cells. Hypotonic lysis buffer (500 µl) containing 5 µl of 0.1 M dithiothreitol (DTT) and 5 µl protease inhibitor cocktail was added to each pellet. (See Appendix 7.19 for all solutions used in the nuclear extraction.) The cells were re-suspended by gentle pipetting and then left on ice, to swell, for 15 min. Cells were viewed under the microscope to ensure that cell lysis had not occurred (which would have indicated that these cells were too fragile for this extraction method). Nuclei were released from the cells by adding 30 µl of 10% Igepal CA-630 (in deionised H_2O) to each sample before briefly vortexing and then centrifuging at 12 000 x g and 4°C for 5 min. The supernatant (cytoplasmic fraction) was aspirated. 70 µl of a high salt nuclear extraction buffer, containing 1 µl of 0.1 M DTT and 1 µl protease inhibitor cocktail, was added to the nuclear pellet and the samples were put on ice, on a shaker for 30 min. The samples were then centrifuged at 20 500 x g and 4°C for 5 min. The supernatant (nuclear extract) was aliquoted and stored at -70°C prior to subsequent analysis.

4.2.3 Protein estimation and polypeptide resolution

Protein estimation was carried out according to the procedure outlined in Chapter 2. The nuclear extracts were then separated on a 12.5% SDS-PAGE gel as previously described.

4.2.4 Western blot analysis of nuclear extracts

Protein (15 μg) from nuclear extracts were separated on a 12.5% SDS-PAGE gel (for high resolution of MUC1 CT) and transferred to nitrocellulose transfer membrane, before being probed with either anti-β-catenin or CT2 (anti-MUC1 CT) antibodies. The appropriate secondary antibodies were applied prior to detection using the West Pico Chemiluminescent Kit (see Chapters 2 and 3 for a more detailed description of the procedure).

4.2.5 Indirect immunofluorescence

WHCO1 and SNO cells, from exponentially growing cultures, were seeded with tissue culture media onto sterile glass cover-slips and maintained at 37°C in an atmosphere of 5% CO_2 overnight to allow the cells to settle and attach to the cover-slip. The following day the medium was aspirated and cells were rinsed 5 times in PBS. Cells were fixed in a 1:1 solution of ice cold methanol and acetic acid for a total of 6 min. The fixing solution was removed by a 5 min wash in dH_2O followed by 3 rinses in PBS. This fixing procedure was used rather than 4% paraformaldehyde (described in Chapter 2) on the suggestion by Dr Gendler's Laboratory (Scottsdale, Arizona) where the antibody had been produced. Cells were permeabalized by applying a solution of 0.25% Triton X-100 for 10 min. Permeabilization was followed by 2 washes in PBS. The cover-slips were then air-dried for 1 min and then areas of cells were delineated using a DAKO pen. Cells were rehydrated in PBS for 30 min before the addition of 20 μl of CT2 antibody (1:250). The cells were incubated in primary antibody for 1 hour at room temperature. The negative control cells were incubated in PBS (containing no antibody) for 1 hour. Both the experimental and control cells were then washed 5 times for 1 min in PBS before the

addition of 20 µl of FITC-conjugated anti-Armenian Hamster IgG antibody (1:500). The cells were incubated in secondary antibody for 1 hour at room temperature in the dark. Secondary antibody was washed off by 6 one minute washes in PBS. 10 µl of elvanol, containing anti-bleach, was added to each well. Glass slides were placed on top of each cover-slip. Cells were viewed as in Chapter 2 using a Zeiss LSM 410 confocal microscope (FITC excitation wavelength 490 nm, emission wavelength 525 nm).

4.2.6 Co-immunoprecipitation of β-catenin and MUC1 CT from nuclear extracts

Protein from nuclear extracts was subject to immunoprecipitation with β-catenin exactly as the membrane extracts were in Chapter 3. The immunoprecipitates, as well as a 2 µl aliquot of SNO whole-cell lysate (for control purposes), were then run on a 12.5% SDS-PAGE gel and were transferred to nitrocellulose according to the previously outlined procedure. The resolved immunoprecipitate, now on nitrocellulose, was probed with CT2, prior to detection with HRP-conjugated goat anti-Armenian Hamster IgG antibody.

4.2.7 EGF treatment and nuclear extractions

After the above co-immunoprecipitation experiments had been performed it was decided that it would be of value to monitor the potential changes in nuclear β-catenin concentration in response to EGF treatment. As in Chapter 2, cells were treated with 10 ng/ml EGF in standard tissue culture medium for a period of 5 min, 30 min, 1 hour or 3 hours. Treatment was followed by nuclear extraction, as detailed above. The extracts then underwent protein estimation prior to western blot analysis.

4.2.8 Western blot analysis of nuclear extracts from EGF treated HOSCC cells

Nuclear protein (15 µg) representing untreated as well as EGF-treated (5 min, 30 min, 1 hour and 3 hours) cells was loaded on a 10% SDS-PAGE gel and electrophoresed according to standard procedure. After transfer to nitrocellulose membrane the resolved

protein was probed for β-catenin using the anti-β-catenin antibody and HRP-conjugated anti-rabbit IgG antibody (see Chapter 2).

4.2.9 Densitometry

Densitometry was conducted according to the procedure outlined in Chapter 2.

4.3 Results

4.3.1 The nuclear extraction isolated numerous proteins

Protein (10 μg) from nuclear extracts representative of each cell line was separated using SDS-PAGE. Numerous bands present in each lane indicate the presence of several polypeptides in the nuclear extracts, potentially including β-catenin at 94 kDa as well as the MUC1 CT (Figure 4.2). The MUC1 CT has been reported (by the producers of the antibody as a personal communication) to electrophorese between 28 and 20 kDa. (See Appendix 7.20 for standard curve of relative molecular weight versus distance migrated). The uniformity of staining in each lane is a good indicator that the protein estimation was accurate and successful.

4.3.2 The MUC1 CT is detectable in the nuclear extracts of 2 cell lines

The nuclear extracts separated by 12.5% SDS-PAGE were subject to western blotting using the anti-MUC1 CT antibody. The banding pattern seen in lanes representative of WHCO1 and SNO, showing a broad band extending from 28 kDa to ~24 kDa and additional distinct lower molecular weight bands of between ~24 and 20 kDa, is typical of a positive reaction of this antibody (Figure 4.3) (Li *et al.,* 2003a). The bands thus indicate that the MUC1 CT is indeed present in nuclear extracts of cell lines WHCO1 and SNO. In addition, a faint band is detectable in the lane representing WHCO5 indicating that the MUC1 CT is also present in the WHCO5 nuclear extract. Although no bands are obvious in lanes representing WHCO3 and WHCO6 it is likely that the concentration of the MUC1 CT in nuclei of these cell lines is below the level of detection of the method used in this experiment. That is, the lack of bands in lanes representing WHCO3 and WHCO6 does not necessarily mean that no MUC1 CT is present, and is more likely a reflection of a much lower concentration of the MUC1 CT in these HOSCC cell lines.

4.3.3 The distribution pattern of the MUC1 CT is not consistent when comparing cell lines WHCO1 and SNO

The cellular distribution of the MUC1 CT was further assessed in cell lines WHCO1 and SNO using an indirect immunofluorescence procedure that employed an antibody directed specifically against a fragment of the MUC1 CT. Figure 4.4 (SNOa and SNOb) shows bright membrane staining (see red arrows) in a high proportion of the cells as well as a high degree of staining throughout the cytoplasm. MUC1 CT staining in WHCO1 is less bright. In contrast to SNO, where there is bright staining throughout the cell and at the membrane, staining in WHCO1 was generally dimmer, with faint staining at the membrane (Figure 4.4 WHCO1a and WHCO1b). In addition, much of the staining in WHCO1 is concentrated to discrete circular particles in the region of the nucleus (see red arrows). In SNO, staining in the nucleus and cytoplasm appeared bright and relatively uniform.

4.3.4 β-catenin is present in nuclear extracts of all 5 HOSCC cell lines investigated

The distinct 94 kDa band in all lanes of Figure 4.5b is a clear demonstration that β-catenin is present in the nucleus of all 5 cell lines investigated. The minor differences in band width and band density are a reflection of the minor differences in concentration of β-catenin. WHCO5 has the highest concentration of nuclear β-catenin (taken to be 100%), followed closely by WHCO3, with 82% of the maximum concentration. WHCO1, WHCO6 and SNO have similar concentrations of nuclear β-catenin with 61% of the maximum, 63% and 56% respectively (Figure 4.5a). (See Appendix 7.21 for raw densitometric data).

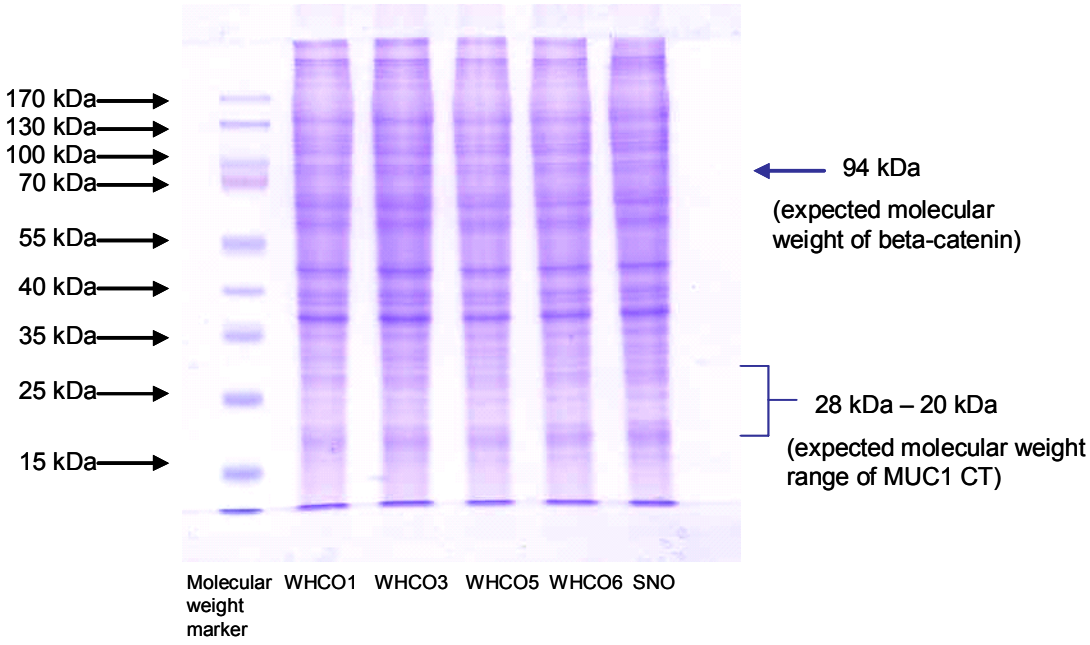

Figure 4.2: HOSCC cells were subject to nuclear extraction. Nuclear extracts were then analyzed by 12.5% SDS-PAGE. Distinct bands in all lanes indicate that the extraction procedure was successful. The uniform degree of staining apparent in each lane shows that the protein estimation was accurate.

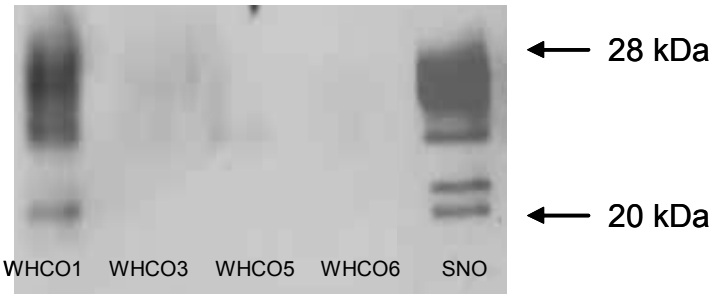

Figure 4.3: The MUC1 CT is present in nuclear extracts of WHCO1, WHCO5 and SNO. Nuclear protein was resolved using 12.5% SDS-PAGE prior to transferring to nitrocellulose and then immunoblotting with CT2 (anti-MUC1 CT antibody). The banding pattern in lanes representative of WHCO1 and SNO nuclear extracts is typical for this antibody (personal communication - Dr Gendler's laboratory, Li *et al*., 2003a).

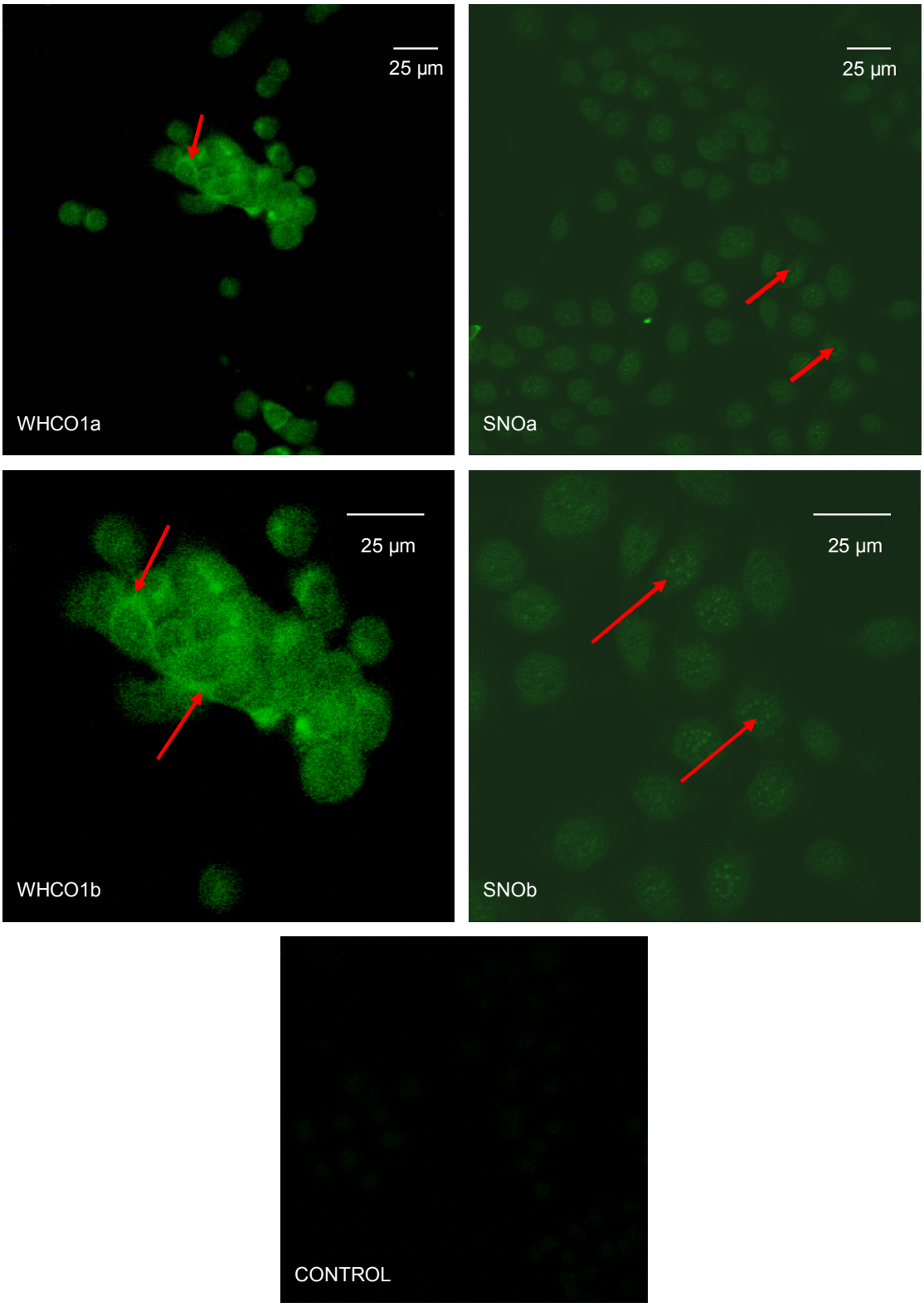

Figure 4.4: The cellular distribution of MUC1 CT was further assessed in cells lines WHCO1 and SNO through indirect immunofluorescence using a MUC1 CT-specific antibody. These data appear to support the data obtained in the western blot. WHCO1b is a magnified version of image WHCO1a, while SNOb is a magnified version of SNOa.

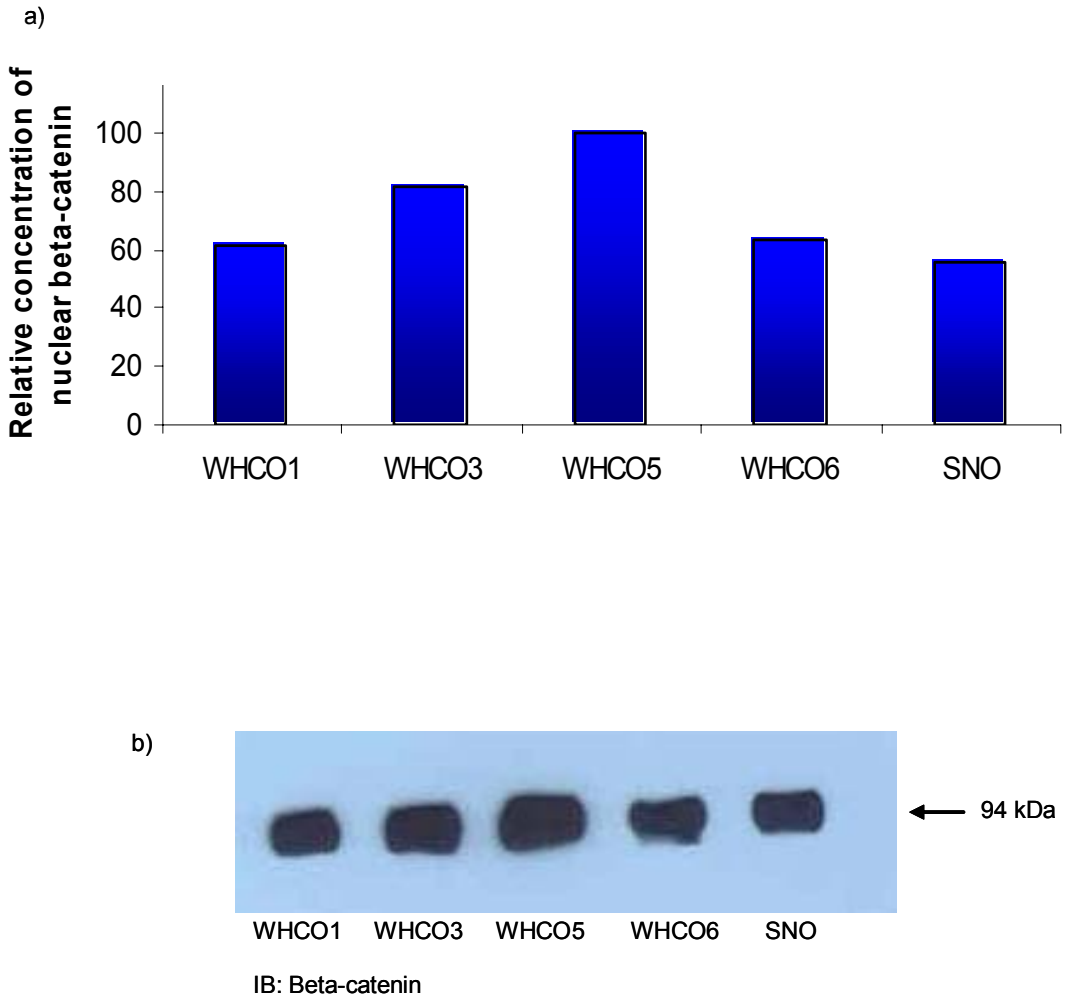

Figure 4.5: β-catenin is present in nuclear protein extracted from 5 HOSCC cell lines. a) Graphical representation of densitometric analysis of bands generated by western blotting. b) β-Catenin-specific immunoblotting of resolved nuclear protein demonstrates the presence of β-catenin in the nucleus of all 5 cell lines investigated. IB=Immunoblotting antibody.

4.3.5 The MUC1 CT and β-catenin co-immunoprecipitate from nuclear extracts

To determine whether the MUC1 CT associates with β-catenin in the nucleus, β-catenin immunoprecipitates from nuclear extracts were analysed by immunoblotting with CT2 (anti-MUC1 CT). The distinct, highly specific, 28 kDa band in lanes representative of HOSCC cell lines clearly demonstrates that the MUC1 CT and β-catenin co-immunoprecipitate from the nuclear extracts of all HOSCC cell lines investigated (Figure 4.6b). Co-immunoprecipitation is considered a valid indicator of complex formation and we thus provide evidence that the MUC1 CT and β-catenin form a nuclear located complex in these lines. As reflected by the differences in band density, there are slight differences in concentration of the complex. WHCO5 has the highest concentration of the complex (taken to be 100%), followed by SNO, with 83% of the maximum, and then WHCO3 with 74% of the maximum. WHCO1 and WHCO6 have the lowest concentration of the complex with 54% and 23% respectively (Figure 4.6a). Lane 6 of Figure 4.6b, containing SNO whole-cell lysate was used as a positive control in this experiment. (See Appendix 7.21 for raw densitometric data.)

4.3.6 EGF, which modulates the association of MUC1 CT and β-catenin at the cell membrane, modulates the concentration of nuclear β-catenin

Figure 4.7 shows that EGF treatment modulates the concentration of nuclear β-catenin in these cell lines. This is demonstrated by the changes in band density at each treatment in the western blots analysed for each of the cell lines. Each cell line is unique in its response to exposure to EGF in terms of the changes in nuclear β-catenin concentration. WHCO1 exhibits a steady decrease in nuclear β-catenin in response to EGF treatment from 100% in the untreated sample to 64% in the sample that had been treated for a period of 3 hours. WHCO3, WHCO5 and WHCO6 exhibit both increases and decreases, however it must be noted that many of these changes appear to be relatively small. WHCO3 exhibits a relative concentration of 71% in the untreated sample, which increases to 94% after 5 min of treatment, followed by a decrease to 74% after 30 min of treatment. In WHCO3, maximum nuclear β-catenin concentration is seen after 1 hour of

treatment. WHCO5 exhibits a relatively high nuclear concentration of β-catenin in the untreated sample (93%), however this drops to only 58% of the maximum concentration after 5 min of treatment before steadily increasing to maximum association after 3 hours of treatment. WHCO6, on the other hand, exhibits an increase in nuclear β-catenin concentration after 5 min of EGF treatment, followed by a relatively steady decrease over the 3 hour treatment period. SNO exhibits little change in β-catenin concentration in response to EGF treatment. SNO has 99% nuclear β-catenin concentration in the untreated sample which is reduced to 90% of the maximum concentration after 30 min of treatment, before increasing again to 99% and then to 100% after 1 hour and 3 hours of treatment respectively. These changes are negligible. (See Appendix 7.22 for raw densitometric data).

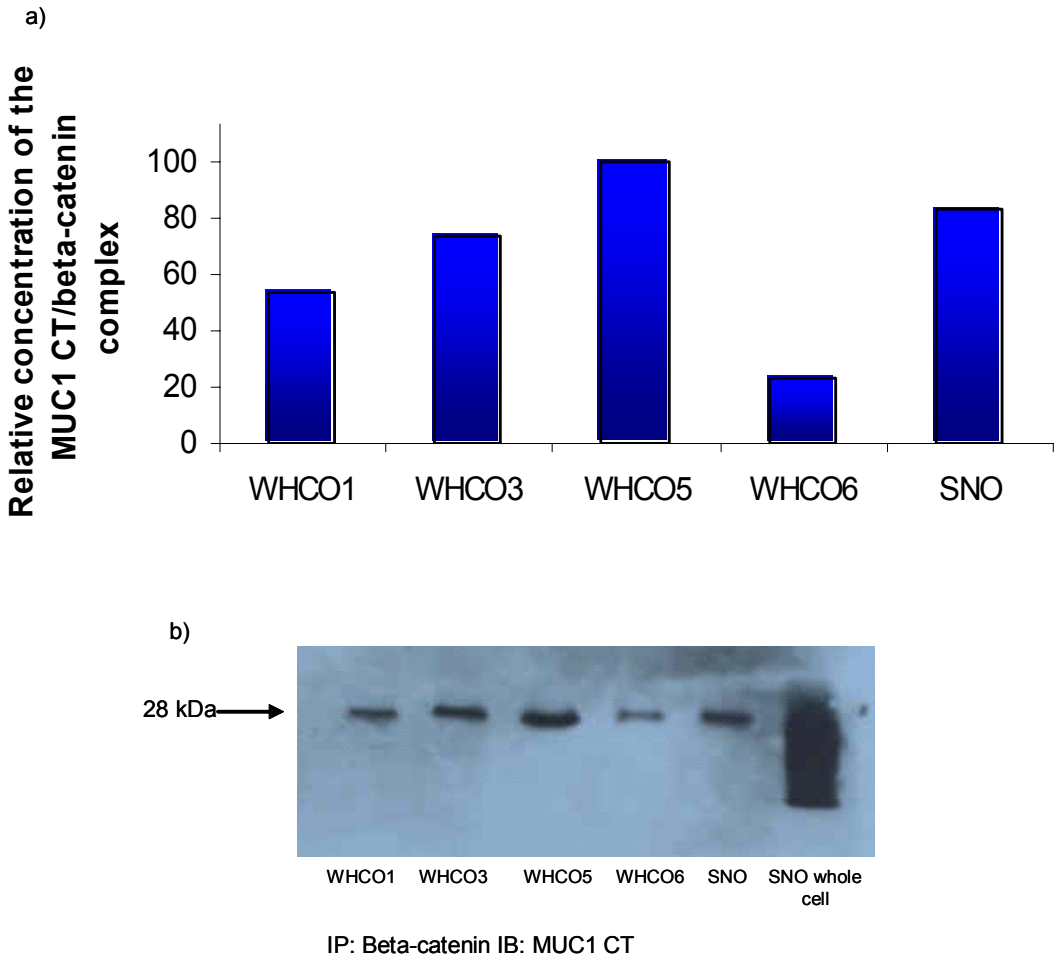

Figure 4.6: MUC1 CT and β-catenin co-immunoprecipitate from nuclear protein extracted from 5 HOSCC cell lines. a) Graphical representation of densitometric analysis of bands generated through MUC1 CT-specific immunoblotting of resolved β-catenin-immunoprecipitated nuclear protein b). Western blot analysis of β-catenin immunoprecipitates indicates the presence of a MUC1 CT/β-catenin complex. IP=Immunoprecipitating antibody, IB=Immunoblotting antibody.

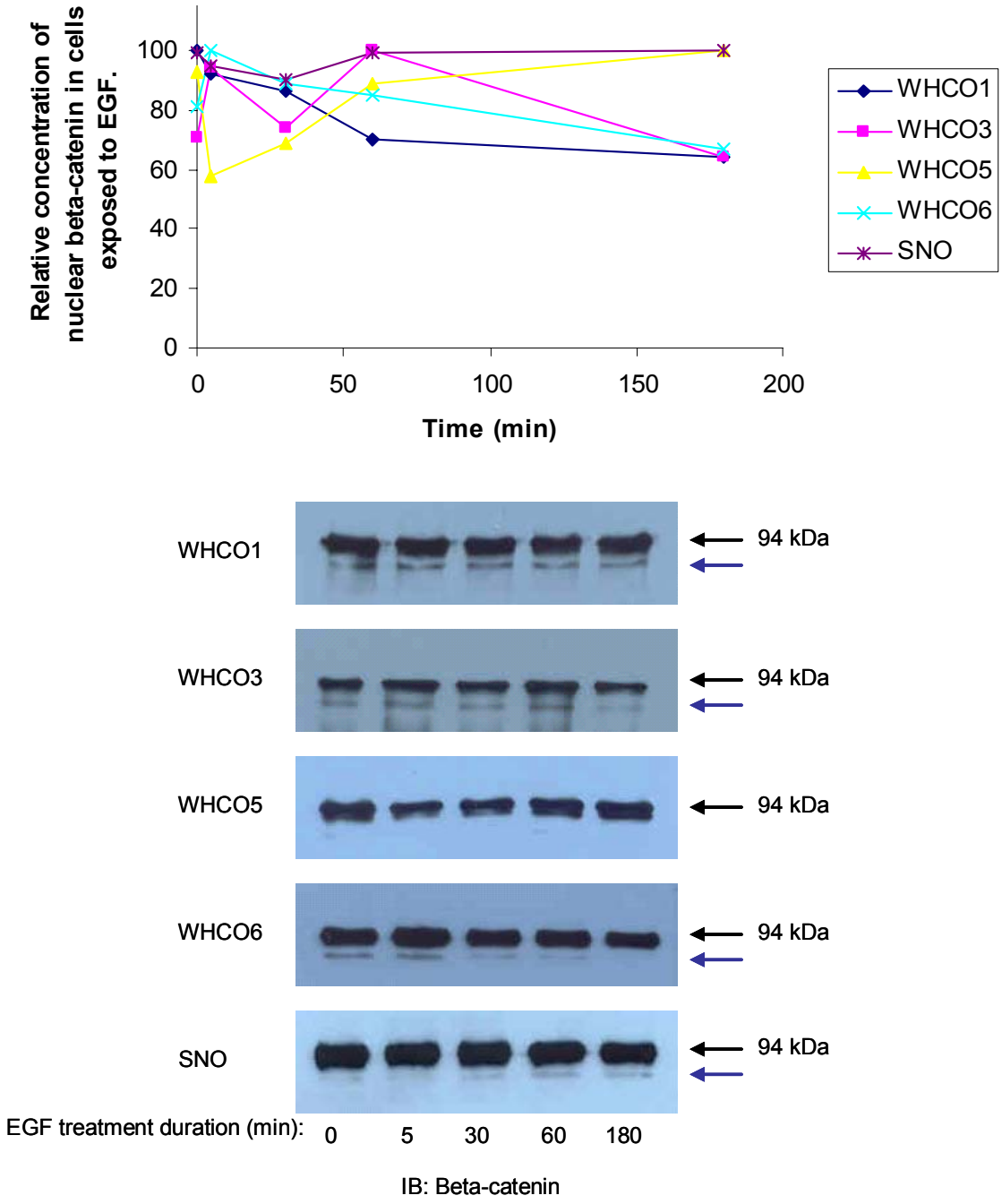

Figure 4.7: EGFR activation modulates the nuclear concentration of β-catenin in 5 HOSCC cell lines. Graphical representation of EGF-induced modulation of β-catenin nuclear concentration, generated by densitometric analysis of β-catenin-specific western blots. Blue arrows indicate a β-catenin degradation product. IB=Immunoblotting antibody.

4.4 Discussion

4.4.1 The presence of the MUC1 CT in the nucleus of HOSCC cells suggests a signalling role for MUC1 in HOSCC

MUC1 has been shown to influence the cellular adhesion properties of cells in which it is overexpressed and aberrantly localized (Wesseling *et al*., 1995, Wesseling *et al*., 1996). The findings that the MUC1 CT is highly conserved across species together with reports that MUC1 associates with a number of important signalling molecules, suggest that MUC1 may play an additional role in morphogenetic signal transduction (Gendler, 2001, Wang *et al.,* 2003, Hattrup and Gendler, 2006 Thompson *et al*., 2006). This chapter details the distribution of the MUC1 CT and its interaction with β-catenin in the nucleus of HOSCC cell lines.

Western blot analysis of nuclear extracts using an antibody specific to the MUC1 CT indicates the presence of the MUC1 CT in the nucleus of 3 out of 5 HOSCC cell lines investigated (that is SNO, WHCO1 and WHCO6). This provides the first demonstration of the MUC1 CT in the nucleus of HOSCC lines. Nuclear localization of the MUC1 CT had previously been limited to pancreatic cancer cells, colon carcinoma cells, multiple myeloma cells, breast carcinoma cells and rat 3Y1 fibroblasts (Huang *et al*., 2003, Li *et al*., 2003b, Li *et al*., 2003c, Wen *et al*., 2003). The detection of MUC1 CT in the nucleus of these cells is of interest considering the potential implications of nuclear MUC1, specifically regarding the potential roles of MUC1 in this cancer-type.

MUC1 CT-specific immunostaining indicated that the MUC1 CT is located throughout the cell, including the nuclear region of cell lines WHCO1 and SNO. Interestingly, SNO displayed a greater degree of staining both at the cell membrane and within the cytoplasm when compared to WHCO1. WHCO1, however, displayed distinct staining in discrete relatively small circular “particles” in the region of the nucleus. The morphology and location of these small particles indicate that they may be nucleoli. Indeed, it has been reported that MUC1 targets γ-catenin to the nucleolus in response to heregulin (HRG) in

breast cancer cells (Li *et al*., 2003a). HRG stimulation increased the association between MUC1 and ErbB2 (a member of the ErbB family). MUC1/ErbB2 association then induced binding of MUC1 to γ-catenin and γ-catenin was targeted to the nucleolus by a mechanism dependant on its interaction with MUC1. Interestingly, the pattern of MUC1 CT specific staining seen here for WHCO1 resembled the pattern of MUC1 CT specific staining generated by Li *et al*. (2003a) for HRG treated breast carcinoma cells. They confirmed that the well-circumscribed nuclear staining was in fact nucleolar staining through the use of a double-staining overlay technique using an anti-MUC1 C-terminus antibody in combination with an anti-nucleolin antibody. The similarity in the staining patterns (between the images shown here and those generated by Li *et al*. (2003a) indicates that the MUC1 CT may localize to the nucleolus in WHCO1 and raises the possibility that the MUC1 CT may interact with γ-catenin in this cell line. Of note is that our immunofluorescence image represents cells that were not exposed to HRG whereas the image of Li *et al*. (2003a) was generated using cells that had been treated with HRG. Thus it is possible that ErbB2 (or either of its heterodimerization partners, ErbB3 or ErbB4) is constitutively active in WHCO1, resulting in targeting of MUC1 and γ-catenin to the nucleolus even in the absence of HRG. The implications of this are important as ErbB2 activation is associated with disruption of tight junctions, loss of epithelial cell polarity and initiation of proliferation (Muthuswamy *et al*., 1999). Constitutive activation of ErbB2 may therefore be a contributing factor to the behaviour of WHCO1 cells.

γ-catenin, like β-catenin, functions in cell adhesion and the Wnt pathway. In addition to forming part of the adherens junction, γ-catenin is also present in desmosomes, where it interacts with desmoglein and desmocollin (Ben-Ze'ev and Geiger, 1998). Similar to MUC1 association with β-catenin, γ-catenin association with MUC1 may disrupt cellular adhesion, this time due to sequestration of γ-catenin away from both the adherens junctions as well as desmosomes. Wnt activation leads to the accumulation of γ-catenin in the cytoplasm and nucleus where it binds to members of the LEF/TCF transcription factor family and activates gene transcription (Kolligs *et al*., 2000). It has been determined that similar to β-catenin, γ-catenin functions as an oncogene when deregulated (Kolligs *et al*., 2000). It would appear that γ-catenin-mediated oncogenic

transformation is largely effected by a dramatic up-regulation of c-myc expression (Kolligs *et al*., 2000).

The nucleolus is a membrane-free nuclear subdomain in which ribosomal RNAs are transcribed and processed into ribosome subunits (Shaw and Jordan, 1995). It is also thought that the nucleolus may function in sequestering specific regulatory factors that are released (and can therefore interact with their binding elements) upon disassembly of the nucleolus during cell cycle progression (Visintin and Amon, 2000). MUC1 targeting of γ-catenin to the nucleolus may therefore be important in enhancing expression of c-myc during disassembly of the nucleolus.

It is possible that the MUC1 CT is found in the nucleolus in SNO as well as in WHCO1. The nucleolar staining in SNO may simply be "swamped" by the bright staining seen in the entire cell, therefore making the nucleolar straining less distinct than what is seen in WHCO1 which exhibits generally dimmer staining.

Together, the immunofluorescence and western blot data confirm the presence of MUC1 CT in the nucleus of at least WHCO1 and SNO. Since it has been suggested that the MUC1 CT may influence the nuclear accumulation of β-catenin, the next steps in this investigation were to assess the presence of nuclear β-catenin in these cell lines as well as to investigate the potential of a MUC1/β-catenin nuclear complex.

4.4.2 MUC1 interaction with β-catenin may be responsible for the disruption of β-catenin turnover in HOSCC

β-catenin is present in the nucleus of all 5 HOSCC cell lines investigated, as demonstrated by western blotting. This is of significance considering that β-catenin is reportedly not detectable in the nucleus of normal oesophageal cells and is thus potentially an indication of disrupted β-catenin turnover (Kimura *et al*., 1999, Ninomiya *et al*., 2000, Saeki *et al*., 2002). As discussed earlier, numerous other cancers exhibit mutations in important components of the β-catenin degradation machinery, resulting in

an accumulation of nuclear β-catenin, and the subsequent up-regulation of tumorigenic and metastatic genes (Morin, 1999). However, these mutations have been reported not to occur in HOSCC (Ninomiya *et al*., 2000, Saeki *et al*., 2002). There must therefore be an alternative mechanism for β-catenin nuclear accumulation in HOSCC.

In this report evidence is presented showing that MUC1 and β-catenin co-immunoprecipitate from nuclear extracts of each cell line. This is the first demonstration that MUC1 forms a complex with β-catenin in the nucleus of HOSCC, or any carcinoma of stratified epithelial origin. The MUC1 CT was not detected in the nuclear extracts of cell lines WHCO3 and WHCO6 in the previous western blot. However, immunoprecipitating with β-catenin is very likely to have concentrated the MUC1 CT, explaining why it was detected as part of the nuclear complex. Thus it is evident that the MUC1 CT is present in the nucleus of all cell lines investigated (in complex with β-catenin) but it is at a much lower concentration in cell lines WHCO3 and WHCO6. Also important to note is that when probing resolved nuclear extracts with the CT2 antibody (see Methods and Materials) the MUC1 CT was detected in a broad band from 28 to 20 kDa in cell lines WHCO1 and SNO. However, only a single highly specific 28 kDa band co-immunoprecipitates with β-catenin both at the membrane (as seen in Chapter 3) as well as in the nucleus (as demonstrated here). This indicates that only a specific fraction of the total pool of the MUC1 CT in these cell lines is present in a complex with β-catenin. There is thus a pool of MUC1 CT in the cell, and within the nucleus, that is not complexed to β-catenin. As detailed above, it has been reported that the MUC1 CT associates with γ-catenin in the nucleus of breast carcinoma cells. The suggestion is that the same may occur here. It is also possible that the remaining pool of the MUC1 CT that is not associated with β-catenin, associates with other, as yet unidentified, proteins. Further analysis of this "unaccounted for" MUC1 CT, particularly in the nucleus, is likely to give important insight into its roles in signalling.

Given that MUC1 and β-catenin form a complex in these cell lines together with the suggestion by Wen *et al.* (2003) that MUC1 stabilizes β-catenin, it is hypothesized that MUC1 plays a role in the deregulation of β-catenin turnover in these cells, resulting in its

nuclear localization. Further supporting this suggestion is the study by Baldus *et al.* (2004). They showed that MUC1 expression correlated with nuclear β-catenin in colorectal carcinomas. Moreover, they demonstrated that MUC1 expression and associated nuclear accumulation of β-catenin were correlated to a worse prognosis in colorectal carcinoma patients. This confirms the functional significance of both MUC1 expression and nuclear accumulation of β-catenin, and suggests that our findings may have important implications with regard to the tumorigenic and/or metastatic behaviour of these HOSCC cells.

Importantly, a recent study by Huang *et al.* (2005) provides a mechanistic basis for MUC1-mediated stabilization of β-catenin. As previously described, GSK3β is responsible for phosphorylating β-catenin and targeting it down the ubiquitination and degradation pathway, and thus plays a key role in maintaining cytoplasmic β-catenin at the appropriate levels. Huang *et al.* (2005) show that MUC1 blocks GSK3β-mediated phosphorylation and subsequent degradation of β-catenin, and in this way increases the level of β-catenin in the cytoplasm and nucleus. It is therefore suggested that this same mechanism of MUC1-mediated β-catenin stabilization exists in HOSCC. This proposal thereby provides an explanation and a potential mechanism for the demonstrated nuclear accumulation of β-catenin in these cells, a phenomenon that has, until now, been poorly understood.

Interestingly however, there is no apparent relationship between the concentration of MUC1 CT in the nucleus and the concentration of β-catenin in the nucleus of the HOSCC cells. That is, if MUC1 was responsible for stabilizing β-catenin we might expect the cell lines with the highest concentration of MUC1 CT in the nucleus to also exhibit the highest concentration of β-catenin in the nucleus. This is not the case; WHCO1 and SNO contain the highest concentrations of nuclear MUC1, but the lowest concentrations of nuclear β-catenin. This could however, simply be a reflection of the complexity of the system. As has already been discussed, in cell lines WHCO1 and SNO the MUC1 CT may have additional roles, such as the mediation of γ-catenin signalling. Similarly, WHCO5, for example, has the highest concentration of nuclear β-catenin. This could be

as a result (for example) of a lower concentration of APC, which as well as being involved in β-catenin degradation also functions to retain β-catenin in the cytoplasm and inhibit its translocation to the nucleus (Krieghoff *et al.,* 2006).

On the other hand, however, these results (showing that nuclear MUC1 and nuclear β-catenin concentrations do not necessarily match) could support the suggestion by Huang *et al.* (2003) that rather than stabilizing β-catenin, MUC1 is an important component of the β-catenin/LEF/TCF transcription factor complex. What is interesting to note in terms of this suggestion, is that the nuclear concentration of the MUC1/β-catenin complex does not appear to be controlled by the concentration of one or other of the components. For example, the concentration of the complex cannot be determined by the concentration of the MUC1 CT in the nucleus, as WHCO5 exhibits a particularly low concentration of nuclear MUC1 CT but has the highest concentration of the complex. Similarly, SNO exhibits the lowest concentration of nuclear β-catenin but the second highest concentration of the complex. Where there is a low concentration of both MUC1 CT and β-catenin, for example in WHCO6, there is a low concentration of the complex. However, where there is a high concentration of either MUC1 CT or β-catenin, there is a high concentration of the complex, such as in WHCO5. This suggests that it is not the concentration of either the MUC1 CT or the β-catenin that is important but the concentration of the complex that is controlled, which is in keeping with the suggestion that the complex, rather than just β-catenin, is important in gene transcription. However, this is speculation and needs to be supported by further experimental evidence. An additional complicating factor is that MUC1 and TCF/LEF may compete for binding to β-catenin since they potentially bind to the same binding site on β-catenin. In order to determine if MUC1 is indeed a component of the transcription factor complex in these cells it would be useful to conduct a MUC1-specific electrophoretic mobility shift assay using the LEF/TCF binding motif as a probe. However, this exigent experiment would have to form the basis of a further study, and could not be included here. It is important to keep in mind that there is nothing to suggest that a "stabilizing" role for MUC1 and a "transcriptional" role are mutually exclusive. It is possible, and even likely, that MUC1

plays a role in stabilizing β-catenin as well as a role in the actual transcription factor complex.

It stands to reason that if MUC1 association with β-catenin stabilizes β-catenin and enhances its translocation to the nucleus, then any increase in association between MUC1 and β-catenin is likely to increase the overall concentration and nuclear translocation of β-catenin. We therefore sought to determine if increases in association between MUC1 and β-catenin generated by EGFR activation, as in the previous chapter, would be reflected as an increase in nuclear β-catenin concentration. If this were to prove true, it would provide an additional mechanism for EGFR-mediated gene transcription.

The results of western blot analysis conducted on nuclear extracts after EGF treatment of the HOSCC cells (designed to reproduce the same changes in MUC1/β-catenin association exhibited at the membrane in the previous chapter) indicate that treatment does modulate the concentration of nuclear β-catenin. Just as each cell line responded differently to EGF treatment in terms of MUC1/β-catenin association at the cell membrane, each cell line responds differently to EGF treatment in terms of the changes in nuclear β-catenin concentration.

4.4.3 EGFR activation modulates the nuclear concentration of β-catenin

WHCO1 exhibits only a minor increase in membranous MUC1/β-catenin association with respect to untreated versus treated, and this occurs after 30 min of treatment. Overall, after the 3 hour treatment period, association between MUC1 and β-catenin is substantially reduced. Interestingly, the concentration of nuclear β-catenin is also substantially reduced after the 3 hour treatment period. This could indicate that the reduction in association between MUC1 and β-catenin at the cell membrane results in degradation of β-catenin, explaining the reduction in nuclear β-catenin. However, these results could also indicate that during the 3 hour period the overall concentration of β-catenin in the cell is being reduced either through inhibition of transcription or through degradation.

In WHCO3, an increase in MUC1/β-catenin association after an hour of treatment is accompanied by a simultaneous increase in nuclear β-catenin. Thus it is possible that in this cell line an increase in association between MUC1 and β-catenin at the cell membrane allows stabilization and nuclear translocation of β-catenin. After 3 hours of treatment there is a dramatic reduction in nuclear β-catenin as well as a decrease in association of the MUC1/β-catenin complex. It is possible that the cell is reacting to the substantial increase in nuclear β-catenin by increasing the functioning of the degradation complex, resulting in a reduction of total cellular β-catenin.

After 5 min of treatment WHCO5 exhibits a dramatic increase in the association of MUC1 and β-catenin at the cell membrane, this is accompanied by a comparably dramatic reduction in nuclear β-catenin. It is possible that the dramatic increase in association of MUC1 and β-catenin at the membrane, brought about by EGFR activation, recruits β-catenin out of the nucleus. This might explain the associated reduction in nuclear β-catenin. Further EGF treatment is associated with a steady increase in nuclear β-catenin as the concentration of the membrane complex drops. Thus, in this case, a massive increase in MUC1/β-catenin association is followed by a steady increase in nuclear β-catenin concentration, potentially suggesting that MUC1 stabilizes β-catenin in WHCO5.

WHCO6 exhibits a substantial increase in MUC1/β-catenin association after 3 hours of treatment. After this same period of treatment the concentration of β-catenin has decreased. Thus, perhaps similar to WHCO5, the substantial increase in MUC1 and β-catenin association at the membrane has recruited β-catenin out of the nucleus to the membrane. SNO, on the other hand exhibits a steady increase in association between MUC1 and β-catenin at the cell membrane, however, there is little change in the concentration of nuclear β-catenin.

Together, these results show that in some cases (WHCO3 and WHCO5) MUC1 association with β-catenin may result in stabilization of β-catenin and thus an increase in nuclear β-catenin concentration. However, the results also show that the translocation of

β-catenin to the nucleus is a complex event and is more likely mediated by numerous converging influences than simply by the interaction of MUC1 with β-catenin. Furthermore, validation of the functional significance of the MUC1/β-catenin complex is required before we can truly grasp the implications of such a complex in the context of cell signalling and gene transcription.

CHAPTER 5: THE NUCLEAR MUC1/β-CATENIN COMPLEX AND ITS RELATIONSHIP WITH MMP7 EXPRESSION

5.1 Introduction

The MUC1/β-catenin nuclear complex has been implicated in activating transcription of Wnt responsive genes in general and the cyclin D1 gene in particular (Huang *et al.*, 2003). In the preceding chapters it has been demonstrated that the MUC1/β-catenin complex is located to the nucleus, as well as to the membrane, in 5 moderately differentiated HOSCC cell lines. The aim here was thus to determine the potential impact of the MUC1/β-catenin nuclear complex on Wnt-related gene transcription in these HOSCC cells.

The matrix metalloproteinase-7 (MMP7) gene contains two TCF binding elements located upstream of the transcriptional start site in its promoter region. It has further been confirmed as a target of β-catenin mediated transactivation (Brabletz, 1999, Crawford et *al*., 1999, Gustavson *et al*., 2004). Moreover, MMP7 expression is associated with a highly invasive phenotype (Liotta *et al*., 1980, Mori *et al*., 1995, Honda *et al*., 1996). Since malignancy is a characteristic of HOSCC, evaluation of MMP7 expression in these lines would be of value. MMP7 was thus selected for further analysis in these HOSCC lines due to the fact that it is both a Wnt responsive gene as well as a gene that may give additional insight into the factors contributing to the transformed behaviour of these cells.

Matrix metalloproteinases (MMPs) are a family of zinc-dependent endoproteinases whose enzymatic activity is directed against components of the ECM (Kleiner and Stetler-Stevenson, 1999). MMPs play an essential role in tissue re-modeling in various physiological and pathological conditions such as development, tissue repair and tumour invasion (Matrisian, 1992, Vansaun and Matrisian, 2006). These proteinases are linked by a core of common domain structures and by their relationship to a family of proteinase inhibitors called the tissue inhibitors of metalloproteinases (TIMPs). TIMPS inhibit MMPs by forming tight-binding non-covalent associations with the active site of the

MMPs (Kleiner and Stetler-Stevenson, 1999). Members of the MMP family are classified into sub-groups, collagenases, gelatinases, stromelysins and others, based predominantly on their substrate specificity (Curran and Murray, 1999). MMP7 is similar to the stromelysins in its substrate specificity; however, it also exhibits characteristics that are unique. Notably, MMP7 is by far the smallest member of the MMP family, and lacks the C-terminal segment encoded by all other MMPs (Wilson and Matrisian, 1996, Kawabata *et al*., 2005). Also, the majority of the MMPs are produced in the stroma surrounding tumour cells, MMP7, however, is localized to the tumour cells themselves (Wilson and Matrisian, 1996).

MMP7 is transcribed and translated to produce a 28 kDa latent pro-form, before being cleaved by proteases such as trypsin, to form an active peptide of 19 kDa (Miyazaki *et al*., 1990). MMP7 expression has been detected in various neoplastic tissues, including colorectal, gastric, breast, pancreatic and oesophageal cancer tissues (Kawabata *et al*., 2005). Importantly, the level of MMP7 expression in colorectal cancers is known to be significantly correlated with clinicopathological characteristics; whereby an inverse relationship between MMP7 expression and 5-year patient survival rate has been observed (Adachi *et al*., 2001). MMP7 has a broad substrate specificity and is capable of degrading proteoglycans, fibronectin, entactin, laminin, gelatin, and elastin (Zeng *et al*., 2002). As such, MMP7 expression is thought to enhance tumour invasion by facilitating ECM degradation. ECM degradation by MMP7 is also important in maintaining the tumour microenvironment, and thus promotes tumour growth (Curran and Murray, 1999). More recently, however, MMP7 has been shown to play additional roles in tumorigenesis through the regulation of several biochemical processes such as the activation, degradation and shedding of non-ECM proteins (Ii *et al*., 2006). For example, proteolysis of insulin-like growth factor binding protein by MMP7 results in increased bioavailability of insulin-like growth factors and enhanced cellular proliferation. Similarly, cleavage of heparin-binding EGF precursor into its mature form also promotes cellular proliferation. On the other hand, MMP7 mediated cleavage of membrane-bound Fas ligand into soluble Fas ligand increases apoptosis of cells adjacent to tumour cells. Interestingly, MMP7 converts E-cadherin to a soluble form which results in the reduction of cell-cell adhesion

and the promotion of invasion (Ii *et al*., 2006). Thus MMP7 expression mediates cancer progression via multiple mechanisms.

Experiments conducted as part of this chapter aimed to investigate the possibility of a relationship between nuclear localization of the MUC1/β-catenin complex and the expression of MMP7 in HOSCC cell lines.

5.2 Methods & Materials

5.2.1 Antibodies

Rabbit anti-MMP7 (Sigma), directed against the N terminal of the catalytic site which contains the highly conserved zinc binding domain, was used in western blot analysis. HRP-bound anti-rabbit IgG antibody (Sigma) was used to detect the anti-MMP7 antibody.

5.2.2 RNA extraction and cDNA synthesis

RNA extraction and cDNA synthesis were carried out according to the procedure described in Chapter 2.

5.2.3 Amplification of a fragment of MMP7

The following primers (from Kawabata *et al*., 2005) were used to amplify a 420 bp fragment of MMP7:

Forward 5′ TCTTTGGCCTACCTATAACTGG 3′
Reverse 5′ CTAGACTGCTACCATCCGTC 3′

The PCR reaction mixtures were prepared according to the procedure described in Chapter 2. Samples were amplified for 30 cycles under the following conditions: 1 min at 95°C, 1 min at 48°C and 1 min 30 seconds at 72°C. PCR products were electrophoresed on a 1% agarose gel.

5.2.4 Western blot analysis

Whole-cell lysate (40 µg) (prepared as described in Chapter 2) was separated on a 12.5% SDS-PAGE gel. Protein was then transferred to nitrocellulose membrane according to the

procedure outlined in Chapter 2. The membrane was blocked in casein-based blocking buffer (Blotto) for 45 min at room temperature. After 6 rinses in PBS, the primary antibody, anti-MMP7 (1:1000) was applied for 1 hour 30 min at room temperature. After 6 PBS washes of 5 min each, HRP-bound anti-rabbit IgG (1:5000) was applied for 1 hour at room temperature. The secondary antibody was rinsed off by washing the membrane 6 times in PBS (5 min each). The membrane was then placed in peroxide: luminol (1:1) for 5 min, in the dark, before exposure to hyperfilm.

5.2.5 Sample preparation for casein zymography

Cells (representative of WHCO1, WHCO5 and SNO) were rinsed 3 times in PBS before being scraped down and transferred to a sterile eppendorf. The cells were centrifuged for 5 min in the Tomy Capsule HF-120 bench top centrifuge (1200 x g) and the supernatant was removed. 200 µl of a denaturing, but non-reducing lysis buffer (see Appendix 7.23) was added to the cell pellet, before briefly vortexing. The samples were incubated at 37°C for 1 hour. For the positive control, 2 µg/µl of α-chymotrypsin was dissolved in the same buffer, and was also incubated at 37°C for 1 hour.

5.2.6 Casein zymography

Two 8% SDS-PAGE gels were set up according to the procedure outlined in Chapter 2, except for the addition of 50 µl of 15% non-fat milk powder (in separating buffer) to the separating gel. One gel was loaded with a maximum volume of 20 µl (equivalent to approximately 40 µg protein) of sample (described above) in 3 lanes, with 2 µl of 2 µg/µl of α-chymotrypsin in a forth lane. The aim of the second gel was to obtain an estimation of the sensitivity of the assay. In this gel, lanes were loaded with 2 µl of 1:10, 1:100, 1:500, 1:1000 and 1:2000 dilutions of the original α-chymotrypsin control sample.

The gels were electrophoresed under non-denaturing conditions (15mA), at 4°C for 2 hours. The gels were washed twice in zymography washing buffer (see Appendix 7.23) for 30 min at room temperature to remove SDS and allow renaturation of proteins. The

gels were developed by incubation in zymography developing buffer (see Appendix 7.23) for 72 hours at 37°C. The gels were then stained and destained according to procedure outlined in Chapter 2 for SDS-PAGE.

5.3 Results

5.3.1 MMP7 expression in HOSCC cell lines

The presence of the expected target fragment of 420 bp in lanes representative of each HOSCC cell line is a clear indication that the MMP7 gene is expressed in all 5 HOSCC cell lines investigated (Figure 5.1). The target fragment was generated by RT-PCR analysis using primers specific to MMP7 cDNA.

5.3.2 The presence of the MMP7 protein

Western analysis was conducted on whole-cell protein lysates using an antibody that detects both the latent form of MMP7 (pro-MMP7) as well as the activated form of MMP7. A specific 19 kDa band is evident in lanes representative of all 5 HOSCC cell lines investigated (Figure 5.2b). Since 19 kDa is the size of the activated form of MMP7, the result indicates the presence of the active form of MMP7 in each of these cell lines. Densitometric analysis of the western blot (see Figure 5.2a) shows that WHCO3 contains the most activated MMP7, closely followed by WHCO5 (83%). WHCO1 (44%) and SNO (30%) contain more of the 19 kDa MMP7 than WHCO6 (29%). There was no band at 28 kDa, which is the size of pro-MMP7. (See Appendix 7.24 for raw densitometric data.)

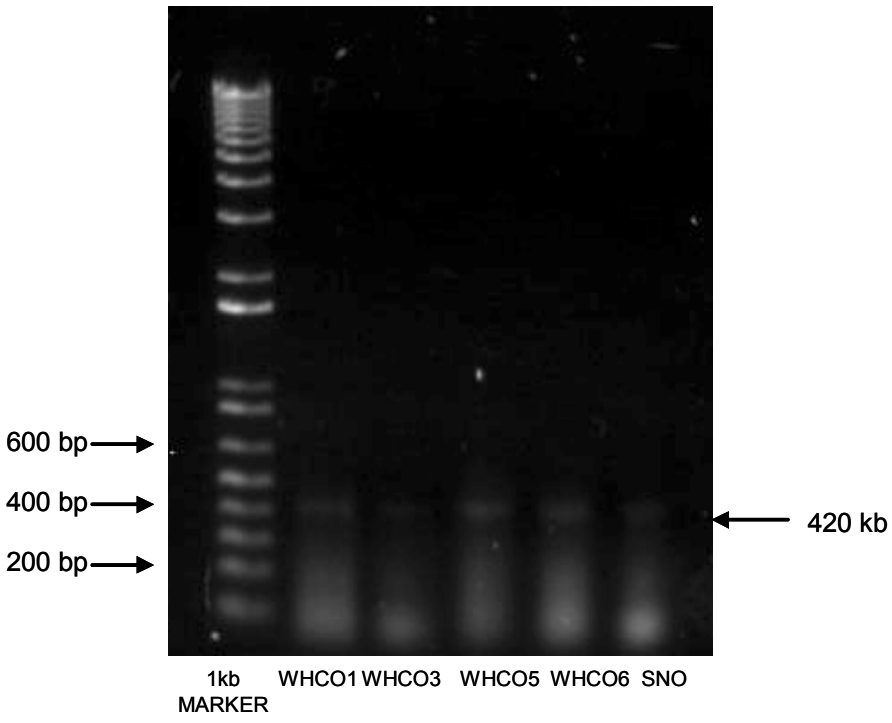

Figure 5.1: MMP7 is expressed in 5 HOSCC cell lines. The presence of a 420 bp target fragment, generated by MMP7-specific RT-PCR, in all lanes shows that the MMP7 cDNA transcript is present in samples representative of all 5 HOSCC cell lines.

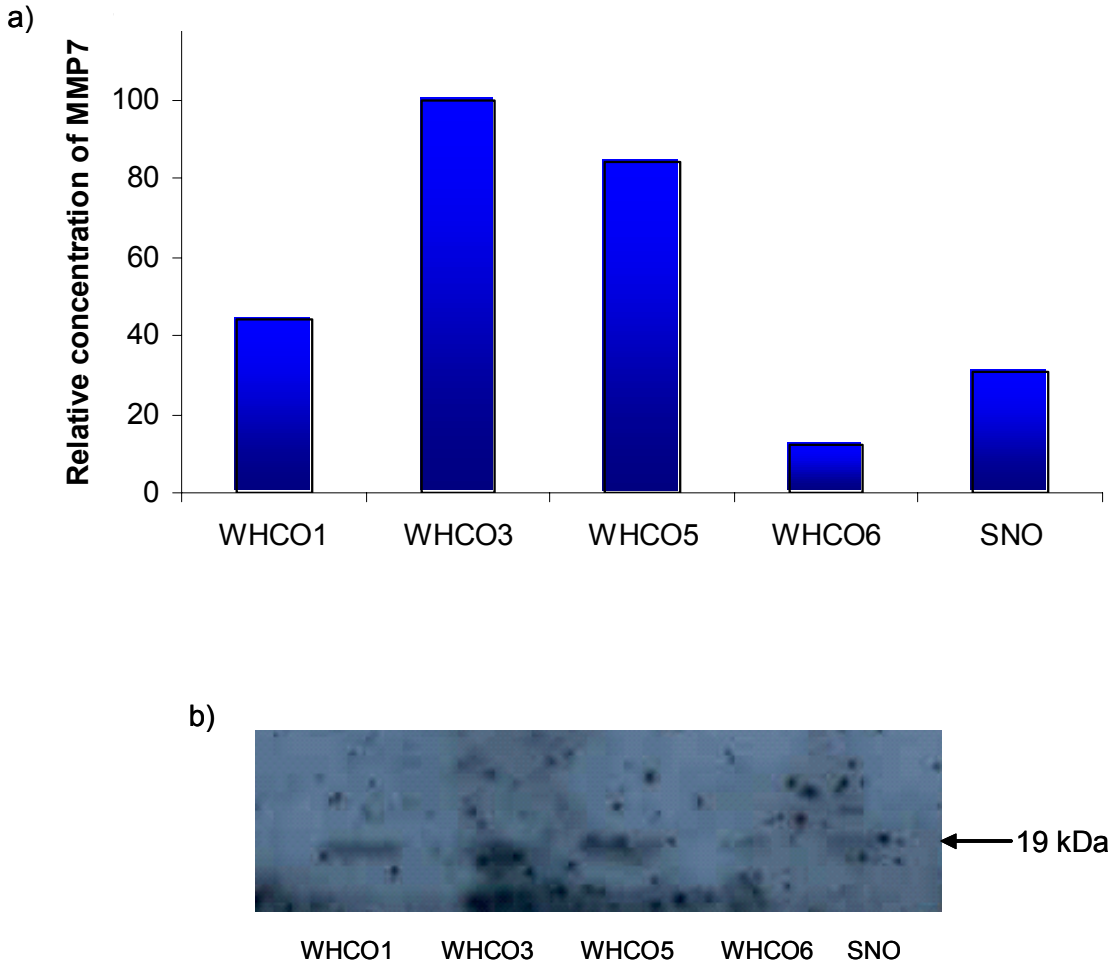

Figure 5.2: The enzymatically active 19 kDa MMP7 protein isoform is present in whole-cell lysates from 5 HOSCC cell lines, as demonstrated by western blotting analysis. The 28 kDa MMP7 pro-form is not apparent in HOSCC cell extracts; however, the active 19 kDa form is detected.

5.3.3 MMP7 activity

The activity of MMP7 was to be investigated using a casein zymography assay. This procedure is based on the ability of both the pro and activated forms of MMP7 to hydrolyze casein. Protein is extracted from cells and separated on a casein-containing 8% SDS-PAGE gel (or in this case a non-fat milk powder containing-gel) in such a way as to minimize denaturation and prevent reduction of the proteins. Subsequent to separation in the SDS-PAGE gel, SDS is washed out of the gel and the protein is allowed to renature. The gel is then placed in a buffer (zymography developing buffer) that supports the activity of MMP7. Active enzyme thus hydrolyses casein, leaving a clear band on a darker background after the Coomassie Blue staining procedure.

In order to confirm that all aspects of the assay were functional and to obtain an estimation of the sensitivity of the assay, a titration was carried out using a sample of α-chymotrypsin. The α-chymotrypsin (2 μg/μl) was prepared according to the standard preparation method for the samples from each of the cell lines. Each dilution (2 μl each of 1:10, 1:100, 1:500, 1:1000, and 1:2000) was loaded into a separate well and the assay carried out as described above. Clear bands are visible in lanes representative of 400 ng (1:10), 40 ng (1:100), 8 ng (1:500) and 4 ng (1:1000) respectively with no band visible in the lane representative of 2 ng (1:2000) of α-chymotrypsin (Figure 5.3a). This indicates that the assay is sensitive enough to detect α-cyhmotrypsin activity down to 4 ng but not to 2 ng of protein. The experiment thus showed that the assay is successful in detecting the activity of proteins able to cleave casein.

In Figure 5.3b, it is apparent that the positive control of α-chymotrypsin yielded a clear band, indicating that the enzyme is active and is capable of cleaving the casein contained in the milk powder. The electrophoresis and separation of the proteins was successful as indicated by the numerous dark bands in lanes containing protein samples. However, there were no clear bands, or lighter patches, in those lanes.

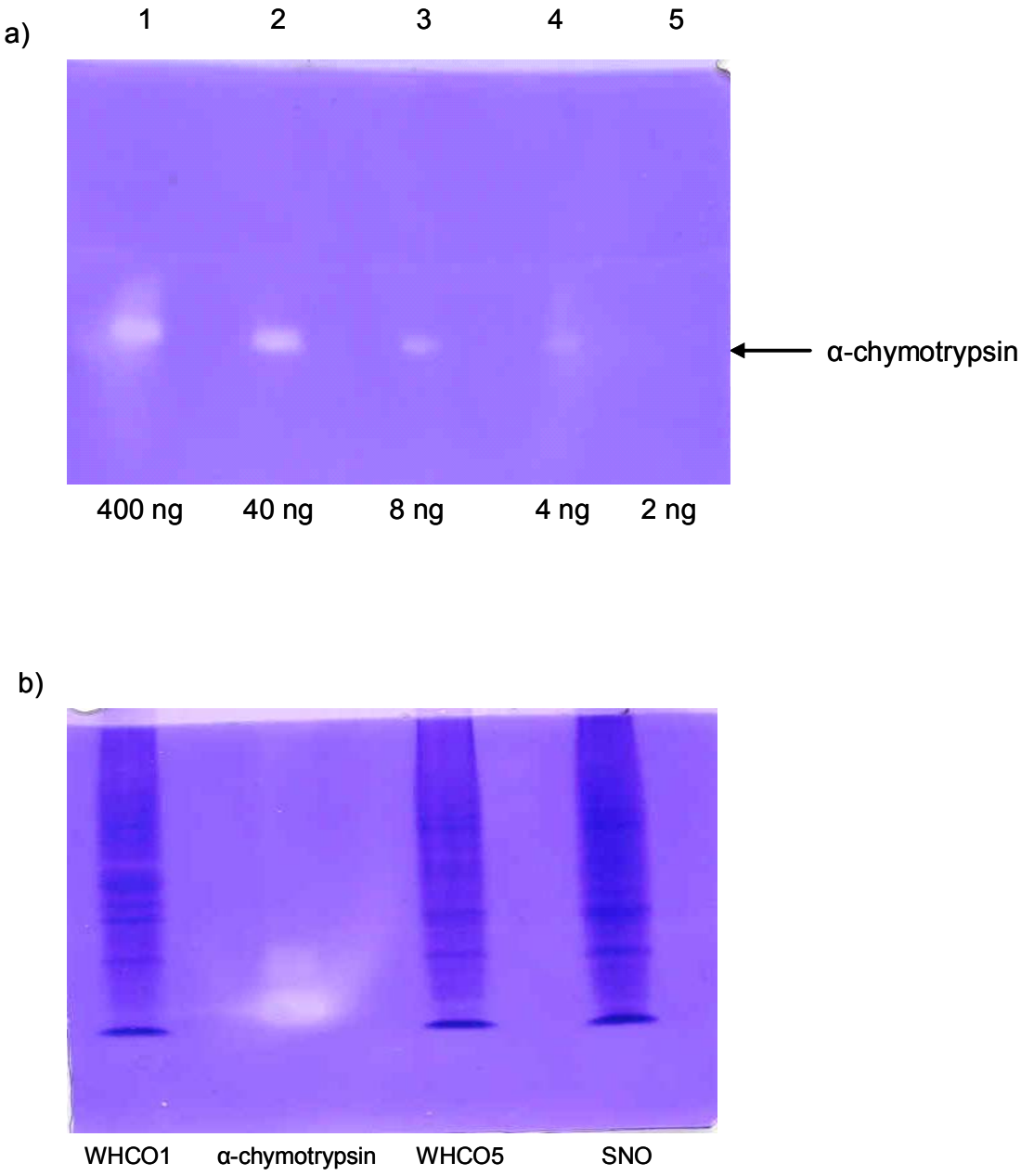

Figure 5.3: **Casein zymography assays successfully detected α-chymotrypsin-mediated casein hydrolysis.** a) The casein zymography assay was able to detect down to 4 ng of α-chymotrypsin that had been electrophoresed through a casein-containing SDS-PAGE gel. b) The α-chymotrypsin positive-control sample successfully hydrolysed the casein, however, no hydrolysis was apparent in lanes containing HOSCC samples.

5.4 Discussion

MMP7 is an endoproteinase that is considered to be important in contributing to the tumorigenic and invasive behaviour of cells in which it is expressed (Kleiner and Stetler-Stevenson, 1999, Zeng *et al*., 2002, Ii *et al*., 2006). Here, it is shown (using RT-PCR) that the MMP7 gene is expressed in 5 moderately differentiated HOSCC cell lines. Moreover, it was shown that the activated 19 kDa MMP7 protein is present in these lines. Interestingly, the 28 kDa pro-MMP7 was not detected by western blot analysis. It must however have been present in the cell lines as it is the 28 kDa pro-MMP7 that undergoes cleavage and generates the active 19 kDa form. It is possible, and even likely, that the 28 kDa form is present in the cell lysates but at a level that is below the level of detection for this experimental method, especially when considering that the 19 kDa bands are themselves of a relatively low optical density (see Appendix for densitometric readings). It is also possible that the extraction procedure may release compartmentalized enzymes and would give rise to protein interactions not otherwise occurring in an intact cell. This may, in turn, result in the cleavage of the 28 kDa pro-form to produce the 19 kDa form.

The casein zymography was not successful in detecting MMP7 activity. However, since the active 19 kDa band was detected in the western blot it is possible that the zymography outcome is more a product of a limitation of the experiment itself, rather than due to an absence of active MMP7. Successful casein zymographies are characterized by numerous clear bands as a result of etching of the casein (see Zeng *et al*., 2002). These bands range from over 130 kDa to 19 kDa, representing numerous proteins that are capable of cleaving casein, that is, casein zymography detects the activity of numerous proteins (including other members of the MMP family) and is not limited to the detection of MMP7 activity. However, Figure 5.3b shows a complete lack of etching at all molecular weights. It is unlikely that these cell lines do not contain any proteins with the capability of hydrolyzing casein. The fact that the positive control (α-chymotrypsin) was successful indicates that the procedure was carried out as it should have been and that no steps were eliminated. The fact that the α-chymotrypsin remained active also indicates that the sample preparation procedure did not irreversibly denature (and thereby deactivate) the

protein. A possible reason for the "negative result" obtained for this experiment is that there is not enough active protein in each lane to result in etching of the casein. Zeng *et al*. (2002) conducted a similar casein zymography using protein samples from colorectal cancer liver metastases. Whereas we were limited (due to the size of the wells) to loading approximately 40 μg of protein per lane, they loaded 125 μg of protein per lane. With this in mind, we investigated the possibility of concentrating the protein samples by adding 100 μl of the zymography sample buffer to a standard cell pellet, rather than 200 μl as described in methods and materials above. However, as the sample buffer is non-reducing the concentrated samples remained extremely viscous and could not be successfully pipetted and loaded. This discussion, therefore, focuses on the results of the RT-PCR and the western blot analyses which together indicate that the MMP7 gene is expressed and that the activated 19 kDa MMP7 protein is present in these HOSCC cell lines.

First there will be a discussion of the potential relationship between MMP7 expression and nuclear localization of the MUC1/β-catenin complex; the discussion will then go on to detail the significance of MMP7 expression in terms of the behaviour of these cells.

In vitro studies have shown that β-catenin, when translocated into the cell nucleus functions as an oncogene by transactivating tumorigenic and metastatic related genes, including MMP7 (Brabletz *et al*., 1999, Ougolkov *et al.*, 2002, Iwaya *et al*., 2003, Wong *et al*., 2004). In murine intestinal tumours MMP7 transcripts show striking overlap with the accumulation of the β-catenin protein. Crawford *et al.* (1999) showed that activation of the MMP7 promoter is up-regulated as much as 12-fold by β-catenin in colon tumour cell lines in a manner that is inversely proportional to the endogenous levels of the β-catenin/TCF complex. Of great interest to the present study was a study conducted by Saeki *et al*. (2002) on the interrelation between the expression of MMP7 and β-catenin in oesophageal cancer. Again, it was shown that MMP7 expression exhibited a striking overlap with nuclear accumulation of β-catenin. Immunohistochemical analysis demonstrated a nuclear accumulation of β-catenin in 12 (35.3%) of the 34 oesophageal squamous cell carcinomas investigated. Seven of those carcinomas (20.6% in total) demonstrated MMP7 expression. These findings thus support the notion that nuclear

translocation of β-catenin is one mechanism contributing to MMP7 expression. Similar findings have been reported for the relationship between the accumulation of nuclear β-catenin and cyclin D1 expression (Utsunomiya *et al*., 2001, Yamazaki *et al*., 2003, Li *et al*., 2005). Importantly, it was recently shown that the interaction between the MUC1 CT and β-catenin is essential for β-catenin-mediated transactivation of cyclin D1 expression (Huang *et al.*, 2003). Considering that, like cyclin D1, MMP7 is a Wnt/β-catenin-target gene, the possibility exists that MUC1/β-catenin interaction is also required for MMP7 expression. The aim of experiments conducted as part of this chapter was to further investigate this possibility.

In the previous chapters it was demonstrated that the MUC1/β-catenin complex is located in the nucleus of all of these cell lines. We have now shown that MMP7 is expressed in all of these lines. However, it is not clear whether it is β-catenin alone, or the MUC1/β-catenin complex that is contributing to the expression of MMP7 in these lines. Nevertheless, what is important to note is that these data do not negate the possibility of a role for MUC1 in β-catenin mediated signalling. With this in mind it is interesting that WHCO6, which exhibits the lowest relative concentration of the nuclear MUC1/β-catenin complex (26%) by a considerable margin, exhibits the lowest relative concentration of MMP7 (12%), also by a considerable margin.

It is also interesting to observe that in the study by Saeki *et al.* (2002) only 7 of the 12 carcinomas that exhibited nuclear β-catenin were positive for MMP7 expression. A possible explanation for this would be a requirement for MUC1 in the activation of transcription of the MMP7 gene, a requirement that is perhaps not met in 5 out of those 12 carcinomas. This however is speculation and further studies would have to be conducted to determine the merit of this suggestion.

The probable role of MMPs *in vivo* is to degrade most components of the ECM (Zeng *et al*., 2002). MMP7 in particular has a broad substrate specificity as well as the highest activity against insoluble elastin. Elastin is the highly cross-linked ECM component of elastic connective tissues such as blood vessels. Zeng *et al*. (2002) suggest that the

capability of MMP7 to degrade vascular basement membranes indicates a potential to facilitate haematogenous metastases. Saeki *et al.* (2002) show that MMP7 expression correlates with penetrating tumour invasion in oesophageal cancer. An additional study revealed that overexpression of MMP7 can affect lymph node metastasis via lymphatic permeation and could thus be an independent prognostic factor for oesophageal carcinoma (Yamashita *et al.,* 2000). Similarly, a third study showed that MMP7 expression at the invasion front is likely to contribute to the more invasive phenotype of carcinoma cells, resulting in the progression of oesophageal squamous cell carcinoma (Yamamoto *et al.,* 1999). Moreover, they showed a correlation between MMP7 expression with disease recurrence and shorter disease-free and overall survival time. Together, these investigations into the clinical significance of MMP7 expression in oesophageal carcinoma highlight MMP7 as an important contributor to the aggressive behaviour of HOSCC cells.

CHAPTER 6: GENERAL DISCUSSION AND CONCLUSION

6.1 MUC1 expression and localization influences cell behaviour

MUC1 is a multi-faceted oncoprotein whose overexpression correlates with aggressiveness of tumours and poor survival of cancer patients (Schroeder *et al*., 2003, Schroeder *et al*., 2004, Patel *et al*., 2005, Hattrup and Gendler, 2006). The oncogenic effects of MUC1 expression appear to stem from its adhesion modulating properties as well as the signalling capabilities of its cytoplasmic tail (Hilkens *et al*., 1992, Regimbald *et al*., 1996, Schroeder *et al*., 2003, Patel *et al*., 2005, Thompson *et al*., 2006). Previous studies have focused largely on MUC1 expression and the associated implications of MUC1 expression in carcinomas derived from simple epithelia. In this study, we set out to investigate MUC1 expression and the potential functional roles of MUC1 in human oesophageal squamous cell carcinoma, an aggressive cancer-type that is derived from a stratified epithelium.

Expression analysis (by RT-PCR) generated the expected MUC1 target fragment of 400 bp in each of the 5 HOSCC cell lines examined. The presence of the target fragment provides a clear demonstration of positive MUC1 expression in these HOSCC cell lines. Moreover, the lack of a band in samples representative of negative controls confirms the specificity of the reaction. The primers used in the experiment were specific for the cytoplasmic tail domain of MUC1 and spanned the region coding for the β-catenin, c-Src and GSK3β binding sites. The fact that each cell line generated the same size fragment of 400 bp indicates that there are no major insertions or deletions occurring within these binding sites. The MUC1 promoter region contains putative binding sites for a number of regulatory proteins. However, at this stage in the investigation, it is not clear what elements are responsible for MUC1 expression in these HOSCC cell lines. It may be postulated that STAT proteins have a role to play in activating MUC1 expression in HOSCC, however, further analysis will be required to conclusively identify the factors contributing to MUC1 expression.

MUC1-specific immunoblotting, conducted on resolved whole-cell extracts, demonstrated the presence of numerous MUC1 isoforms in all 5 HOSCC cell lines. This is in keeping with previous reports that have shown MUC1 to be highly polymorphic as a result of allelic polymorphisms in the tandem repeat region, the expression of alternatively spliced isoforms as well as differential glycosylation (due to transformation-associated changes in expression of glucosyltransferases) (Gendler and Spicer, 1995, Taylor-Papadimitriou *et al.,* 1999, Gendler, 2001).

There is a high degree of uniformity among the 5 HOSCC cell lines assessed here, in terms of the specific isoforms that are present. The homogeneous nature of MUC1 isoform expression in these lines (as demonstrated by identical western blotting profiles) may imply that the MUC1 alleles are identical across the cell lines (i.e. each genome contains the sequence for the same number of tandem repeats), that the same alternatively spliced isoforms are present, and that the cells express the same profile of glucosyltransferases. This is in stark contrast to what has been demonstrated for breast carcinoma (Walsh *et al*., 2000). A survey of 14 breast carcinoma cell lines was characterized by a considerable heterogeneity in terms of MUC1 expression. There was little uniformity, both in terms of MUC1 mRNA expression (as demonstrated by northern blot analysis) and in terms of the presence of various protein isoforms (as demonstrated by western blotting). Only 2 (out of 14) of the breast cancer cell lines exhibited identical MUC1-specific western blotting profiles whereas all 5 of the HOSCC cell lines investigated exhibited the same western blot profile. The mechanisms leading to the heterogeneity of MUC1 expression in breast carcinoma are not clear. It has yet to be determined whether this heterogeneity represents clonal differences in MUC1 transcriptional activation or temporal changes in expression within individual cells, perhaps related to the cell cycle (Walsh *et al.,* 2000).

Regardless of the heterogeneity of expression in breast, it is apparent that there are no clonal differences in the HOSCC cell lines with regards to MUC1 transcriptional activation as well as MUC1 glycosylation. This is interesting as it suggests that whatever the mechanism controlling MUC1 expression in HOSCC (at least in moderately

differentiated HOSCC), it is maintained and is uniform across all the HOSCC cell lines investigated. Notably, the cell lines used in this investigation are all derived from moderately differentiated carcinomas. It may therefore be interesting to investigate whether a similar uniformity of MUC1 expression exists across cell lines derived from both poorly differentiated and well differentiated carcinomas.

The antibody used in the above-described immunoblotting procedure is specific for an under-glycosylated form of an epitope located within the tandem repeat region of the MUC1 extracellular domain. Antibody binding is therefore an indication that MUC1 is aberrantly, and specifically under-glycosylated in these HOSCC cell lines. This has implications relating to the cellular distribution of MUC1, the ability of MUC1 to adhere to selectins and the interaction of MUC1 with the immune system (Regimbald *et al*., 1996, Altschuler *et al*., 2000, Taylor-Papadimitriou and Burchell, 2002). O-linked glycans potentially target MUC1 to the apical membrane, thus modifications in the glycosylation pattern of MUC1 may result in its aberrant localization over the entire cell membrane (Altschuler *et al*., 2000). The rate of clathrin-mediated MUC1 endocytosis is up-regulated in cases where MUC1 is under-glycosylated. This may result in the accumulation of aberrantly glycosylated MUC1 within the cytoplasm of cells, an event that has been reported for tumour cells (Rahn *et al*., 2001). The data presented here, indicating that MUC1 is both aberrantly glycosylated and localized within the cytoplasm of HOSCC cells, is in keeping with this concept.

Aberrant glycosylation may generate (or expose) specific epitopes of MUC1 that are known to act as ligands for selectin molecules present on endothelial cells lining vessels of the circulatory system (Regimbald *et al*., 1996). Importantly, MUC1-mediated attachment of neoplastic cells to vessel walls may promote cell migration, thereby enhancing the metastatic capabilities of those cells. The interaction of MUC1 with the immune system, on the other hand, is more complex. Under-glycosylation of MUC1 may unmask core protein epitopes that were previously hidden by long complexly branched carbohydrates (Taylor-Papadimitriou and Burchell, 2002). These novel epitopes, should they come into contact with cells of the immune system while either still tethered to the

cell surface or after they have been shed from the cell surface, will be recognized as foreign. An immune response will then be mounted against cells expressing the novel (MUC1) epitope (Taylor-Papadimitriou and Burchell, 2002). However, although the response is elicited specifically against cells expressing MUC1, MUC1 itself may protect against immune system attack by sterically hindering interactions between MUC1 and immune system effector cells, such as CTLs (Chan *et al*., 1999). Thus, the apparent aberrant glycosylation of MUC1 in these cells may impact upon various aspects of cell behaviour, including the interaction of these cells with the immune system.

In healthy cells, MUC1 is restricted to the apical membrane (Hilkens *et al*., 1992). Our data indicates that in these HOSCC cell lines, apical localization is lost and MUC1 is located over the entire cell membrane as well as within the cytoplasm. Considering both the above described implications of aberrant MUC1 glycosylation as well as the fact that loss of polarization is characteristic of cancer cells, this is not surprising. Moreover, this pattern of MUC1 cellular distribution is in keeping with what has previously been reported for other tumour cells and cell lines (Rahn *et al*., 2001, Hollingsworth and Swanson, 2004). Importantly, the circumferential and cytoplasmic staining, as demonstrated in these HOSCC cells, are associated with metastasis and a poor prognosis in carcinomas of the breast and lung as well as in colorectal adenocarcinomas (Rahn *et al*., 2001, Guo *et al*., 2006). A further demonstration of the significance of MUC1 circumferential localization in tumour cells was provided by a recent study that investigated the anti-tumour effect of the anti-KL-6/MUC1 antibody (Doi *et al.,* 2006). Anti-KL-6 recognizes a particular MUC1 tumour-associated sialylated sugar chain. Breast carcinoma cell lines expressing MUC1 abundantly over the cell membrane, grown in suspension culture without aggregation, were exposed to anti-KL-6. The antibody induced capping of MUC1 and resulted in E-cadherin-mediated cell-cell adhesion. Moreover, anti-KL-6 enhanced the cytotoxic activity of lymphokine-activated killer cells. It appears that the capping of MUC1 restores functioning of cell surface proteins including adhesion molecules and tumour antigens, leading to inhibition of tumour proliferation due to cell-cell adhesion and increased accessibility of immune effector cells. Keeping in mind the relationship that exists between MUC1 expression/aberrant

localization and prognosis in other cancer-types, it may be of value to investigate the potential relationship between MUC1 expression and aberrant localization with prognosis in HOSCC.

Integrins are crucial regulators of cell behaviour (Giancotti and Rouslatti, 1999). It is therefore of significance that MUC1 expression (and membrane localization) is associated with the disruption of integrin function in melanoma cells (Wesseling *et al.,* 1995). Specifically, MUC1 expression has been shown to inhibit the ability of melanoma cells to adhere to various components of the ECM, including laminin, fibronectin and collagen. It is postulated that the large extended extracellular domain of MUC1 masks the integrins and thereby prevents integrin-mediated attachment to the ECM, potentially enhancing cell motility (Wesseling *et al*., 1995). The implications of inhibition of integrin functioning are demonstrated, and put into clear perspective, by cancers that exhibit a down-regulation of specific integrins. For example, loss of the α1 integrin subunit appears to be an important characteristic exhibited by lung cancer cells (Suzuki *et al*., 1993). Moreover, the loss of α1 integrin expression in these cells is thought to contribute to the invasive and/or metastatic behaviour of lung cancer (Suzuki *et al*., 1993). In the same vein, decreased levels of cell surface β1 integrin and β4 integrin subunits are thought to confer anchorage-independent growth to the MCF-7 breast carcinoma cell line (Suzuki and Takahashi, 1999). Importantly, there appeared to be less β1 integrin in lymph node metastases of oesophageal squamous cell carcinoma than in the associated primary tumour (Takayama *et al*., 2003). Thus, MUC1 expression and potential inhibition of integrin binding, and therefore functioning, may mimic integrin down-regulation and promote invasion as well as anchorage-independent growth in these HOSCC cells.

MUC1 has been implicated in the disruption of adherens junction formation (Hilkens *et al*., 1992, Wesseling *et al*., 1996). Adherens junctions are necessary for the maintenance of epithelial tissue architecture (Harington and Syrigos, 2000). In order for the adherens junction to function, E-cadherin at the cell surface must bind to E-cadherin on adjacent cells as well as to β-catenin within the cell (Conacci-Sorrell *et al*., 2002). Disruption of adherens junction formation is associated with epithelial-mesenchymal transition, a

process whereby cells acquire a fibroblastic-like phenotype followed by the propensity to migrate (described in Chapter 1) (Cano *et al*., 2000, Larue and Bellacosa, 2005). Reduction or loss of E-cadherin expression (resulting in reduced formation of adherens junctions) is significantly associated with poor differentiation, increased invasiveness, a high incidence of lymph node metastasis, haematogenous recurrence and a poor prognosis in a number of carcinomas, including those of the head and neck, and breast (Andrews *et al*., 1997, Lim and Lee, 2002). A recent study conducted on HOSCC indicated that patients with tumours exhibiting E-cadherin expression were more likely to survive than those exhibiting a loss of E-cadherin expression (Lin *et al*., 2004). MUC1 inhibits adherens junction functioning via 2 distinct mechanisms. On one hand, the rod-like extracellular domain of MUC1 inhibits the interaction between E-cadherin molecules on adjacent cells (Wesseling *et al.,* 1996), and on the other hand, intracellular MUC1-binding to β-catenin sequesters β-catenin away from adherens junctions (Yamamoto *et al*., 1997). We have demonstrated that not only does MUC1 interact with β-catenin at the membrane of these HOSCC cell lines, but that this association can be increased by the activation of EGFR, a growth factor receptor that is highly overexpressed in these cell lines (Veale and Thornley, 1989). Thus, MUC1-mediated disruption of adherens junction formation in these HOSCC cells (elicited both by the membrane localization of MUC1 as well as by MUC1's interaction with β-catenin) is likely to be profound. In order to confirm the effect of MUC1 expression on cell adhesion in these cells it would be necessary to modulate expression of MUC1, perhaps using RNA interference (RNAi) technology, and perform adhesion assays comparing adhesive characteristics before and after expression modulation. Interestingly, inhibition of c-Src, which would reduce the association between MUC1 and β-catenin (see Chapter 3), activates the functioning of E-cadherin-mediated cell adhesion and suppresses metastasis in cancer cells (Nam *et al*., 2002). Perhaps c-Src inhibition, by inhibitor PP2, should be considered as a potential method of treatment for cancers, such as HOSCC, in which MUC1 is expressed and associates with β-catenin.

In terms of the potential mitogenic effects of MUC1 expression, Schroeder *et al*. (2001) implicated MUC1 in EGFR signalling in the mouse mammary gland. They detected a

sharp increase in ERK1/2 activation in MUC1 transgenic mammary glands compared with MUC1 null and wild-type animals. Their explanation and the implications of this are as follows. Phosphorylation of MUC1 (presumably by EGFR activation) results in association of MUC1 with Grb2/SOS, which is an effector of EGFR signalling. Since MUC1 and EGFR physically interact, association of MUC1 with Grb2/SOS recruits Grb2/SOS into close proximity with EGFR. This results in an increase in association between EGFR and Grb2/SOS, which is followed by Ras activation and phosphorylation of Raf, MEK and ERK1/2. ERK1/2 then translocates to the nucleus and induces the transcription of genes involved in mitogenesis, differentiation and apoptosis. The activation of this pathway is often associated with tumorigenesis. The study by Schroeder *et al*. (2001) therefore defines an additional role for MUC1 as a potentiator of EGFR signalling, with MUC1 expression resulting in increased activation of ERK1/2. The question remains as to whether the same might occur in the HOSCC cell lines, i.e. does MUC1 expression enhance EGFR signalling in these cells? Although we have not directly addressed this question, it must be considered that MUC1 expression may result in ERK1/2 activation and subsequent gene transcription, thereby further contributing to the transformed behaviour of these HOSCC cells.

In Chapter 2 we discussed the possibility that EGFR activation may trigger MUC1 expression via STAT activation. In a recent study, Li *et al*. (2005) showed that down-regulation of MUC1, by treatment of KB carcinoma cells with small interfering RNA, inhibited expression of EGFR both at the mRNA and protein levels. This result demonstrates a role for MUC1 in the regulation of EGFR expression. It thus appears that MUC1 and EGFR may regulate each others expression via a positive feedback system. To illustrate, EGFR activates STAT which results in the expression of MUC1. MUC1 then up-regulates EGFR expression which results in STAT activation and subsequent MUC1 expression, and so on (see Figure 6.1). Although this is the first time this has been suggested, the hypothesis is supported by previous reports of EGFR overexpression in these HOSCC lines together with the present demonstration of MUC1 expression in these lines (Veale and Thornley, 1989). This system thereby presents an enticing target for

therapeutic intervention, as inhibition of expression of either gene (both of which are associated with the cancer phenotype) may result in the down-regulation of the other.

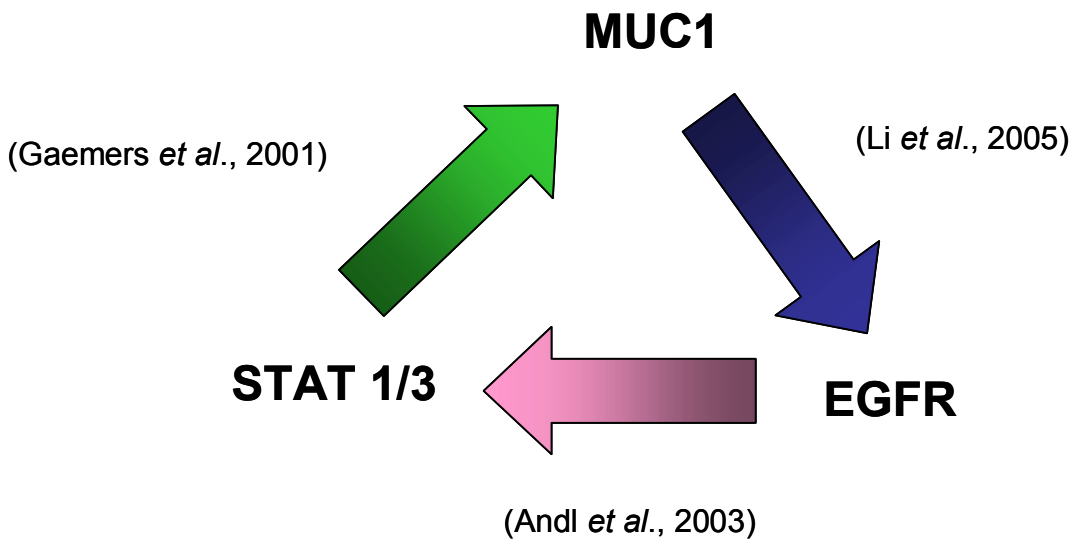

Figure 6.1: MUC1 and EGFR may enhance one another's expression via a positive feedback system.

6.2 MUC1 is implicated in Wnt signalling

The MUC1 cytoplasmic tail is highly conserved across species and is thought to play a role in morphogenetic signal transduction (Gendler, 2001, Hattrup and Gendler, 2006). We investigated the potential nuclear localization of the MUC1 CT using MUC1 CT-specific immunocytochemistry and western blotting. In the SNO cell line, immunofluorescence data indicated that the MUC1 CT is located at the cell membrane, within the cytoplasm and potentially in the nucleus. The WHCO1 cell line exhibited less CT-specific staining overall, but what became apparent was a pattern of CT-staining that resembled nucleolar staining. Indeed, it has been established that the MUC1 CT may be responsible for targeting γ-catenin to the nucleolus in response to growth factor signalling in breast carcinoma cell lines (Li *et al*., 2003a). γ-Catenin functions as an oncogene when

it translocates to the nucleus and up-regulates the expression of c-myc, which enhances cell growth (Kolligs *et al*., 2000). The apparent nucleolar localization of the MUC1 CT in WHCO1 raises the possibility that, similar to what occurs in breast, the MUC1 CT targets γ-catenin to the nucleolus and plays a role in γ-catenin-mediated gene transcription in some HOSCC cell lines. Co-immunoprecipitation analysis will better define the relationship and potential physical interaction between MUC1 and γ-catenin in these cell lines.

Nuclear localization of the MUC1 CT in cell lines WHCO1 and SNO was further confirmed by western blotting. The obvious existence of the MUC1 CT in the nucleus of these 2 cell lines further supports a role for the MUC1 CT in signal transduction. Since recent reports have implicated the MUC1 CT in β-catenin mediated signalling (Huang *et al*., 2003, Wen *et al*., 2003), we continued the investigation by assessing the presence of nuclear β-catenin in the 5 HOSCC cell lines.

A correlation between nuclear β-catenin and tumorigenesis has been well established (reviewed in Polakis, 2000). Here, we have demonstrated the presence of β-catenin in the nucleus of all 5 HOSCC cell lines investigated. This is in keeping with what has previously been reported for HOSCC (De Castro *et al*., 2000; Ninomiya *et al*., 2000, Saeki *et al*., 2002). Considering that nuclear β-catenin is not detectable in normal oesophagus (Ninomiya *et al*., 2000, Saeki *et al*., 2002), nuclear β-catenin, as seen in these HOSCC cells, is likely to be an indication of deregulated β-catenin turnover. Mutations and deletions of phosphorylation sites in the amino terminus resulting in stabilization and nuclear translocation of β-catenin have been observed in numerous human tumours and cancer cell lines, including colon, hepatocellular, ovarian and endometrial (Bienz and Clevers, 2000, Park *et al*., 2005). Elevated β-catenin levels resulting from mutations in other components of the Wnt signalling pathway, such as loss-of-function APC mutations are also commonly found. For example, in colon cancer, it is estimated that nearly 85% of tumours contain mutations in APC (Michaelson and Leder, 2001). However, these mutations have been reported not to occur in oesophageal cancer (Powell *et al*., 1994, Choi *et al*., 2000, Ninomiya *et al*., 2000). There must therefore be an alternative

mechanism for the stabilization and subsequent nuclear translocation of β-catenin in HOSCC. We thus propose that β-catenin stabilization in these HOSCC cell lines, and potentially in HOSCC in general, is dependant on its interaction with MUC1; an interaction that we have shown exists in these HOSCC cells. In support of this suggestion, Huang *et al*. (2005) recently showed that MUC1 interaction with β-catenin blocks GSK3β-mediated phosphorylation and degradation of β-catenin. We therefore present, and provide data in support of, a previously unreported mechanism for β-catenin stabilization and nuclear translocation in HOSCC.

Further investigation (specifically co-immunoprecipitation of nuclear extracts) indicated the presence of a MUC1 CT/β-catenin complex in the nucleus of all 5 HOSCC cell lines. This complex has been reported to occur in carcinomas of the pancreas and colon, as well as in myeloma cells; however, this is the first demonstration of the complex in the nucleus of HOSCC lines. The nuclear localization of a MUC1/β-catenin complex further confirms a role for MUC1 in β-catenin-mediated signalling in HOSCC. This role, however, has not yet been fully elucidated. MUC1 may contribute to β-catenin stabilization (through the inhibition of GSK3β-mediated degradation), enhancing its accumulation in the cytoplasm and then acting as a shuttle during its nuclear translocation (Wen *et al*., 2003). Recent evidence has shown that further than simply acting as a stabilizer, MUC1 may be an essential component of the β-catenin/LEF/TCF transcription factor complex. Indeed, we demonstrated that expression of the Wnt responsive gene MMP7 correlates with nuclear localization of the MUC1/β-catenin complex.

In order to explore the concept that the MUC1/β-catenin association impacts upon β-catenin nuclear translocation, we modulated the association between MUC1 and β-catenin, using EGF, and determined if this had any effect on the concentrations of nuclear β-catenin. The results indicated that altering the association between MUC1 and β-catenin at the membrane did in fact result in the modulation of the concentration of β-catenin in the nucleus. Although the relationship was complex, it must be noted that in cell lines WHCO3 and WHCO5, increases in association between MUC1 and β-catenin

were accompanied by increases in nuclear β-catenin. Thus it is possible that, in support of our hypothesis, MUC1 interaction with β-catenin assists in its nuclear translocation.

MMP7 (a Wnt-responsive gene product) is a member of a family of proteases that are responsible for degradation of various components of the ECM, and as such, its expression is thought to play a role in the progression of various human tumours (Kleiner and Stetler-Stevenson, 1999, Vansaun and Matrisian, 2006). MMP7 expression in HOSCC in particular, has been associated with an increased propensity to invade as well as being associated with recurrence and a poor prognosis (Saeki *et al*., 2002). Thus, regardless of the potential contribution of MUC1 to the expression of this gene, the data provided here, showing that MMP7 is expressed in these HOSCC cells, gives additional insight into the molecular mechanisms contributing to the behaviour of these particular cell lines. As these cell lines were all derived from South African patients it is possible that MMP7 expression is a characteristic of HOSCC in South Africa, or at least of moderately differentiated HOSCC in South Africa. Clearly, further analysis of a larger number of samples needs to be carried out in order to determine if this is the case. However, the determination of MMP7 expression as a characteristic of HOSCC in South Africa may be important in informing the approach to treatment of this cancer-type. It would thus be worthwhile to pursue such an investigation.

Investigations into MUC1 expression in stratified epithelia are limited to descriptive reports of presence versus absence and speculation about the protective role of MUC1 (Wantake, 2002, Gipson, 2004, Hebbar *et al*., 2005). According to our knowledge, this is the first molecular analysis of MUC1 to be conducted on cell lines derived from tumours of stratified epithelial origin (as opposed to simple epithelial origin). Our results, particularly the demonstration of MUC1 membrane localization and complex formation with β-catenin both at the cell membrane and in the nucleus, suggest that the mechanisms of MUC1 action are similar in carcinomas of both simple and stratified epithelial origin. This is not altogether surprising considering the indications that MUC1 may play similar roles in non-epithelial cancers such as astrocytoma, melanoma and neuroblastoma (Oosterkamp *et al*., 1997). Indeed, the MUC1/β-catenin interaction has been

demonstrated in haematologic malignancies, such as in multiple myeloma (Li *et al*., 2003b, Li *et al*., 2004). Together, these findings suggest that the role of MUC1 is maintained across numerous cancer-types, and is not restricted to cancers derived from simple epithelia. This is an encouraging finding as it suggests that cancer treatments designed to target MUC1 (discussed below) are likely to have comparable results across different cancer-types.

The potential implications of MUC1 expression in terms of cell adhesion, EGFR signalling and β-catenin-mediated signal transduction have already been discussed. However, MUC1 has also been implicated in resistance to apoptosis. The results of one particular study support a model in which expression of MUC1 by carcinoma cells (in response to oxidative stress) decreases oxidant levels and thereby attenuates reactive oxygen species (ROS)-induced apoptosis. This is important as carcinoma cells may have exploited this mechanism by overexpressing MUC1 to achieve a survival advantage under conditions of oxidative, or other forms of, stress (Yin *et al*., 2004). In support of that finding, a subsequent study showed that MUC1 attenuates the apoptotic response to DNA damage and that MUC1 confers resistance to genotoxic anticancer agents (Ren *et al*., 2004). Further studies have indicated that MUC1 may elicit its anti-apoptotic function through the activation of the anti-apoptotic PI3K/Akt and Bcl-x(L) pathways and/or through the suppression of the p53-dependent apoptotic response (Raina *et al*., 2004, Wei *et al*., 2005). A relationship between MUC1 and anti-apoptotic signalling is in keeping with the association between MUC1 expression and an aggressive cancer phenotype.

This chapter, as well as previous chapters, has detailed at length the concept that MUC1 expression influences cell behaviour. A recent, significant study further strengthens and provides evidence for this hypothesis. Tsutsumida *et al*. (2006) investigated the influence of MUC1 expression on various aspects of cell behaviour by down-regulating MUC1 expression by RNAi in pancreatic cancer cell lines. MUC1-suppressed clones showed significantly decreased proliferation both *in vitro* and *in vivo*. Adhesion of MUC1-supressed cells to type IV collagen and fibronectin was increased. Additionally and perhaps of most interest here, results of implantation of experimental cells to cecum and

pancreas showed significant reduction of metastasis to lymph nodes, lung or peritoneal sites, when compared to control cells (in which MUC1 expression was not down-regulated). This study thus provides an unequivocal demonstration of the potential impacts of MUC1 expression on cell behaviour, particularly with regards to metastatic capabilities. There is little to suggest that MUC1 expression might not have similar implications for oesophageal cells. MUC1 expression in HOSCC cells, as demonstrated here, may therefore be a key factor contributing to the aggressive behaviour of HOSCC cells.

6.3 Clinical trials are highlighting the considerable potential of MUC1-specific cancer therapies

Although MUC1 expression may grant a cancer cell properties that contribute to its ability to proliferate and metastasize, it may, if developers of a range of new cancer therapeutics are accurate, prove to be disadvantageous to the cancer cell. Aberrant, specifically under-, glycosylation of MUC1 in cancer cells exposes core-protein epitopes that are masked in fully glycosylated isoforms (Von Mensdorff-Pouilly *et al*., 2000). Cancer-associated MUC1 is thus antigenically distinct from MUC1 expressed by normal cells. This, together with the fact that MUC1 is overexpressed in numerous cancers, as well as the fact that MUC1 appears to be highly immunogenic, makes MUC1 a particularly attractive target for therapeutic intervention (Von Mensendorff-Pouilly *et al*., 2000, Liu *et al*., 2004, Karsten *et al*., 2005).

A number of MUC1-specific immunotherapies are currently being developed and investigated for their tumour-suppressive properties. At least 3 of these – TG 4010 (Transgene), Stimuvax®/BLP25 (Biomura), and BrevaRex® (ViRexx Medical Corporation) – are yielding positive results in (human) clinical trials (Cohen and Kaufman, 2004, Liu *et al*., 2004, North *et al*., 2006). The strategy behind these immunotherapeutic compounds is to induce a strong immune response against MUC1 in order to selectively destroy MUC1 expressing tumour cells. TG 4010, for example, is based on recombinant vaccinia virus expressing the MUC1 antigen and human

interleukin-2 (IL-2), a cytokine that plays an important role in immune stimulation (Cohen and Kaufman, 2004, Liu *et al*., 2004). It has been designed to induce a MUC1-specific cellular and humoral immune response, as well as a non-specific activation of the immune system via the vaccinia virus infection and activation by IL-2. This vaccine has successfully completed phase I clinical trials for non-small-cell lung cancer, metastatic renal cancer and prostate cancer, and phase II clinical trials are currently underway (Cohan and Kaufman, 2004). According to Transgene, the preliminary results of these studies can be expected in 2007. Stimuvax® is based on a synthetic 25 amino acid sequence of cancer-associated MUC1 encapsulated in a specially designed liposomal delivery system. In September 2004, the FDA granted fast track status to the investigation of Stimuvax® for its proposed use in the treatment of non-small-cell lung carcinoma. Thus far, studies on the liposomal vaccine have yielded encouraging results for both non-small-cell lung cancer and prostate cancer (North *et al*., 2006). The murine monoclonal antibody BrevaRex®, a highly specific anti-MUC1 antibody recognizing the tandem repeat protein backbone, has demonstrated anti-tumour activity against MUC1-expressing human tumour xenografts. Utilizing a metastatic MUC1-transfected tumour cell line in a mouse model, BrevaRex® prevented tumour generation in over 60% of the mice tested, and increased murine median survival from 51 days to over 120 days (Qi *et al*., 2001). Anti-MUC1 antibodies potentially protect against tumour progression and metastasis by binding to MUC1-expressing cancer cells, capping MUC1 on the cell surface, restoring cell-cell interaction, counteracting immunosuppressive effects, and inhibiting MUC1 intracellular signalling (Akewanlop *et al*., 2001, Snijdewint *et al*., 2001 Patel *et al*., 2005). Phase I human clinical trials conducted on BrevaRex® indicated that injection with the antibody results in the formation of immune-complexes and the induction of MUC1-specific immune responses in cancer patients with advanced disease (De Bono *et al*., 2004). The outcome of the study was extremely positive and indicated that the agent (the anti-MUC1 antibody) merits further evaluation in clinical trials.

Patel *et al*. (2005), on the other hand, are currently evaluating retrovirally delivered RNAi as a mechanism to down-regulate the expression of MUC1 in thyroid cancer cells, as a cancer treatment strategy. Thus far they have achieved stable MUC1 suppression and are

conducting *in vitro* and *in vivo* assays to study the tumorigenic properties of MUC1-supressed cells when compared with the unsuppressed parent line. It is important to note that although the concept of susceptibility of MUC1-expressing cells to immune system attack remains controversial, it seems that MUC1-specific therapies are extremely promising.

Our data demonstrate that 5 (out of 5) HOSCC cell lines positively express MUC1. Moreover, since the antibody used in immunofluorescence assays binds only under-glycosylated MUC1, antibody binding indicates that MUC1 is under-glycosylated in these cells, and is therefore likely to be antigenically distinct from MUC1 expressed by healthy cells. These results, together with the existing immunohistochemical data showing MUC1 expression in HOSCC (Kijima *et al*., 2001), identify HOSCC as a prime candidate for MUC1-specific therapy. This is of particular importance considering the ineffectual nature of conventional therapies in treating HOSCC.

6.4 MUC1 may be a key factor contributing to HOSCC behaviour

Oesophageal squamous cell carcinoma is a particularly aggressive cancer and exhibits a prognosis that is significantly worse than that of other digestive tract cancers (Yamamoto *et al*., 1999). In spite of this, the molecular mechanics governing this highly invasive cancer-type have not yet been clearly defined (Hu *et al*., 2001). MUC1 has proven to be an exceptionally dynamic protein involved in numerous aspects of cell behaviour and malignancy. It is suggested that MUC1 expression, and its interaction with β-catenin, as demonstrated in these HOSCC cells, may contribute to the malignant behaviour characteristic of HOSCC. This dissertation therefore provides insight into a previously unexplored domain of HOSCC behaviour. Further study may confirm MUC1 expression, and interaction with β-catenin, as central to events leading to metastatic behaviour in HOSCC, and may present MUC1 as an important therapeutic target in this cancer-type.

CHAPTER 7: APPENDIX

7.1 Tissue culture

DMEM medium

1.37% DMEM

0.37% Sodium Bicarbonate

2% penicillin (500 U/ml)/streptomycin (0.5%) solution

Hams F12

1.07% Hams F12 medium

0.0118% Sodium bicarbonate

2% penicillin (500 U/ml)/streptomycin (0.5%) solution

Mix DMEM:Hams F12 3:1

Filter sterilize and store at 4°C

Trypsin/Ethylenediaminetetra-acetic acid (EDTA)

0.02% EDTA in PBS

0.1% trypsin in PBS

Mix EDTA:Trypsin 1:1 to give a final concentration of 0.01% EDTA/0.05% trypsin

7.2 Phosphate buffered saline (PBS)

0.1 M Sodium chloride

10 mM Disodium hydrogen orthophosphate

3 mM Potassium chloride

1 mM Potassium dihydrogen orthophosphate

Adjust to pH 7.6

Make up to volume with dH_2O and autoclave

7.3 Agarose gel electrophoresis

Tris acetic acid EDTA (TAE) buffer (20X)

1.6 M Tris(hydroxymethyl)aminomethane (Tris)

0.6 M Sodium acetate

40 M EDTA

Adjust to pH 7.2 with acetic acid

Make up to volume with dH_2O

Ethidium bromide (EtBr)

10 ng/ml EtBr in dH_2O

Agarose gel loading buffer

50% TAE

50% Glycerol

0.01% Bromophenol blue

7.4 cDNA synthesis

MMLV-RT reaction buffer (5X)

50 mM Tris-HCl pH 8.3

75 mM Potassium chloride

3 mM Magnesium chloride

10 mM DTT

Nucleotide mix

dNTPs are supplied as sodium salts of dATP, dCTP, dGTP, dTTP each at 10 mM in dH_2O at pH 8.3

MMLV-RT

The enzyme is supplied in 20 mM Tris-HCl pH 7.7, 200 mM sodium chloride, 0.1 mM EDTA, 1 mM DTT, 0.01% Nonidet-P40 and 50% glycerol.

7.5 Primer design

MUC1 CT-specific primers were generated using the web-based interactive primer design program GeneFisher. The MUC1 sequence was obtained through NCBI Entrez Nucleotide (http://www.ncbi.nlm.nih.gov). The input sequence was a 418 bp sequence representative of the cytoplasmic tail end of the gene (excluding introns) that included binding sites for β-catenin, c-Src and Grb2. The input sequence was as follows:

5'TCAATCAGTATAAAACGGAAGCAGCCTCTCGATATAACCTGACGATC
TCAGACGTCAGCGTGAGTGATGTGCCATTTCCTTTCTCTGCCCAGTCTG
GGGCTGGGGTGCCAGGCTGGGGCATCGCGTCGCTGGTGCTGGTCTGTG
TTCTGGTTGCGCTGGCATTGTCTATCTCATTGCCTTGGCTGTCTGTCAG
TGCCGCCGAAAGAACTACGGGCAGCTGGACATCTTTCCAGCCCGGGAT
ACCTACCATCCTATGAGCGAGTACCCCACCTACCACACCCATGGGCGC
TATGTGCCCCCTAGCAGTACCGATCGTAGCCCCTATGAGACGGTTTCT
GCAGGTAATGGTGGCAGCAGCCTCTCTTACACAAACCCAGCAGTGGC
AGCCACTTCTGCCAACTTGTAGGGGCACGTCGCC3'

The parameters used for primer selection were as follows:
Primer size: 18-24 bp
GC content: 45-65%
Melting temperature: 55-60°C

PCR distance: 300-500 bp

Characteristics of the selected primers were calculated using OligoAnalyzer (http://www.idtdna.com/analyzer/Applications/OligoAnalyzer) and are as follows:

Forward primer melting temperature: 59.3°C

Forward primer hairpin loop: ΔG=0.01, melting temperature=37.0°C

Forward primer self-dimer: ΔG=-6.76

Reverse primer melting temperature: 58.8°C

Reverse primer hairpin loop: ΔG=-0.85, melting temperature=48.1°C

Reverse primer self-dimer: ΔG=-6.21

PCR product length: 400 bp

7.6 PCR

PCR reaction buffer (10X)

20 mM Tris-HCl pH 7.5

100 mM Potassium chloride

1 mM DTT

0.1 mM EDTA

0.5% Tween

0.5% Nonidet-P40

15 mM Magnesium chloride

7.7 Laemmli lysis buffer

0.05 M Tris

0.15 M SDS

10% glycerol

5% β-mercaptoethanol

Make up to volume with dH_2O and adjust pH to 6.8

7.8 Protein estimation

Tri-chloroacetic acid (TCA)

7% TCA

Make up to volume with dH_2O

0.25% Coomassie blue

0.25% coomassie blue

50% methanol

Dissolve, then add

10% acetic acid

Make up to volume with dH_2O

Destain

12% ethanol

10% acetic acid

Make up to volume with dH_2O

Elution solution

67% methanol

32% dH_2O

1% concentrated ammonia

7.9 SDS-PAGE

10% SDS-PAGE gel

Separating gel:

1.0 g acrylamide

2.5 ml separating buffer (1.5 M Tris pH 8.8)

400 µl SDS (50 mg/ml 0.17 M)

400 µl *N′,N′*-Methylenebisacrylamide (25 mg/ml 0.16 M)

Make up to 10 ml with dH_2O, then immediately prior to pouring add:

180 µl ammonium persulphate (APS) (1.25%)

25 µl *N′,N′,N′,N′*- tetramethylene-diamine (TEMED) (0.25%)

Stacking gel:

0.5 g acrylamide

2.5 ml stacking buffer (0.5 M Tris pH 6.8)

400 µl SDS (50 mg/ml)

400 µl bis-acrylamide (25 mg/ml)

Make up to 10 ml with dH_2O, then immediately prior to pouring add:

180 µl APS

25 µl TEMED

Reservoir buffer

0.2 M Glycine

25 mM Tris pH 8.3

3 mM SDS

Make up to volume with dH_2O

0.25% Coomassie blue

0.25% coomassie blue

50% methanol

Dissolve, then add

10% acetic acid

Make up to volume with dH_2O

Destain

10% ethanol

10% acetic acid

Make up to volume with dH_2O

7.10 Western blot analysis

Western blot transfer buffer

25 mM Tris pH 8.3

0.5 M Glycine

20% methanol

Make up to volume with dH_2O

Blocking buffer (Blotto)

50 mM Tris pH 7.8

2 mM Calcium chloride

5% non-fat milk powder

0.01% antifoam

0.05% Triton X-100

Make up to volume with dH_2O

Developer

6.4 M Metol

0.6 M Sodium sulphite

80 mM Quinol

0.45 M Sodium carbonate

34 mM Potassium bromide

Fixer

0.8 M Sodium thiosulphate

0.2 M Sodium metabisulphite

7.11 Immunocytochemistry

4% Paraformaldehyde

Solution A: 0.2 M Sodium dihydrogen orthophosphate

Solution B: 0.6 M Sodium hydroxide

Take 166 ml of Solution A

Add 34 ml of Solution B

Heat to 60 – 80°C

Add 8 g paraformaldehyde

Stir until clear

Filter and cool

pH 7.2

Elvanol

0.1 M Tris

20% polyvinyl alcohol

50% glycerol

Make up to volume with dH_2O

7.12 PCR fragment size determination

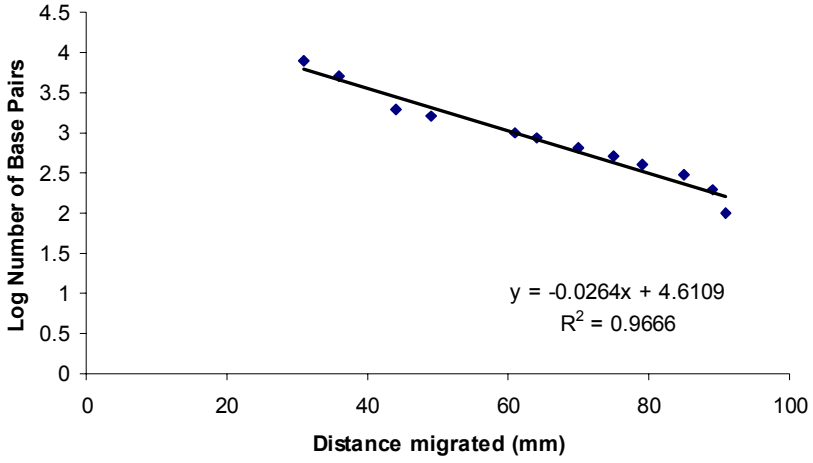

Figure 7.1: 1% Agarose Gel: Standard curve of number of base pairs (log) vs distance migrated (mm).

7.13 Determination of protein concentration

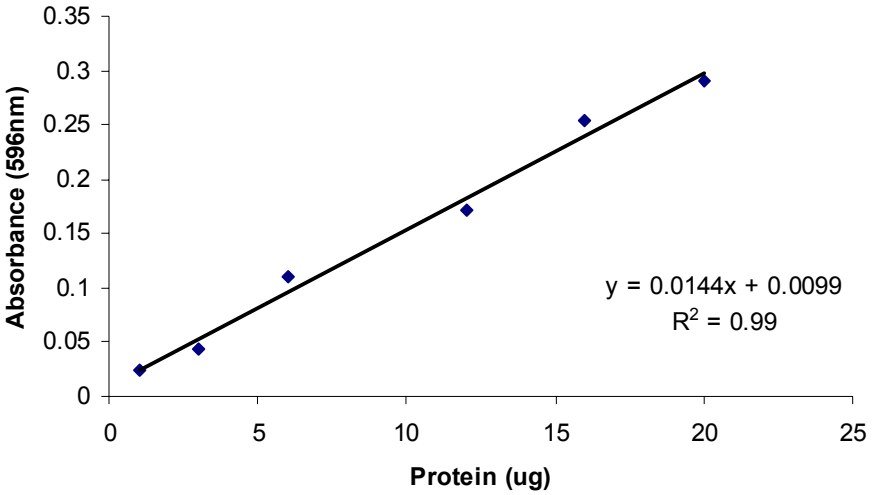

Figure 7.2: Standard curve of absorbance (at 596 nm) versus protein concentration (μg/μl).

7.14 Determining the relative molecular weight of proteins separated by 10% SDS-PAGE

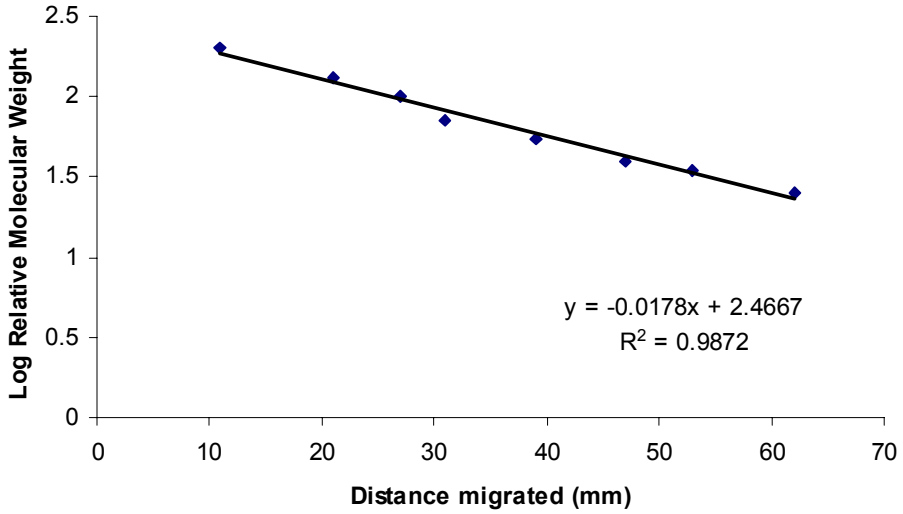

Figure 7.3: Standard curve of relative molecular weight (log) versus distance migrated (mm).

7.15 TritonX-100 membrane extraction buffer

0.5% Triton X-100
50 mM Tris pH 8.5
150 mM Sodium chloride
1 mM Calcium chloride
1 mM Magnesium chloride
0.01% aprotinin
4 μg/ml pepstatin A
10 μg/ml leupeptin

7.16 Immunoprecipitation buffer

20 mM Tris pH 8.0
0.5% Nonidet P-40
0.9% Sodium chloride

7.17 Raw densitometric data of experiments designed to investigate changes in association between MUC1 and β-catenin

Table 7.1: Optical density values obtained through LabWorks analysis of bands generated by MUC1 CT-specific western blot analysis of β-catenin membrane immunoprecipitates

CELL LINE	EGF Exposure Duration (min)				
	0	**5**	**30**	**60**	**180**
WHCO1	69.93	46.56	71.97	45.20	1.90
WHCO3	38.11	27.42	45.56	148.28	32.70
WHCO5	37.18	60.26	41.37	26.26	12.93
WHCO6	68.80	408.64	570.90	166.20	901.71
SNO	42.20	91.20	105.61	111.54	95.03

7.18 Raw densitometric data of experiments designed to investigate changes in membrane concentration of β-catenin

Table 7.2: Optical density values obtained by LabWorks analysis of bands generated by β-catenin-specific western blot analysis of β-catenin membrane immunoprecipitates

CELL LINE	EGF Exposure Duration (min)				
	0	**5**	**30**	**60**	**180**
WHCO1	208.17	352.97	330.68	312.01	120.86
WHCO3	130.93	110.61	142.61	155.88	54.46
WHCO5	172.12	180.65	232.71	313.46	242.93
WHCO6	302.99	382.81	692.34	654.00	37.23
SNO	76.80	50.47	84.42	100.28	36.13

7.19 Nuclear extraction buffers

Hypotonic lysis buffer

10 mM HEPES pH 7.9

1.5 mM Magnesium chloride

10 mM Potassium chloride

Nuclear extraction buffer

20 mM HEPES

1.5 mM Magnesium chloride

0.42 M Sodium chloride

0.2 mM EDTA

25% glycerol

7.20 Determining the relative molecular weight of proteins separated by 12.5% SDS-PAGE

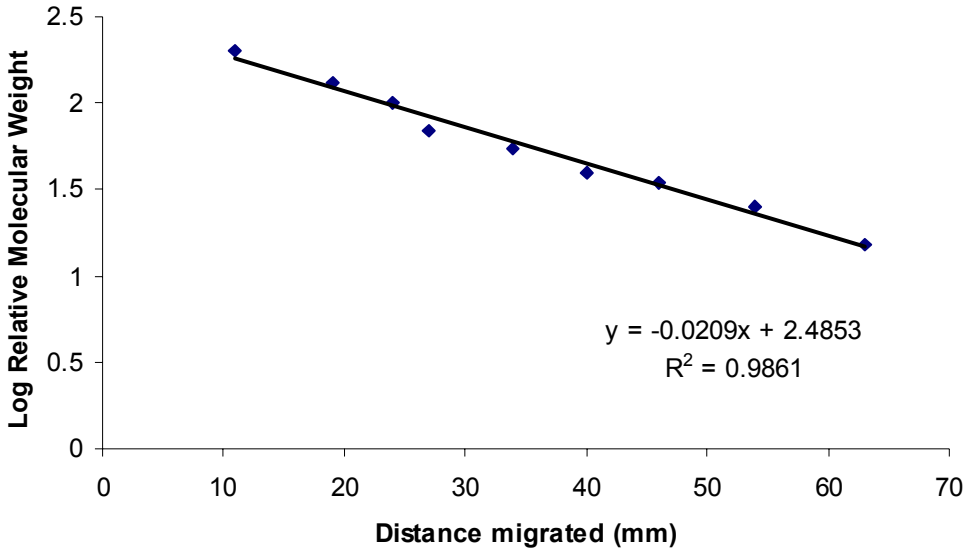

Figure 7.4: Standard curve of relative molecular weight (log) versus distance migrated (mm).

7.21 Raw densitometric data of experiments investigating the presence of nuclear β-catenin and the presence nuclear MUC1/β-catenin complex

Table 7.3: Optical density values obtained by LabWorks analysis of bands generated by western blot analysis of nuclear protein

CELL LINE	Nuclear β-catenin	Nuclear MUC1/β-catenin complex
WHCO1	178.73	47.3
WHCO3	240.26	64.78
WHCO5	293	88.07
WHCO6	184.59	20.57
SNO	164.08	72.84

7.22 Raw densitometric data of experiments investigating the changes in nuclear β-catenin concentration in response to EGFR activation

Table 7.4: Optical density values obtained by LabWorks analysis of bands generated by β-catenin-specific western blot analysis of β-catenin membrane immunoprecipitates

CELL LINE	EGF Exposure Duration (min)				
	0	**5**	**30**	**60**	**180**
WHCO1	1075.90	990.85	921.09	752.49	687.74
WHCO3	189.43	250.15	197.22	267.29	169.38
WHCO5	434.77	271.02	321.66	416.22	468.45
WHCO6	218.86	268.69	238.37	227.86	181.10
SNO	314.91	300.94	287.18	316.30	318.20

7.23 Zymography reagents

Zymography (non-reducing) sample buffer

0.05 M Tris pH 6.8

0.15 M SDS

10% glycerol

Zymography washing buffer

2.5% Triton-X 100

50 mM Tris

pH 7.6

Zymography developer

50 mM Tris-HCl pH 7.6

200 mM Sodium chloride

10 mM Calcium chloride

7.24 Raw densitometric data of experiments investigating the presence of MMP7 in HOSCC cells

Table 7.5: Optical density values obtained by LabWorks analysis of bands generated by MMP7-specific western blot analysis of whole-cell extracts

CELL LINE	MMP7
WHCO1	26.1
WHCO3	59.04
WHCO5	49.49
WHCO6	17.07
SNO	18.25

CHAPTER 8: REFERENCES

Adachi, Y., Yamamoto, H., Itoh, F., Arimura, Y., Nishi, M., Endo, T. and Imai, K. (2001). Clinicopathologic and prognostic significance of matrilysin expression at the invasive front in human colorectal cancers. *Int. J. Cancer,* **95:**290-294.

Akewanlop, C., Watanabe, M,, Singh, B., Walleer, M., Kufe, D. and Hayes, D.F. (2001). Phagocytosis of breast cancer cells mediated by MUC-1 monoclonal antibody, DF3, and its bispecific antibody. *Cancer Res.,* **61:**4061-4065.

Altschuler, Y., Kinlough, C.L., Poland, P.A., Bruns, J.B., Apodaca, G., Weisz, O.A. and Hughey, R.P. (2000). Clathrin-mediated endocytosis of MUC1 is modulated by its glycosylation state. *Mol. Biol. Cell,* **11:**819-831.

Andl, C.D., Mizushima, T., Nakagawa, H., Oyama, K., Harada, H., Chruma, K., Herlyn, M., Rustgi, A.K. (2003). Epidermal Growth Factor Receptor Mediates Increased Cell Proliferation, Migration, and Aggregation in Esophageal Keratinocytes *in Vitro* and *in Vivo*. *J. Biol. Chem.*, **278:**1824-1830.

Andrews, N.A., Jones, A.S., Helliwell, T.R. and Kinsella, A.R. (1997). Expression of the E-cadherin-catenin complex in primary squamous cell carcinomas of the head and neck and their nodal metastases. *Br. J. Cancer,* **75:**1474-1480.

Baldin, V., Lukas, J., Marcote, M.J., Pagano, M. and Draetta, G. (1993). Cyclin D1 is a nuclear protein required for cell cycle progression in G1. *Genes Dev.,* **7:**812-821.

Baldus, S.E., Monig, S.P., Huxel, S., Landsberg, S., Hanisch, F.G., Engelmann, K., Schneider, P.M., Thiele, J., Holscher, A.H. and Dienes, H.P. (2004). MUC1 and β-catenin are coexpressed at the invasion front of colorectal carcinomas and are both correlated with tumor prognosis. *Clin. Cancer Res.,* **10:**2790-2796.

Ben-Ze'ev, A. and Geiger, B. (1998). Differential molecular interactions of β-catenin and plakoglobin in adhesion, signaling and cancer. *Curr. Opin. Cell Biol.,* **10:**629-639.

Bey, E., Alexander, J., Whitcutt, J.N., Hunt, J.A. and Gear, J.H.S. (1976). Carcinoma of the oesophagus in Africans: establishment of a continuously growing cell line from a tumour specimen. *In Vitro,* **12:**107-114.

Bienz, M. and Clevers, H. (2000). Linking colorectal cancer to Wnt signaling. *Cell,* **103:**311-320.

Bienz, M. (2004). β-Catenin: A pivot between cell adhesion and Wnt signalling. *Current Biol.,* **15:**64-67.

Brabletz, T., Jung, A., Dag, S., Hlubek, F. and Kirchner, T. (1999) Beta-catenin regulates the expression of the matrix metalloproteinase-7 in human colorectal cancer. *Am. J. Pathol.,* **155:**1033-1038.

Bramhall, S., Noack, N., Wu, M. and Loewenburg, J.R. (1969). A simple colorimetric method for determination of protein. *Anal. Biochem.,* **31:**146-148.

Brayman, M., Thathiah, A. and Carson, D.D. (2004). MUC1: A multifunctional cell surface component of reproductive tissue epithelia. *Reproductive Biol. Endocrinol.,* **2:**4.

Brembeck, F.H., Rosario, M. and Birchmeier, W. (2006). Balancing cell adhesion and Wnt signaling, the key role of β-catenin. *Curr. Opin. Genet. Dev.,* **16:**51-59.

Bussemakers, M.J. and Schalken, J.A. (1996). The Role of Cell Adhesion Molecules and Proteases in Tumor Invasion and Metastasis. *World J. Urol.,* **14:**151-156.

Cadigan, K.M. and Liu, Y.I. (2006). Wnt signaling: complexity at the surface. *J. Cell Sci.,* **119:**395-402.

Cano, A., Perez-Moreno, M.A., Rodrigo, I., Locanscio, A., Blanco, M.J., del Barrio, M.G., Portillo, F. and Nieto, M.A. (2000). The transcription factor snail controls epithelial-mesenchymal transitions by repressing E-cadherin expression. *Nat. Cell Biol.,* **2:**76-83.

Carlos, T.M. and Harlan, J.M. (1994). Leukocyte-endothelial adhesion molecules. *Blood,* **84:**2068-2101.

Carthew, R.W. (2005). Adhesion proteins and the control of cell shape. *Curr. Opin. Genet. Dev.,* **15:**358-363.

Ceresa, B.P. (2006). Regulation of EGFR endocytic trafficking by rab proteins. *Histol. Histopathol.,* **21:**987-993.

Chan, A.K., Lockhart, D.C., von Beinstorff, W., Spanjaard, R.A., Joo, H.G. and Eberkin, T.J. (1999). Soluble MUC1 secreted by human epithelial cancer cells mediates immune suppression by blocking T-cell activation. *Int. J. Cancer,* **82:**721-726.

Choi, Y.W., Heath, E.I., Heitmiller, R., Forastier, A.A. and Wu, T.T. (2000). Mutations in beta-catenin and APC genes are uncommon in esophageal and esophagogastric junction adenocarcinomas. *Mod. Pathol.,* **13:**1055-1059.

Classon, M. (2002). The retinoblastoma tumor suppressor in development and cancer. *Nat. Rev. Genet.,* **2:**910-917.

Cohen, S. and Kaufman, H.L. (2004).TG-4010 Transgene. *Curr. Opin. Investig. Drugs,* **5:**1319-1328.

Conacci-Sorrell, M., Zhurinsky, J. and Ben-Ze'ev, A. (2002). The cadherin-catenin adhesion system in signaling and cancer. *J. Clin. Investigation,* **109:**987-991.

Crawford, H.C., Fingleton, B.M., Rudolph-Owen, L.A., Goss, K.J., Rubinfeld, B., Polakis, P. and Matrisian, L.M. (1999). The metalloproteinase matrilysin is a target of beta-catenin transactivation in intestinal tumors. *Oncogene,* **18:**2883-2891.

Curran, S. and Murray, G.I. (1999). Matrix metalloproteinases in tumour invasion and metastasis. *J. Pathol.,* **189:**300-308.

Danen, E.H. (2005). Integrins: regulators of tissue function and cancer progression. *Curr. Pharm. Des.* **11:**881-891.

Davies, H. (2002). Mutations of the BRAF gene in human cancer. *Nature,* **417:**949-954.

De Bono, J.S., Rha, S.Y., Stephenson, J., Schultes, B.C., Monroe, P., Eckhardt, G.S., Hammond, L.A., Whiteside, T.L., Nicodemus, C.F., Cermak, J.M., Rowinsky, E.K. and Tolcher, A.W. (2004). Phase I trial of a murine antibody to MUC1 in patients with metastatic cancer: evidence for the activation of humoral and cellular antitumor immunity. *Annals Oncol.,* **15:**1825-1833.

De Castro, J., Gamallo, C., Palacious, J., Moreno-Bueno, G., Rodriguez N., Feliu J. and Gonzalez-Baron, M. (2000). β-Catenin expression pattern in primary oesophageal squamous cell carcinoma. Relationship with clinicopathologic features and clinical outcome. *Virchows Arch.,* **437:**599-604.

Doi, M., Yokoyama, A., Kondo, K., Ohnishi, H., Ishikawa, N., Hattori, N. and Kohno, N. (2006). Anti-tumor effect of the anti-KL-6/MUC1 monoclonal antibody through exposure of surface molecules by MUC1 capping. *Cancer Sci.,* **97:**420-429.

Felding-Habermann, B., Mueller, B.M., Romerdahl, C.A. and Cheresh, D.A. (1992). Involvement of integrin alpha V gene expression in human melanoma tumorigenicity. *J. Clin. Invest.,* **89:**2018-2022**.**

Friedberg, E.C. (2003). DNA damage and repair. *Nature,* **421:**436-400.

Fujita, K., Denda, K., Yamamoto, M., Matsumoto, T., Fujime, M. and Irimura, T. (1999). Expression of MUC1 mucins inversely correlated with post-surgical survival of renal cell carcinoma patients. *Br. J. Cancer,* **80:** 301-308.

Gaemers, I.C., Vos, L.H., Volders, H.H., van der Valk, S.W. and Hilkens, J. (2001). A STAT-responsive Element in the Promoter of the Episialin/MUC1 Gene Is Involved in Its Overexpression in Carcinoma Cells. *J. Biol. Chem.,* **276:** 6191-6199.

Gendler, S.J., Burchell, J.M., Duhig, T., Lamport, D., White, R., Parker, M., Taylor-Papadimitriou, J. (1987). Cloning of partial cDNA encoding differentiation and tumor-associated mucin glycoproteins expresses by human mammary epithelium. *Proc. Natl. Acad. Sci. U.S.A.,* **84:**6060-6064.

Gendler, S.J., Lancaster, C.A., Taylor-Papadimiriou, J., Duhig, T., Peat, N., Burchell, J., Pemberton, L., Lalani, E.N. and Wilson, D. (1990). Molecular cloning and expression of human tumor-associated Polymorphic epithelial mucin. *J. Biol. Chem.,* **265:**15286-15293.

Gendler, S.J. and Spicer, A.P. (1995). Epithelial mucin genes. *Annu. Rev. Physiol.,* **57:**607-634.

Gendler, S.J. (2001). MUC1, The Renaissance Molecule. *J. Mammary Gland Bio. Neoplasia,* **6:**339-353.

Giancotti, F.G. and Rouslatti, E. (1990). Elevated levels of the alpha 5 beta 1 fibronectin receptor suppress the transformed phenotype of Chinese hamster ovary cells. *Cell,* **60:**849-859.

Giancotti, F.G. and Rouslatti, E. (1999). Integrin signaling. *Science,* **285:** 1028-1032.

Gibault, L., Metges, J.P., Conan-Charlet, V., Lozac'h, P., Robaszkiewicz, M., Bessaguet, C., Layarde, N. and Volant, A. (2005). Diffuse EGFR staining is associated with reduced overall survival in locally advanced oesophageal squamous cell cancer. *Br. J. Cancer,* **93:**107-115.

Gipson, I.K. (2004). Distribution of mucins at the ocular surface. *Exp. Eye Res.,* **78:**379-388.

Goodison, S., Urquidi, V. and Tarin, D. (1999). CD44 cell adhesion molecules. *Mol. Pathol.,* **52:**189-96.

Graham, F.L., Smiley, J., Russell, W.C. and Nairn, R. (1977). Characteristics of a human cell line transformed by DNA from human adenovirus type 5. *J. Gen. Virol.,* **36:**59-74.

Guddo, F., Glatromanolaki, A., Koukourakis, M.I., Reina, C., Vignola, A.M. and Chlouverakis, G. (1998). MUC1 (episialin) expression in non-small cell lung cancer is independent of EGFR and c-erbB-2 expression correlates with poor survival in node positive patients. *J. Clin. Pathol.,* **51:**667-671.

Guo, O., Tang, W., Inoqaki, Y., Midorikawa, Y., Kokudo, N., Sugawara, Y., Nakata, M., Konishi, T., Nagawa, H. and Makuachi, M. (2006). Clinical significance of subcellular localization of KL-6 mucin in primary colorectal adenocarcinoma metastatic tissues. *World J. Gasteroenterol.,* **12:** 54-59.

Gustavson, M.D., Crawford, H.C., Fingleton, B. and Matrisian, L.M. (2004). Tcf binding sequence and position determines beta-catenin and Lef-1 responsiveness of MMP-7 promoters. *Mol. Carcinog.,* **41:**125-139.

Haegel, H., Larue, L. and Ohsugi, M. (1995). Lack of catenin affects mouse development at gastrulation. *Development,* **121:**3529-3537.

Hanahan, D. and Weinberg, R.A. (2000). The Hallmarks of Cancer. *Cell,* **100:**57-70.

Hanski, C., Drechsler, K., Hanisch, F.G., Sheehan, J., Manske, M., Ogorek, D., Klussmann, E., Hanski, M.L., Blank, M., Xing, P.X., McKenzie, I.F.C., Devine, P.L. and Riecken, E.D. (1993). Altered glycosylation of the MUC-1 protein core contributes to the colon carcinoma-association increase of mucin-bound sialyl-Lewis(x) expression. *Cancer Res.,* **53:**4082-4088.

Harington, K.J. and Syrigos, K.N. (2000). The role of E-Cadherin-Catenin Complex: More Than an Intercellular Glue? *Annals Surgical Oncol.,* **7:**783-788.

Harris, T.J.C. and Peifer, M. (2005). Decisions, decisions: β-Catenin chooses between adhesion and transcription. *Trends Cell Biol.,* **15:**234-237.

Hattrup, C.L. and Gendler, S.J. (2006). MUC1 alters oncogenic events and transcription in human breast cancer cells. *Breast Cancer Res.*, **8:**37.

Hayes, D.F., Mesa-Tejuda, R., Papisidero, L.D., Croghan, G.A., Korzun, A.H. and Norton, L. (1991). Prediction of prognosis in primary breast cancer by detection of a high molecular weight mucin-like antigen using monoclonal antibodies DF3, F36122 and CU18: a cancer and leukemia group B study. *J. Clin. Oncol.,* **9:**1113-1125.

Hazan, R.B., Norton, L. (1998). The epidermal growth factor receptor modulates the interaction of E-cadherin with the actin cytoskeleton. *J. Biol. Chem.,* **273:**9078-9084.

Hebbar, V., Damera, G. and Sachder, G.P. (2005). Differential expression of MUC genes in endometrial and cervical tissues and tumors. *BMC Cancer,* **5:**124.

Hilkens, J., Ligtenberg, M.J.L., Vos, H.L. and Litvinov, V. (1992). Cell-membrane associated mucins and their adhesion-modulating property. *TIBS,* **17:**359-363.

Hirai, T., Kuwahara, M., Yoshida, K., Kagawa, Y., Hihara, J. and Yamashita, Y. (1998). Clinical results of transhiatal esophagectomy for carcinoma of the lower thoracic esophagus according to biological markers. *Dis. Esophagus,* **11:**221-225.

Hirohashi, S. and Kanai, Y. (2003). Cell adhesion system and human cancer morphogenesis. *Cancer Sci.,* **94:**575-581.

Hollingsworth, M.A. and Swanson, B.J. (2004). Mucins in cancer: Protection and control of the cell surface. *Nat. Rev. Cancer,* **4:**45-60.

Hollstein, M., Sidransky, D., Vogelstein, B. and Harris, C.C. (1991). p53 mutations in human cancers. *Science,* **253:**49-53.

Honda, M., Mori, M., Ueo, H., Sugimachi, K. and Akiyoshi, T. (1996). Matrix metalloproteinase-7 expression in gastric carcinoma. *Gut,* **39:**444-448.

Hu. Y.C., Lam, K.Y., Law, S., Wong, J. and Srivastava, G. (2001). Identification of Differentially Expressed Genes in Esophageal Squamous Cell Carcinoma (ESCC) by cDNA Expression Array: Overexpression of *Fra-1, Neogenin, Id-1,* and *CDC25B* Genes in ESCC. *Clin. Cancer Res.,* **7:**2213-2221.

Huang, L., Ren, J., Chen, D., Li, Y., Kharbanda, S. and Kufe, D. (2003). MUC1 cytoplasmic domain coactivates Wnt target gene transcription and confers transformation. *Cancer Biol. Ther.,* **2:**702-706.

Huang, L., Chen, D., Liu, D., Yin, L., Kharbanda, S. and Kufe, D. (2005). MUC1 Oncoprotein Blocks Glycogen Synthase Kinase 3β-Mediated Phosphorylation and Degradation of β-Catenin. *Cancer Res.,* **65:**10413-10422.

Hynes, R.O. and Zhou, (2000). The evolution of cell adhesion. *J. Cell Biol.,* **150:**89-96.

Hynes, R.O. (2002). Integrins: bidirectional , allosteric signaling machines. *Cell,* **10:**673-687.

Ii, M., Yamamoto, H., Adachi, Y., Maruyama, Y. and Shinomura, Y. (2006). Role of matrix metalloproteinase-7 (matrilysin) in human cancer invasion, apoptosis, growth, and angiogenesis. *Exp. Biol. Med.,* **231:**20-27.

Isaacson, C. (2005). The change of the staple diet of black South Africans from sorghum to maize (corn) is the cause of the epidemic of squamous carcinoma of the oesophagus. *Med. Hypothesis,* **65:**658-660.

Iwaya, K., Ogawa, H., Kuroda, M., Izumi, M., Ishida, T. and Mukai, K. (2003). Cytoplasmic and/or nuclear staining of beta-catenin is associated with lung metastasis. *Clin. Exp. Metastasis,* **20:**525-52.

Jones, L.J.G. and Veale, R.B. (2003). Redistribution of β-catenin in response to EGF and lithium signaling in human oesophageal squamous carcinoma cell lines. *Cancer Cell Int.,* **3:**13.

Kannagi, R. (2004). Molecular mechanism for cancer associated induction of sialyl Lewis X and sialyl Lewis A expression – The Warburg effect revisited. *Glycoconj. J.,* **70:**353-364.

Karsten, U., von Mensdorff-Pouilly, S. and Goletz, S. (2005). What makes MUC1 a tumor antigen? *Tumour Biol.,* **26:**217-220.

Kawabata, K., Murakami, A. and Ohigashi, H. (2005). Nobiletin, a citrus flavonoid, downregulates matrix metalloproteinase-7 (matrilysin) expression in HT-29 human colorectal cancer cells. *Biosci. Biotechnol. Biochem.,* **69:**307-314**.**

Kijima, H., Chino, O., Oshiba, G., Tanaka, H., Kenmochi, T., Kise, Y., Shimada, H., Abe, Y., Tokunaga, T., Yamakazi, H., Nakamura, M., Tanaka, M., Makuuchi, H. and Ueyama, Y. (2001). Immunohistochemical MUC1 (DF3 antigen) expression of human oesophageal squamous cell carcinoma. *Anticancer Res.,* **21:**1285-1289.

Kikuchi, A. (2000). Regulation of β-catenin signaling in the Wnt pathway. *Biochem. Biophys. Res. Commun.,* **286:**243-248.

Kimura, Y., Shiozaki, H., Doki, Y., Yamamoto, M., Utsunomiya, T., Kawanishi, K., Fukuchi, N., Inoue, M., Tsujinaka, T. and Monden, M. (1999). Cytoplasmic beta-catenin in esophageal cancers. *Int. J. Cancer,* **84:**174-178.

Kinlough, C.L., Poland, P.A., Bruns, J.B., Harkelroad, K.L. and Hughey, K.P. (2004). MUC1 membrane trafficking is modulated by multiple interactions. *J. Biol. Chem.,* **279:**53071-53077.

Kleiner, D.E. and Stetler-Stevenson, W.G. (1999). Matrix metalloproteinases and metastasis. *Cancer Chemother. Pharmacol.,* **43:**42-51.

Knudson, A.G. (2002). Cancer genetics. *Am. J. Med. Genet.,* **111:**96-102.

Kolligs, F.T., Kolligs, B., Hajra, K.M., Hu, G., Tani, M., Cho, K.R. and Fearon, E.R. (2000). γ-Catenin is regulated by the APC tumor suppressor and its oncogenic activity is distinct from that of β-catenin. *Genes and Dev.,* **14:**1319-1331.

Kondo, K., Kohno, N., Yokoyama, A. and Hiwada, K. (1998). Decreased MUC1 expression induces E-cadherin-mediated cell adhesion of breast cancer cell lines. *Cancer Res.,* **58:**2014-2019.

Kontani, K., Taguchi, O., Narita, T, Izawa, M, Hiraiwa, N., Zenita, K., Takeuchi, T., Murai, S. and Kannagi, R. (2001). Modulation of MUC1 mucin as an escape mechanism of breast cancer cells from autologous cytotoxic T-lymphocytes. *Br. J. Cancer,* **84:**1258-1264.

Krieghoff, E., Behrens, J. and Mayr, B. (2006). Nucleo-cytoplasmic distribution of beta-catenin is regulated by retention. *J. Cell Sci.,* **119:**1453-1463.

Kuwano, H., Kato, H., Miyazaki, T., Fukuchi, M., Masuda, N., Nakajima, M., Fukai, Y., Sohda, M., Kimura, H. and Faried, A. (2005). Genetic alterations in esophageal cancer. **35:**7-18.

Laemmli, U.K. (1970). Cleavage of structural proteins during the assembly of the head of bacteriophage T4. *Nature,* **227:**680-685.

Lagow, E., De Souza, M.M. and Carson, D.D. (1999). Mammalian reproductive tract mucins. *Hum. Reprod. Update,* **5:**280-292.

Lam, A.K.Y. (2000). Molecular biology of esophageal squamous cell carcinoma. *Critical Rev. Oncol./Hematol.,* **33:**71-90.

Larue, L., Ohsugi, M. and Hirchenhain, J. (1994). E-cadherin null mutant embryos fail to form a trophoectoderm epithelium. *Proc. Natl. Acad. Sci. U.S.A.,* **91:**8263-6367.

Larue, L. and Bellacosa, A. (2005). Epithelial-mesenchymal transition in development and cancer: role of phosphatidyl inositol 3´ kinase/AKT pathways. *Oncogene,* **24:**7443-7454.

Lehrbach, D.M., Nita, M.E. and Cecconello, I. (2003). Molecular aspects of esophageal squamous cell carcinoma carcinogenesis. *Arq. Gastroenterol.,* **40:**256-261.

Li, Y., Bharti, A., Chen, D., Gong, J. and Kufe, D. (1998). Interaction of Glycogen Synthase 3β with the DF3/MUC1 Carcinoma-associated Antigen and β-Catenin. *Mol. Cell Biol.,* **18:**7216-7224.

Li, Y., Ren, J., Yu, W., Li, Q., Kuwahara, H., Yin, L. and Kufe, D. (2001a). The Epidermal Growth Factor Receptor Regulates Interaction of the Human DF3/MUC1 Carcinoma Antigen with c-Src and β-catenin. *J. Biol. Chem.,* **276:**35239-35242.

Li, Y., Kuwahara, H., Ren, J., Wen, G. and Kufe, D. (2001b). The c-src tyrosine kinase regulates signaling of the Human DF3/MUC1 carcinoma-associated antigen with GSK3β and β-catenin. *J. Biol. Chem.,* **276:**6061-6064.

Li, Y., Yu, W.H., Ren, J., Chen, W., Huang, L., Kharbunda, S., Loda, M. and Kufe, D. (2003a). Heregulin targets γ-catenin to the nucleolus by a mechanism dependent on the DF3/MUC1 oncoprotein. *Mol. Cancer Res.,* **1:**765-775.

Li, Y., Chen, W., Ren, J., Yu, W.H., Li, Q., Yoshida, K. and Kufe, D. (2003b). DF3/MUC1 signaling in multiple myeloma cells is regulated by interleukin-7. *Cancer Biol. Ther.,* **2:**187-193.

Li, Y., Liu, D., Chen, D., Kharbunda, S. and Kufe, D. (2003c). Human DF3/MUC1 carcinoma-associated protein functions as an oncogene. *Oncogene,* **22:**6107-6110.

Li, Q., Ren, J. and Kufe, D. (2004). Interaction of human MUC1 and beta-catenin is regulated by Lck and ZAP-70 in activated Jurkat T cells. *Biochem. Biophys. Res. Comm.,* **315:**471-476.

Li, Y.J., Wei, Z.M., Meng, Y.X. and Ji, X.R. (2005). β-catenin up-regulates the expression of cyclin D1, c-myc and MMP-7 in human pancreatic cancer: Relationships with carcinogenesis and metastasis. *World J. Gasteroenterol.,* **11:**2117-2123.

Lim, S.C. and Lee, M.S. (2002). Significance of E-cadherin/beta-catenin complex and cyclin D1 in breast cancer. *Oncol. Rep.,* **9:**915-928.

Lin, Y.C., Wu, M.Y., Li, D.R., Wu, X.Y. and Zheng, R.M. (2004). Prognostic and clinicopathological features of E-cadherin, α-catenin, β-catenin, γ-catenin and cyclin D1 expression in human oesophageal squamous cell carcinoma. *World J. Gasteroenterol.,* **10:**3235-3239.

Liotta, L.A., Tryggvason, K., Garbisa, S., Hart, I., Foltz, C.M. and Shalie, S. (1980). Metastatic potential correlates with enzymatic degradation of basement membrane collagen. *Nature,* **284:**67-68.

Liu, M., Acres, B., Balloul, J.M., Bizouarne, N., Paul, S., Slos, P. and Squiban, P. (2004). Gene-based vaccines and immunotherapeutics. *PNAS,* **101:**14567-14571.

Locascio, A. and Nieto, M.A. (2001). Cell movements during vertebrate development: Integrated tissue behaviour versus individual cell migration. *Curr. Opin. Genet. Dev.,* **12:**464-469.

Logan, C.Y. and Nusse, R. (2004). The Wnt signaling pathway in development and disease. *Annu. Rev. Cell Dev. Biol.,* **20:**781-810.

Mareel, M., Leroy, A. (2002). Clinical, cellular and molecular aspects of cancer invasion. *Phsiol. Rev.,* **83:**33-376.

Matrisian, L.M. (1992). The matrix-degrading metalloproteinases. *BioEssays,* **14:**455-463.

Mayo, L.D. (2002). The PTEN, p53 tumor-suppressor-oncoprotein network. *Trends Biochem.,* **27:**462-467.

McCabe, M.L. and Dlamini, Z. (2005). The molecular mechanisms of oesophageal cancer. *Int. Immunopharmacol.,* **5:**1113-1130.

McCuckin, M.A., Walsh, M.D., Hohn, B.G., Ward, B.G. and Wright, R.G. (1995). Prognostic significance of MUC1 epithelial mucin expression in breast cancer. *Hum. Pathol.,* **26:**432-439.

Michaelson, J.S. and Leder, P. (2001). β-catenin is a downstream effector of Wnt-mediated tumorigenesis in the mammary gland. *Oncogene,* **20:**5093-5099.

Miyazaki, K., Hattori, Y., Umenishi, F., Yasumitsu, H. and Umeda, M. (1990). Purification and characterization of extracellular matrix-degrading metalloproteinase, matrin (pump-1), secreted from human rectal carcinoma cell line. *Cancer Res.,* **50:**7758-7764.

Moniaux, N., Escande, F., Porchet, N., Aubert, J.P. and Batra, S.K. (2001). Structural organization and classification of the human mucin genes. *Front Biosci.,* **6:**1192-1206.

Moniaux, N., Andrianifahanana, M., Brana, R.E. and Batra, S.K. (2004). Multiple roles of mucins in pancreatic cancer, a lethal and challenging malignancy. *Br. J. Cancer,* **91:**1633-1638.

Mori, M., Barnard, G.F., Mimori, K., Ueo, H., Akiyoshi, T. and Sugimachi, K. (1995). Overexpression of matrix metalloproteinase-7 mRNA in human colon carcinomas. *Cancer,* **75:**1516-1519.

Morin, P.J. (1999). β-Catenin signaling and cancer. *Bioessays,* **21:**1021-1030.

Muthuswamy, S.K., Gilman, M. and Brugge, S. (1999). Controlled dimerization of ErbB receptors provides evidence for differential staining by homo- and heterodimers. *Mol. Cell Biol.,* **19:**6845-6857.

Nair, K.S., Naidoo, R. and Chetty, R. (2005). Expression of cell adhesion molecules in oesophageal carcinoma and its prognostic value. *J. Clin. Pathol.,* **58:**343-351.

Nakagawa, H., Zukerberg, Togawa, K. (1995). Human cyclin D1 oncogene and esophageal squamous cell carcinoma. *Cancer,* **76:**541-549.

Nelson, W.J. and Nusse, R. (2004). Convergence of Wnt, β-catenin, and cadherin pathways. *Science,* **303:**1483-1487.

Nicolson, G.L. (1982). Cancer metastasis. Organ colonization and the cell-surface properties of malignant cells. *Biochim. Biophys. Acta,* **695:**113-176.

Ninomiya, I., Endo, Y., Fushida, S., Sasagawa, T., Miyashita, T., Fujimura, T., Nishimura, G., Tani, T., Hashimoto, T., Yagi, M., Shimizu, K., Ohsa, T., Yonemura, Y., Inoue, M., Sasaki, T., Miwa, Y. (2000). Alteration of β-catenin expression in esophageal squamous cell carcinoma. *Int. J. Cancer,* **85:**757-761.

Normanno, N., De Luca, A., Bianco, C., Strizzi, K., Mancino, M., Maiello, MR., Carotenuto, A., De Feo, G., Caponigro, F., Salomon, D.S. (2006). Epidermal growth factor (EGFR) signaling in cancer. *Gene,* **366:**2-16.

North, S.A., Graham, K., Bodnar, D. and Venner, P. (2006). A pilot study of the liposomal MUC1 vaccine BLP25 in prostate specific antigen failures after radical prostatectomy. *J. Urol.,* **176:**91-95.

Novak, A., and Dedhar, S. (1999). Signaling through β-catenin and Lef/Tcf. *Cell Mol. Life Sci.,* **56:**523-537.

Nowell, P.C. (2002). Tumor progression: a brief historical perspective. *Semin. Cancer Biol.,* **12:**261-266.

Oosterkamp, H.M., Scheiner, L., Stefanova, M.C., Lloyd, K.O. and Finstad, C.L. Comparison of MUC1 Mucin Expression in Epithelial and Non-epithelial Cancer Cell Lines and Demonstration of a new short variant form (MUC-1/Z). *Int. J. Cancer,* **72:**87-94.

Ougolkov, A.V., Yamashita, K., Mai, M. and Minamoto, T. (2002). Oncogenic beta-catenin and MMP-7 (matrilysin) cosegregate in late stage clinical colon cancer. *Gasteroenterol.,* **122:**60-71.

Ozawa, M., Baribault, H. and Kremler, R. (1989a). The cytoplasmic domain of the cell adhesion molecule uvomorulin associates with three independent proteins structurally related in different species. *EMBO J.,* **8:**1711-1717.

Ozawa, A., Ueda, M., Ando, N., Shimizu, N. and Abe, O. (1989b). Prognostic significance of epidermal growth factor receptor in esophageal squamous cell carcinomas. *Cancer,* **63:**2169-2173.

Panday, P., Kharbunda, S., Kufe, D. (1995). Association of the DF3/MUC1 breast cancer antigen with Grb2 and the SOS/Ras exchange protein. *Cancer Res.,* **55:**4000-4003.

Parenti, A.R., Rugge, M., Frizzera, E., Ruol, A., Noventa, F. and Ancona, E. (1995). p53 overexpression in the multistep process of esophageal carcinogenesis. *Am. J. Surg. Pathol.,* **19:**1418-1422.

Park, J.Y., Park, W.J., Nam, S.W., Kim, S.Y., Lee, S.H., Yoo, N.J., Lee, J.Y. and Park, C.K. (2005). Mutations of beta-catenin and AXIN I genes are a late event in human hepatocellular carcinogenesis. *Liver Int.,* **25:**70-76.

Patel, K.N., Maghami, E., Wreeamann, V.B., Shaha, A.R., Shah, J.P., Ghossein, R. and Singh, B. (2005). MUC1 plays a role in tumor maintenance in aggressive thyroid carcinomas. *Surgery,* **138:**994-1002.

Patton, S., Gendler, S.J. and Spicer, A.P. (1995). The epithelial mucin, MUC1, of milk, mammary gland and other tissues. *Biochem. Biophys. Acta,* **1241:**407-424.

Pecina-Slaus, N. (2003). Tumor suppressor gene E-cadherin and its role in normal and malignant cell. *Cancer Cell Int.,* **3:**17.

Pignatelli, M. and Vessey, C.J. (1994). Adhesion Molecules: Novel Molecular Tools in Tumor Pathology. *Hum. Pathol.,* **25:**849-856.

Polakis, P. (2000). Wnt signaling and cancer. *Genes Dev.,* **14:**1837-1851.

Powell, S.M., Papadopoulous, N., Kinzler, K.W., Smolinski, K.N. and Meltzer, S.J. (1994). APC gene mutations in the mutation cluster region are rare in oesophageal cancer. *Gasteroenterol.,* **107:**1759-1763.

Qi, W., Schultes, B.C. and Liu, D. (2001). Characterization of an anti-MUC1 monoclonal antibody with potential for immunotherapy of cancer. *Hybrid Hybridomics,* **20:**313-323.

Rahn, J.J., Dubbagh, L., Pasdar, M. and Hugh, J.C. (2001). The importance of MUC1 cellular localization in patients with breast carcinoma: an immunohistologic study of 71 patients and a review of the literature. *Cancer,* **91:**1973-1982.

Rahn, J.J., Shen, Q., Mah, B.K. and Hugh, J.C. (2004). MUC1 initiates a calcium signal after ligation by intercellular adhesion molecule-1. *J. Biol. Chem.* **279:**29386-29390.

Raina, D., Kharbanda, S. and Kufe, D. (2004). The MUC1 Oncoprotein Activates the Anti-apoptotic Phosphoinositide 3-Kinase/Akt and Bcl-xL Pathways in Rat3Y1 Fibroblasts. *J. Biol. Chem.,* **279:**20607-20612 .

Regimbald, L.H., Pilarski, L.M., Longenecker, B.M., Reddish, M.A., Zimmermann, G. and Hugh, J.C. (1996). The breast mucin MUC1 as a novel adhesion ligand for endothelial intercellular adhesion molecule 1 in breast cancer. *Cancer Res.,* **56:**4244-4249.

Ren, J., Li, Y. and Kufe, D. (2002). Protein kinase C delta regulates function of the DF3/MUC1 carcinoma antigen in β-catenin signaling. *J. Biol. Chem.,* **277:**17616-17622.

Ren, J., Agata, N., Chen, D., Li, Y., Yu ,W.H., Huang, L., Raina, D., Chen, W., Kharbanda, S. and Kufe, D. (2004). Human MUC1 carcinoma-associated protein confers resistance to genotoxic anticancer agents. *Cancer Cell* **5:**163-175.

Roose, J. and Clevers, H. (1999). TCF transcription factors: molecular switches in carcinogenesis. *Biochem. Biophys. Acta,* **1424:**23-37.

Saeki, H., Tanaka, S., Sugimachi, K., Kimura, Y., Miyazaki, M., Ohga, T. and Sugimachi, K. (2002). Interrelation between expression of matrixmetalloproteinase 7 and β-catenin in esophageal cancer. *Digestive Dis. Sci.,* **47:**2738-2742.

Sagara, M., Yonezawa, S., Nagata, K., Tezuka, Y., Natsugoe, S., Xing, P.X., McKenzie, I.F., Aikou, T. and Sato, E. (1999). Expression of mucin 1 (MUC1) in esophageal squamous-cell carcinoma: its relationship with prognosis. *Int. J. Cancer,* **84:**251-257.

Salomon, D.S., Kim, N., Saeki, T. and Ciardiello, F. (1990). Transforming growth factor-α: an oncodevelopmental growth factor. *Cancer Cells,* **2:**389-397.

Salomon, D.S., Sacco, P., Roy, S., Simcha, I., Johnson, K., Wheelock, M. and Ben Ze'ev, A. (1997). Regulation of β-catenin levels and localization by overexpression of plakoglobin and inhibition of the ubiquitination-proteasome system. *J. Cell Biol.,* **139:**1325-1335.

Satoh, S., Hindoa, Y., Hayashi, T., Burdick, M.D., Imai, K. and Hollingsworth, M.A. (2000). Enhancement of metastatic properties of pancreatic cancer cells by MUC1 gene encoding an anti-adhesion molecule. *Int. J. Cancer,* **88:**507-518.

Schol, DJ., Meulenbroek, MF., Snijdewint, FG., Von Mensdorff-Pouilly, S., Verstraeten RA, Murakami, F., Kenemans, P. and Hilgers., J. (1998). 'Epitope fingerprinting' using overlapping 20-mer peptides of the MUC1 tandem repeat sequence. *Tumour Biol.,* **19:**35-45

Schroeder, J.A., Thompson, M.C., Mockenstrum, G. and Gendler, S.J. (2001). Transgenic MUC1 Interacts with Epidermal Growth Factor Receptor and Correlates with Mitogen-activated Protein Kinase Activation in the Mouse Mammary Gland. *J. Biol. Chem.,* **276:**13057-13064.

Schroeder, J.A., Adriance, M.C., Thompson, M.C., Camenisch, T.D. and Gendler, S.J. (2003). MUC1 alters β-catenin-dependant tumor formation and promotes cellular invasion. *Oncogene,* **33:**1324-1332.

Schroeder, J.A., Masri, A.A., Adriance, M.C., Tessier, K., Kotlarczyk, K.C., Thompson, M.C. and Gendler, S.J. (2004). MUC1 overexpression results in mammary gland tumorigenesis and prolonged alveolar differentiation. *Oncogene,* **23:** 5739-5747.

Sepulveda, J.L., Gkretsi, V., Wu, C. (2005). Assembly and signaling of adhesion complexes. *Curr. Top. Dev. Biol.,* **68:**183-225.

Shamma, A., Doki, Y. and Shiozaki, H. (1998). Effect of cyclin D1 and associated proteins on proliferation of esophageal squamous cell carcinoma. *Int. J. Oncol.,* **13:**455-460.

Shaw, P.J. and Jordan, E.G. (1995). The nucleolus. *Annu. Rev. Cell Dev. Biol.,* **11:**93-121.

Shibamoto, S., Hayakawa, M., Takeuchi, K., Hori, T., Oku, N., Miyazawa, K., Kitamura, N., Takeichi, M. and Ito, F. (1994). Tyrosine phosphorylation of β-catenin and plakoglobin enhanced by hepatocyte growth factor and epidermal growth factor in human carcinoma cells. *Cell Adhes. Commun.,* **1:**295-305.

Shiozaki, H., Kadowaki, T., Doki, Y., Inoue, M., Tamura, S., Oka, H., Iwazawa, T., Matsui, S., Shimaya, K., Takichi, M. (1995). Effect of epidermal growth factor on cadherin-mediated adhesion in a human oesophageal cancer cell line. *Br. J. Cancer,* **71:**250-258.

Shook, D. and Keller, R. (2003). Mechanisms, mechanics and function of epithelial-mesenchymal transitions in early development. *Mech. Dev.,* **120:**1351-1383**.**

Snijdewint, F.G., Von Mensendorff-Pouilly, S., Karutna-Wanamarta, A.H., Verstraeten, A.A., Livingston, P.O., Hilgers, J. and Kenemans, P. (2001). Antibody-dependent cell-mediated cytotoxicity can be induced by MUC1 peptide vaccination of breast cancer patients. *Int. J. Cancer,* **93:**97-106.

Song, Z.B., Gao, S.S., Yi, X.N., Li, Y.J., Wang, Q.M., Zhuang, Wang, L.D. (2003). Expression of MUC1 in oesophageal squamous-cell carcinoma and its relationship with prognosis of patients from Linzhou city, a high incidence area of Northern China. *World J. Gastroenterol.,* **9:**404-407.

Springer, T.A. (1990). Adhesion receptors of the immune system. *Nature,* **346:**425-434.

Stang, E. F. D., Blystad, M., Kazazic, V., Bertelsen, T., Brodahl, C., Raiborg, H. Stenmark, S. and Madshus, I.H. (2004). Cbl-dependent ubiquitination is required for progression of EGF receptors into clathrin-coated pits. *Mol. Biol. Cell,* **15**:3591-3604.

Stemmermann, G., Heffelfinger, S.C., Noffsinger, A., Hui, Y.Z., Miller, M.A. and Fenoglio-Preiser, C.M. The molecular biology of esophageal and gastric cancer and their precursors: oncogenes, tumor suppressor genes and growth factors. *Human Pathol.,* **25:**968-981.

Sunpaweravong, P., Sunpaweravong, S., Pattawibul, P., Mitarnum, W., Zeng, C., Baron, A.E., Franklin, W., Said, S., and Varella-Garcia, M. (2004). Epidermal growth factor receptor and cyclin D1 are independently amplified and overexpressed in esophageal squamous cell carcinoma. *J. Cancer Res. Clin. Oncol.,* **131:**111-119.

Takechi, M. (1988). The cadherins: cell-cell adhesion molecules controlling animal morphogenesis. *Development,* **102:**639-655.

Takeno, S., Noguchi, T., Fumoto, S., Kimura, Y., Shibata, T. and Kawahara, K. (2004). E-cadherin expression in patients with esophageal squamous cell carcinoma: promoter hypermethylation, snail overexpression, and clinicopathologic implications. *Am. J. Clin. Pathol.,* **122:**78-84.

Tamura, S., Shiozaki, H., Miyata, M. (1996). Decreased E-cadherin expression is associated with haematogeneous recurrence and poor prognosis in patients with squamous cell carcinoma of the oesophagus. *Br. J. Surg.,* **83:**1608-1614.

Taylor-Papadimitriou, J. and Finn, O.J. (1997). Biology, biochemistry and immunology of carcinoma-associated mucins. *Trends Immunol. Today,* **18:**105-107.

Taylor-Papadimitriou, J., Burchell, D.W. and Dalziel, M.M. (1999). MUC1 and Cancer. *Biochim. Biophys. Acta,* **1455:**301-313.

Taylor-Papadimitriou, J. and Burchell, J. (2002). MUC1 and the immunobiology of cancer. *J. Mammary Gland Biol. Neoplasia,* **7:**209-21.

Thompson, E.J., Shaanmugam, K., Hattrup, C.L., Kotlarczyk, K.L., Gutierrez, A., Bradley, J.M., Mukherjee, P. and Gendler, S.J. (2006). Tyrosines in the MUC1 cytoplasmic tail modulate transcription via the extracellular signal-regulated kinase ½ and nuclear factor kappaB pathways. *Mol. Cancer. Res.,* **4:**489-497.

Trowbridge, I.S. and Helenius, A. (1998). Lectins as chaperones in glycoprotein folding. *Curr. Opin. Struct. Biol.,* **8:**587-592.

Utsunomiya, T., Doki, Y., Takemoto, H., Shiozaki, H., Yano, M., Sekimoto, M., Tamura, S., Yasuda, T., Fujiwara, Y. and Monden, M. (2001). Correlation of beta-catenin and cyclin D1 expression in colon cancers. *Oncology,* **61:**226-233.

Van der Flier, A. and Sonnenberg, A. (2001). Function and interactions of integrins. *Cell Tissue Res.,* **305:**285-298.

Van de Wiel-Van Kemenade, E., Ligtenberg, M.J., de Boer, A.J., Buijs, F., Vos, H.L., Melief, C.J., Hilkens, J. and Figdor, C.G. (1993). Episialin (MUC1) inhibits cytotoxic lymphocyte-target cell interaction. *J. Immunol.,* **15:**767-776.

Van Klinken, B.J., Dekker, J., Buller, H.A. and Einerhand, A.W. (1995). Mucin gene structure and expression: protection vs. adhesion. *Am. J. Physiol. Gastrointest. Liver Physiol.,* **269:**613-627.

Van Zyneck, E.R. (1973). Survey of cancer of the oesophagus in relation to other neoplasms. *S. Afr. Med. J.,* **47:**325-331.

Vansaun, M.N. and Matrisian, L.M. (2006). Matrix metalloproteinases and cellular motility in development and disease. *Birth Defects Res. C. Embryo Today,* **78:**69-79.

Veale, R.B. and Thornley, A.L. (1989). Increased single class low-affinity EGF receptors expressed by human oesophageal squamous cell carcinoma cell lines. *S. Afr. J. Sci.*, **85:**375-379.

Vernon, A.E. and LaBonne, C. (2004). Tumor metastasis: A new twist on epithelial-mesenchymal transitions. *Curr. Biol.,* **14:**719-721.

Visintin, R., Amon, A. (2000). The nucleolus: the magician's hat for cell cycle tricks. *Curr. Opin. Cell Biol.,* **12:**372-377.

Vogelstein, B. and Kinzler, K.W. (2004). Cancer genes and the pathways they control. *Nat. Med.,* **10:**789-799.

Von Mensdorff-Pouilly, S., Verstraeten, A.A., Kenemans, P., Snijdewint, F.G.M., Kok, A., Van Kamp, G.J., Paul, M.A., Van Diest, P.J., Meijer, S. and Hilgers, J. (2000): Survival in early breast cancer patients is favorably influenced by a natural humoral immune response to polymorphic epithelial mucin. *J. Clin. Oncol.,* **18:**574-583.

Wang, H., Lillehog, E.P., Kim, K.C. (2003). Identification of four sites of stimulated tyrosine phosphorylation in the MUC1 cytoplasmic tail. *Biochem. Biophys. Res. Commun.,* **310:**341-346.

Wang, H., Lillehog, E.P., Kim, K.C. (2004). MUC1 tyrosine phosphorylation activates the extracellular signal-regulated kinase. *Biochem. Biophys. Res. Commun.,* **321:**448-454.

Wantake, H. (2002). Significance of mucin on the ocular surface. *Cornea,* **21:**7-22.

Wei, X., Xu, H. and Kufe, D. (2005). Human MUC1 oncoprotein regulates p53-responsive gene transcription in the genotoxic stress response. *Cancer cell,* **7:**167-178.

Wen, Y., Caffrey, T.C., Wheelock, M.J., Johnson, K.R. and Hollingsworth, M.A. (2003). Nuclear association of the cytoplasmic tail of MUC1 and β-catenin. *J. Biol. Chem.,* **278:**38029-38039.

Wesseling, J., van der Valk, S.W., Vos, H.L., Sonnenberg, A. and Hilkens, J. (1995). Episialin (MUC1) Overexpression Inhibits Integrin-mediated Cell Adhesion to Extracellular Matrix Components. *J. Cell Biol.,* **129:**255-265.

Wesseling, J., van der Valk, S.W. and Hilkens, J. (1996). A mechanism for inhibition of E-cadherin mediated cell-cell adhesion by the membrane associated mucin episialin/MUC1. *Mol. Biol. Cell,* **7:**565-577.

Wilson, C.L. and Matrisian, L.M. (1996). Matrilysin: an epithelial matrix metalloproteinase with potentially novel functions. *Int. J. Biochem. Cell Biol.,* **28:**123-136.

Wong, N.A. and Pignatelli, M. (2002). β-Catenin- A linchpin in colorectal carcinogenesis. *Am. J. Pathol.* **160:**389-401.

Wong, S.C., Lo, E.S., Lee, K.C., Chan, J.K. and Hsiao, W.L. (2004). Prognostic and diagnostic significance of beta-catenin nuclear immuno-staining in colorectal cancer. *Clin. Cancer. Res.,* **10:**1401-1408.

Yamamoto, M., Bharti, A., Li, Y. and Kufe, D. (1997). Interaction of the DF3/MUC1 Breast Carcinoma-associated Antigen and β-Catenin in Cell Adhesion. *J. Biol. Chem.,* **272:**12492-12464.

Yamamoto, H., Adachi, Y., Itoh, F., Iku, S., Matsuno, K., Kusano, M., Arimura, Y., Endo, T., Hinoda, Y., Hosokawa, M. and Imai, K. (1999). Association of matrilysin expression with recurrence and poor prognosis in human eosophageal squamous cell carcinoma. *Cancer Res.,* **59:**3313-3316.

Yamashita, K., Mori, M., Shiraishi, T., Shibuta, K. and Sugimachi, K. (2000). Clinical significance of matrix metalloproteinase-7 expression in esophageal carcinoma. *Clin. Cancer Res.,* **6:**1169-1174.

Yamazaki, K., Hanami, K., Nagao, T., Asoh, A., Sugano, I. and Ishida, Y. (2003). Increased cyclin D1 expression in cancer of the ampulla of Vater: relevance to nuclear beta catenin accumulation and k-ras gene mutation. *Mol. Pathol.,* **56:**336-341.

Yano, H., Shiozaki, H. and Kobayashi, K. (1991). Immunohistochemical detection of the epidermal growth factor receptor in human esophageal squamous cell carcinoma. *Cancer,* **67:**91-98.

Yarden, Y. and Sliwkowski, M.X. (2001). Untangling the ErbB signaling network. *Nat. Rev. Mol. Cell Biol.,* **2:**127-137.

Yonezawa, S. and Sato, E. (1997). Expression of mucin antigens in human cancers and its relationship with malignancy potential. *Pathol. Int.,* **47:**813-830.

Yin, L., Huang, L. and Kufe, D. (2004). MUC1 oncoprotein activates the FOXO3a transcription factor in a survival response to oxidative stress. *J. Biol. Chem.,* **279:**45621-45727.

Zeng, Z.S., Shu, W.P., Cohen, A.M. and Guillem, J.G. (2002). Matrix metalloproteinase-7 expression in colorectal cancer liver metastases: evidence for involvement of MMP-7 activation in human cancer metastases. *Clin. Cancer Res.,* **8:**144-148.

Zhang, K., Beackstrom, D., Brevinge, H. and Hansson, G.C. (1996). Secreted MUC1 mucins lacking their cytoplasmic part and carrying sialyl-Lewis a and x epitopes from a tumor cell line and sera of colon carcinoma patients can inhibit HL-60 leukocyte adhesion to E-selectin-expressing endothelial cells. *J. Cell Biochem.,* **60:**538-549.